Spring 2006

Passive and Active Nonlinear Control of Ship Roll Motions Using U-Tube Tanks

Thongchai Phairoh
Old Dominion University

PASSIVE AND ACTIVE NONLINEAR CONTROL OF SHIP ROLL MOTIONS USING U-TUBE TANKS

by

Thongchai Phairoh
B.Eng, King Mongkut's Institute of Technology North Bangkok, Thailand, 1986
M.Eng, King Mongkut's Institute of Technology North Bangkok, Thailand, 1997

A Thesis Submitted to the Faculty of
Old Dominion University in Partial Fulfillment of the
Requirement for the Degree of

DOCTOR OF PHILOSOPHY

MECHANICAL ENGINEERING

OLD DOMINION UNIVERSITY
May 2006

Approved by:

Dr. Jen-Kuang Huang (Director)

Dr. Han P. Bao (Member)

Dr. Gene J. -W. Hou (Member)

Dr. Brett Newman (Member)

ABSTRACT

PASSIVE AND ACTIVE NONLINEAR CONTROL OF SHIP ROLL MOTIONS

USING U-TUBE TANKS

Thongchai Phairoh
Old Dominion University, 2006
Director: Dr. Jen-Kuang Huang

A U-tube water tank is first designed to roll a ship floating on still water. The 6-degree of freedom (DOF) dynamic model of U-tube tank is derived and the effects of its parameters on ship roll motion are studied. Numerical simulations show that the U-tube tank is an effective stimulator to roll the ship on still water. For a rolling ship, the U-tube tank can be used as a damper to reduce ship roll motion quickly.

Active control of ship roll motion with a proportional and derivative (PD) controller, linear quadratic regulator (LQR), generalized predictive control (GPC), and deadbeat predictive control (DPC) is studied using a U-tube water tank as actuator is studied. For the predictive control, system identification is applied to update the parameters of the linear ship roll model with a U-tube tank when the ship dynamics changes. Numerical simulations show that GPC has the best performance and the U-tube tank is effective in ship roll mitigation.

Nonlinear ship roll mitigation with passive U-tube tank, U-tube tank using feedback linearization with completely known system parameters, and U-tube tank using adaptive fuzzy feedback linearization control with unknown system parameters, are also studied. In numerical simulation, a passive U-tube tank and feedback linearization help to reduce ship roll motion and capsizing compared to a ship without the U-tube tank.

Feedback linearization is the most effective means of controlling ship roll motion, and adaptive feedback linearization is more effective than a passive U-tube tank.

To ALL OF MY TEACHERS

ACKNOWLEDGMENTS

I would like to express my sincere appreciation to my advisor, Dr. Jen Kuang Huang for his guidance and valuable advice in various aspects. These have been most important things in completing this thesis. He is not only my academic advisor but he also treated me like his cousin. I am grateful to Dr. Brett Newman, Dr. Han Bao, Dr. Gene Hou and Dr. Keith Williamson for spending their valuable time as members of my dissertation committee, and for their useful suggestions and recommendations. In addition to the members, I feel fortunate to work and discuss ship roll mitigation with Dr. Drexter Bird of Craft Engineering Inc.

I would like to thank the Mechanical Engineering Department for financial support, Diane Mitchell for helping me with department paperwork, Laura for correcting my writing, and the office of dean for help with the final correction dissertation format and grammar.

I am most grateful to my parents especially my mother, Boonsomkroh, for raising and taking care of me. I thank my mother in law, Sriupsorn, for taking care of my daughter. Special thanks to my wife, Sariyamon and my daughter, Ruksamadi, for their encouragement.

TABLE OF CONTENTS

Page

LIST OF TABLES

LIST OF FIGURES

NOMENCLATURE

A_t, A_p	Area of the reservoir, and duct respectively
$\mathbf{a}_p$	Particle acceleration
$B(\phi, \dot{\phi})$	Nonlinear damping moment
b	Friction coefficient of resistance
$C(\phi)$	Nonlinear restoring moment
CG (ship)	Center of mass of the ship
d_1	Linear roll damping coefficient
$\mathbf{F}_s, X_s, Y_s, Z_s$	Stimulator force and its component in X_0, Y_0, and Z_0 respectively
$\mathbf{f}, \mathbf{f}_{acc}, \mathbf{f}_{grav}, \mathbf{f}_{fric}$	Body force per unit mass and its component generated by acceleration, gravitation, and friction force respectively
$\mathbf{g}$	Gravitational acceleration
H	Equilibrium water height in U-tube tank
h	Water height in U-tube tank deviation from it's equillibrum
h_c	control horizon
$h_{0/w}, h_{0/p}$	Water height amplitude due to external excitation, and pump pressure respectively
h_0	Water height amplitude due to external excitation and pump pressure
h_p	predicted output
$\mathbf{I}, \mathbf{J}, \mathbf{K}$	Unit vectors of the inertial frame in X, Y and Z respectively
I	Ship roll moment of inertia and added mass
I_n	Identity matrix with dimension n
$\mathbf{i}, \mathbf{j}, \mathbf{k}$	Unit vectors of body fixed frame in X_0, Y_0 and Z_0 respectively
K_1	Restoring moment coefficient
K_{st}, K_{wave}	Stimulator moment and external moment acting on the ship roll
K_0	Wave moment acting on the ship roll
L	Duct length

L_x, L_y, L_z	Distance of the center of the duct to the center of gravity of the ship in the X_0-direction, Y_0-direction, and Z_0-direction respectively
l	Length of streamline in U-tube tank from starboard to port
$\mathbf{M}_{st}, K_s, L_S, M_s$	Stimulator moment and its component in X_0, Y_0, and Z_0 respectively
m	Mass of fluid in U-tube tank
m, n, r	Number of system output, number of system order, and number of system output
P	Particle or pressure
P_0	Pump pressure amplitude
$\mathbf{r}_{P/0}$	Position vector of P with respect to CG (ship)
$\mathbf{r}_0, r_{0X}, r_{0Y}, r_{0Z}$	Position vector of the CG (ship) with respect to inertial reference frame and its component in X, Y, and Z respectively
T	Kinetic energy
U	Potential energy
$\mathbf{u}_l$	Unit vector of streamline in U-tube tank
$\mathbf{u}_f$	Fluid velocity along streamline in U-tube tank
$\mathbf{v}_p, u(t), v(t), w(t)$	Velocity of particle P and its component in X_0, Y_0, and Z_0 respectively
μ	Mass ratio
$\mathbf{\Omega}, \dot{\phi}, \dot{\theta}, \dot{\varphi}$	Angular velocity and its component in X_0, Y_0, and Z_0 respectively
$\phi_{0/w}, \phi_{0/p}$	Ship roll amplitude due to external moment and pump pressure respectively
$\phi_{\phi-K}$, $\phi_{\tau-K}$	Phase ship of ship roll and tank angle with respect to wave moment respectively
ϕ_0	Ship roll amplitude due to external moment and pump pressure
ϕ_1	Phase shift of pump pressure
ϕ_2	Phase shift of external moment
ρ	Fluid density in U-tube tank
ω_s	Natural frequency of ship roll motion

ω_t	Natural frequency of fluid motion in U-tube tank
ω_e	Encounter frequency of wave moment
ρ	Fluid density in U-tube tank
τ	Tank angle which is the water height h divided by $L/2$

CHAPTER I

INTRODUCTION

A ship has six degrees of freedom (DOF) (surge, sway, heave, roll, pitch, and yaw) that allow it to move when forces act upon it. Forces acting upon a ship come from thrusters which may include propeller forces, control surfaces such as rudder forces, and environmental forces such as waves, wind, current, loading and unloading, and water motion in an internal compartment.

A ship has restoring forces that counter the effects of roll, pitch, and heave enabling a ship to oscillate in the sea. Loading and unloading are difficult operations, so operators should be trained under sea conditions. The real environment can be simulated by using a ship roll stimulator so that training can be conducted as needed. Active U-tube tanks, gyroscopes, and a moving mass can be used to stimulate the ship roll motion. Gyroscopes have precision moving parts and rotate with high speed, so they are not suitable ship roll stimulators. An active U-tube tank is selected because its weight can be removed easier than a moving mass. For a ship roll stimulator, if the maximum ship roll amplitude is less than 6 degrees, then linear ship roll is considered for design and analysis of a ship roll stimulator. This U-tube was designed by Bird and Lucero (1999).

After a U-tube tank is installed as a ship roll stimulator, two questions may be asked: For aid in loading and unloading, can a U-tube tank be applied to reduce ship roll motion? Can an active U-tube tank help to reduce capsizing in severe seas? For both questions, yes is the answer, if an appropriate controller is implemented. Loading and unloading normally occur with small ship roll motion, so active ship roll mitigation can

be designed by using a linear ship roll model. Capsizing occurs with large ship roll motion, so the active ship roll controller should be designed by using a nonlinear ship roll model.

1.1 Objectives

First, a mathematical model of an active U-tube tank is derived. Second, the optimal passive U-tube tank for ship roll mitigation is studied by considering the optimal values of water motions natural frequency in a U-tube tank and the friction coefficient between water and the U-tube tank. Third, a linear controller is applied to the linear ship roll model and linear U-tube tank model. Finally, a nonlinear controller is applied to a nonlinear ship roll model with uncertain parameters.

1.2 Outlines

Passive and active U-tube tanks were studied for ship roll mitigation. In chapter 2, a nonlinear mathematical model of a U-tube tank was derived, and a comparison was made with the experimental data. In chapter 3, optimal U-tube tank parameters were considered for a passive U-tube tank. For an active U-tube tank, a linear ship roll model was used for a linear control design. Selected linear controllers are a proportional and derivative (PD) controller, linear quadratic controller (LQR), generalized predictive controller (GPC), deadbeat predictive controller (DPC) and adaptive predictive controller. In chapter 4, nonlinear ship roll and a U-tube tank were considered for a passive and active U-tube tank. Adopted nonlinear controllers were linearization feedback and adaptive fuzzy control based on feedback linearization. The effects of a

passive and an active U-tube tank on ship capsizing were compared.

1.3 Literature Review

1.3.1 Ship Modeling

Abkowitz (1969), Fossen and Fjellstad (1995) derived the equation of ship motion. However, due to the difficulties with obtaining the hydrodynamic forces and with nonlinear multi-DOF problems, the general models are usually linearized or the degree of freedom is reduced for analysis. The reduction of the full ship model to a 1-DOF one is commonly done. Coupling of surge, sway, and yaw motion is considered for dynamic positioning. Chen et al. (1999), and Yim et al. (2004) derived the couple of roll, heave, and sway motion in beam seas, and show that restoring forces and moments depend on ship roll, heave, wave height and wave slope. Oh et al. (1993), and Neves (1999), (2003) studied the coupling of heave, pitch, and roll motions in following seas and show that a restoring moment depends on ship roll, pitch, heave, and wave height. Falazano (1990) presented that water on the deck changed the restoring moment curve. Hua et al. (1999) represented the metacentric height of a ship with a Volterra series.

1.3.2 Ship Motion Analysis

The analysis of nonlinear rolling motions has been focused on the decouple a 1-DOF roll equation. The steady state periodic solutions excited by periodic excitation for such a system can be obtained by perturbation techniques such as the harmonic balance method, the method of multiple scales, and the averaging method. For random excitation, Roberts (1982) studied 1-DOF roll motion under roll excitation using the stochastic averaging method.

For the geometric approach, Thompson (1989b), (1990), (1990b) investigated ship capsizing in regular seas using a numerical simulation emphasizing transient behavior. Shaw and co-workers predict the capsizing criteria for regular and irregular seas. Chen et al. (1998) applied them to multiple degree of freedoms. Jiang et al. (2000) presented capsizing in irregular beam seas by considering damping as a memory function.

1.3.3 Ship Roll Stabilization

Control algorithms for active ship roll mitigation are developed by following the development of control theory. A fin, rudder, moving mass, and U-tube tank are active methods of ship roll stabilization. From publication papers, fins and rudders are most concerned with the control application. An active U-tube tank is also implemented for ship roll mitigation, which works well at any ship velocity.

For rudder control, a robust controller was studied by Stoustrup et al. (1994), a fuzzy logic controller was implemented by Nejim (2000) and an adaptive controller was undertaken by Amerogen et al. (1990).

For fin stabilizer, a robust controller was applied by Hickey et al. (1997) and a neuro-fuzzy controller was applied by Guo (2003).

For U-tube tank, Webster (1967) presented an analysis of control activated anti-roll U-tube tank systems. A passive U-tube tank was modeled by Lloyd (1989). Phairoh and Huang (2005) derived nonlinear forces and moment generated by an active U-tube tank. Chen et al. (2000) proposed a nonlinear controller to the couple of motion in sway, heave and roll which is derived by Chen et al. (1997). Chen and Hsu (2003) applied fuzzy

logic control to an active U-tube tank. Yamagushi and Shinkai (1995) applied model reference adaptive control to control a pump to drive water in a U-tube tank. Phairoh and Huang (2005) applied adaptive predictive control to ship roll mitigation.

For a semi active U-tube tank, water flow in the U-tube tank is controlled by adjusting air valves at the top of the connection pipe. Pole placement design was studied by Roberts and Barboza (1988), and optimal control was undertaken by Zhang et al. (2004). For the other type of semi active U-tube tank, the flow of the water tank is controlled by adjusting the valve area of pipe. Webster et al. (2003) used learning process, and on-off control to control the valve area of pipe.

A fluid tank and U-tube tank are not used only in ship roll mitigation but are also applied in high rise buildings to reduce building vibration due to winds or earthquakes. Yalla et al. (2001) presented a semi-active U-tube tank applied to structural control.

Combinations of actuator were also considered in ship roll mitigation. For fin and rudder, optimal control was applied by Shao et al. (1994), robust control was implemented by Sharif et al. (1997), fuzzy logic and MIMO were compared by Sutton (1989), and gain scheduling control was implemented by Tanguay and Lebret (2004). Burns (1991) applied optimal control to stabilize pitch, heave, and roll motion by using rudder angle, engine speed, and four fins.

1.3.4 Selected Controller

The general predictive control (GPC) was introduced by Clarke et.al. (1987). GPC is a time domain method that uses a mathematical model to describe the input-output relationship of the system and to design the controller minimizing a desired cost function.

Juang and Phan (1997a, b) developed a GPC by using the autoregressive with exogenous input (ARX) model to describe the input-output relationship and applied it to vibration control problems. Kvaternik et al. (2001) applied this GPC to improve aeroelastic stability in airplanes.

Chen et al. (1992) and Juang (1994) derived a system identification algorithm which can identify a state-space model from input-output test data. Juang et al. (1993) developed the Observer/Kalman Filter Identification (OKID) algorithm.

Slotine and Li (1991) introduced feedback linearization to the control of a nonlinear system. It relies on exact cancellation of nonlinear term in order to get linear input-output behavior, then the input-output behavior is no longer linear. Sastry and Bodson (1989) used parameter adaptive control to help make more robust the cancellation of nonlinear terms when parametric uncertainties occur in the nonlinear terms. A fuzzy system and neural network can be used to represent nonlinear function; this occurs when nonlinear function functions are not known exactly. He et al. (1998), Ge et al. (1999) used a neural network to represent the nonlinear function. Wang (1993), Chen et al. (1996) and Park (2003) applied a fuzzy system for an indirect adaptive controller, and Yang and Ren (2003) applied a fuzzy system for a direct adaptive controller.

CHAPTER 2

SHIP ROLL STIMULATION BY USING U-TUBE TANK

A ship has six degrees of freedom (surge, sway, heave, roll, pitch, and yaw) that allow it to move when forces act upon it. Forces acting upon a ship come from thrusters which may include propeller forces, control surfaces such as rudder forces, and environmental forces such as waves, wind, current, and loading and unloading.

A ship has restoring forces that counter the effects of roll, pitch, and heave enabling a ship to oscillate in the sea condition. Due to a smaller moment of inertia, ship roll motion is more significant than the other oscillations. From Lewis (1989), in the roll motion, the magnification factor (i.e. the magnitude ratio of the amplitude of a ship oscillation with respect to the magnitude of the sinusoidal input) can be 10 or more for a bare hull and can be 7 or more for a ship equipped with bilge keels. However, the magnification factor of heave is less than 1.3, and the magnification factor of pitch is less than 1.5. Roll motion also makes passengers uncomfortable and makes the process of loading and unloading difficult.

Various active and passive systems may be used for ship roll cancellation. Possible active systems include active flume tanks, gyroscopes, active fins, and rudders. Passive systems may consist of water tanks and bilge keels.

Passive water tanks have two basically different structures. One is free surface and the other one is U-tube tank. For free surface, Kim (2002) simulated the coupling between fluid motion in the tank, with and without baffle, and ship rolling based on finite difference method. For U-tube tank, Lloyd (1989) used one-dimensional Euler's equation

to derive the equation of fluid motion in U-tube. Based on this equation, Gawad et al (2001) studied the effect of U-tube tank parameters to the ship roll motion. A limitation of the passive tank is its inability to effectively reduce ship roll at frequencies encountered at sea. It can, however, reduce ship roll motion near the ship roll natural frequency.

U-tube tank can also be used for active ship roll mitigation. Yamaguchi et al (1995) showed U-tube anti-roll tanks that had an impeller in the center of the cross tube. The ship roll mitigation was demonstrated by using an active U-tube tank with adaptive control algorithm. Chen et al (2000) also used U-tube anti-roll tank with robust control.

Active U-tube tank can be used to stimulate the ship roll motion. This system will provide a realistic, elevated sea state environment for operator training and evaluation of future research and development efforts to improve cargo load and unloading operations. The mathematical model of stimulator is required for studying system behavior and selecting the size of the stimulator. In this study, the model of U-tube anti-roll tanks is developed with two inputs from wave moment and pump pressure. The stimulator forces and moments are calculated. The effects of stimulator parameters to stimulator dynamics, the time domain behavior of ship roll and stimulator, and the relationship between pump pressure and wave moment are considered.

In this study, an active flume tank consists of two water reservoirs mounted in the outboard container cells and connected to a bow thruster inside a duct. A schematic diagram of the active tank is shown in Figure 2.1. The water, driven by an axial pump, has a varying flow rate and is used to generate forces and moments acting on the ship.

The axial pump is assumed to be the pressure source. The fluid motion in the U-tube is assumed to be one dimensional, from the reservoir, to duct, and other reservoir.

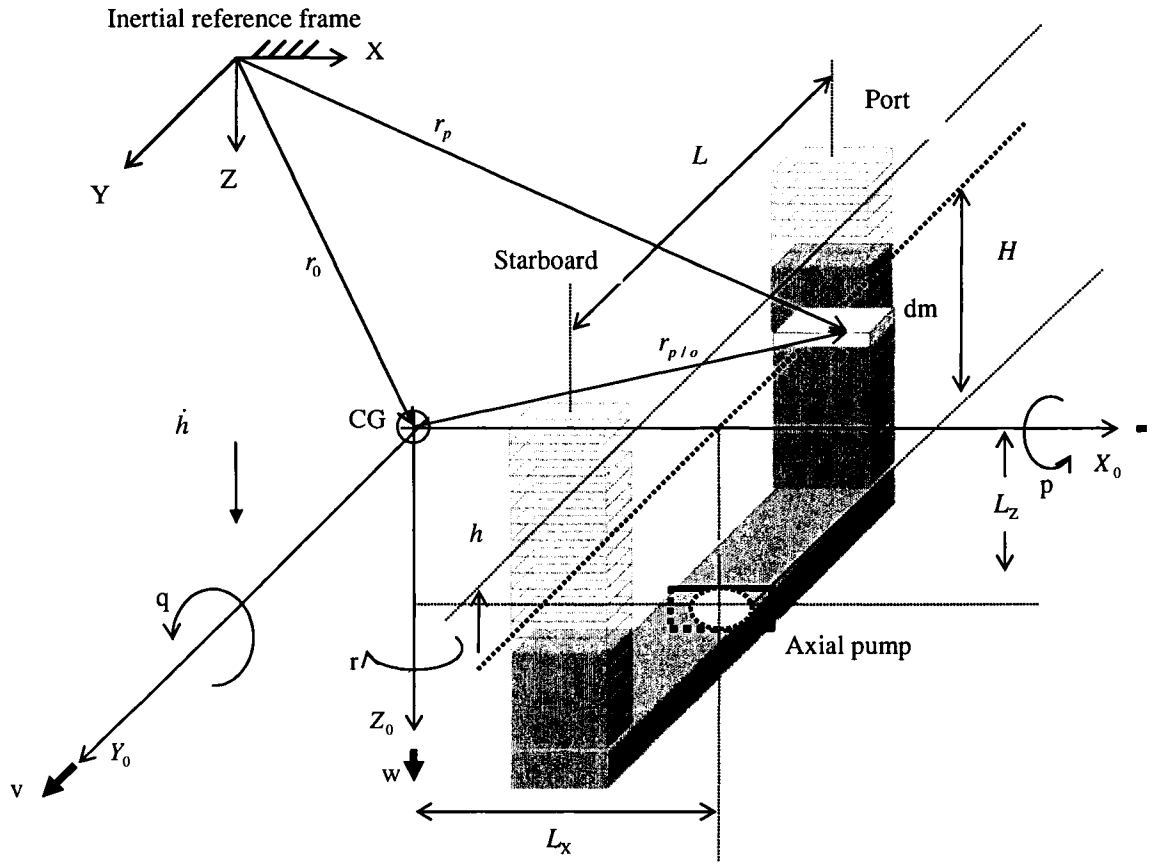

Figure 2.1 Schematic diagram of active U-tube tank.

2.1 Equation of Tank Fluid Motion

In this part, the motion equation of the fluid in the active U-tube tank is considered. Fluid motion in the active tank generates force and moment acting on the ship.

2.1.1 Fluid Motion in U-tube Tank

The fluid motion is assumed to be the motion of a group of particles. As shown in Figure 2.1, the center of mass of the ship is located at CG (ship). A position vector from the origin of the inertial reference frame to the CG (ship) is

$$\mathbf{r}_0 = r_{0X}(t)\mathbf{I} + r_{0Y}(t)\mathbf{J} + r_{0Z}(t)\mathbf{K} \tag{2.1}$$

The ship velocity at CG (ship) is

$$\mathbf{v}_0 = \frac{d\mathbf{r}_0}{dt} = \dot{r}_{0X}(t)\mathbf{I} + \dot{r}_{0Y}(t)\mathbf{J} + \dot{r}_{0Z}(t)\mathbf{K} \tag{2.2}$$

This can be described in the body fixed frame as

$$\mathbf{v}_0 = \frac{d\mathbf{r}_0}{dt} = u(t)\mathbf{i} + v(t)\mathbf{j} + w(t)\mathbf{k} \tag{2.3}$$

Let P represent a particle in the U-tube tank. Then its position vectors in the vertical reference frame is

$$\mathbf{r}_p = \mathbf{r}_0 + \mathbf{r}_{P/0} \tag{2.4}$$

The velocity of the particle P with respect to body fixed frame becomes

$$\mathbf{v}_p = \frac{d\mathbf{r}_p}{dt} = u(t)\mathbf{i} + v(t)\mathbf{j} + w(t)\mathbf{k} + \boldsymbol{\Omega}\times\mathbf{r}_{p/0} + \dot{\mathbf{r}}_{p/0} \tag{2.5}$$

or $\mathbf{v}_p = \mathbf{v}_0 + \boldsymbol{\Omega}\times\mathbf{r}_{p/0} + \dot{\mathbf{r}}_{p/0}$,

where $\boldsymbol{\Omega} = p(t)\mathbf{i} + q(t)\mathbf{j} + r(t)\mathbf{k}$ is the ship angular velocity, and $\mathbf{v}_0 = u(t)\mathbf{i} + v(t)\mathbf{j} + w(t)\mathbf{k}$ is the ship CG velocity. The derivatives of $(r_{0X}(t), r_{0Y}(t), r_{0Z}(t))$ and (ϕ, θ, ψ) are related to the components of the velocities in the body-fixed system by the transformation

$$\begin{bmatrix} \dot{r}_{0X} \\ \dot{r}_{0Y} \\ \dot{r}_{0Z} \\ \dot{\phi} \\ \dot{\theta} \\ \dot{\psi} \end{bmatrix} = \begin{bmatrix} C\psi C\theta & -C\phi S\psi + C\psi S\theta S\phi & S\theta S\psi + C\psi C\phi C\theta & 0 & 0 & 0 \\ S\psi C\theta & -C\phi C\psi + S\psi S\theta S\phi & -S\phi C\psi + S\psi S\phi S\theta & 0 & 0 & 0 \\ -S\theta & C\theta S\phi & C\theta C\phi & 0 & 0 & 0 \\ 0 & 0 & 0 & 1 & S\phi T\theta & C\phi T\theta \\ 0 & 0 & 0 & 0 & C\phi & -S\phi \\ 0 & 0 & 0 & 0 & S\phi/C\theta & C\phi/C\theta \end{bmatrix} \begin{bmatrix} u \\ v \\ w \\ p \\ q \\ r \end{bmatrix}$$

, where S, C, and T represent the sine, cosine, and tangent functions respectively.

The acceleration of the particle P with respect to the body fixed frame is

$$\mathbf{a}_p = \frac{d\mathbf{v}_p}{dt} = \mathbf{a}_0 + \boldsymbol{\Omega} \times \mathbf{v}_0 + \dot{\boldsymbol{\Omega}} \times \mathbf{r}_{p/0} + 2\boldsymbol{\Omega} \times \dot{\mathbf{r}}_{p/0} + \boldsymbol{\Omega} \times (\boldsymbol{\Omega} \times \mathbf{r}_{p/0}) + \ddot{\mathbf{r}}_{p/0} \tag{2.6}$$

where $a_0 = \dot{u}(t)\mathbf{i} + \dot{v}(t)\mathbf{j} + \dot{w}(t)\mathbf{k}$ is the ship CG acceleration.

By using Euler's equation, Lloyd (1989) derived fluid motion equation

$$\frac{\partial u_f}{\partial t} + u_f \frac{\partial u_f}{\partial l} = -\frac{1}{\rho} \frac{dP}{dl} + \mathbf{f} \cdot \mathbf{u}_l . \tag{2.7}$$

In addition, one can assume that the velocity in the reservoir is equal, the velocity in the duct is equal, and there is no transition effect of fluid flow at the connection between the duct and reservoirs. Then the fluid motion is simplified to be

$$\frac{du_f}{dt} = -\frac{1}{\rho} \frac{dP}{dl} + \mathbf{f} \cdot \mathbf{u}_l \tag{2.8}$$

The force per unit mass $\mathbf{f}$ acting on fluid element includes the acceleration force, the gravitational force, and the frictional force, i.e.

$$\mathbf{f} = \mathbf{f}_{acc} + \mathbf{f}_{grav} + \mathbf{f}_{fric}$$

The acceleration force per unit mass $\mathbf{f}_{acc}$ is mass acceleration in Equation (2.6). The gravitational force per unit mass $\mathbf{f}_{grav}$ is $\mathbf{g} \cdot \mathbf{u}_l$. The frictional force per unit mass $\mathbf{f}_{fric}$ is $-bu_f \mathbf{u}_l$. The equation of motion becomes

$$\frac{du_f}{dt} = \ddot{\mathbf{r}}_{p/0} \cdot \mathbf{u}_l - \frac{1}{\rho}\frac{dP}{dl} - \left\{\mathbf{a}_0 + \boldsymbol{\Omega} \times \mathbf{v}_0 + \dot{\boldsymbol{\Omega}} \times \mathbf{r}_{p/0} + 2\boldsymbol{\Omega} \times \dot{\mathbf{r}}_{p/0} + \boldsymbol{\Omega} \times \left(\boldsymbol{\Omega} \times \mathbf{r}_{p/0}\right)\right\} \cdot \mathbf{u}_l + \mathbf{g} \cdot \mathbf{u}_l - bu_f \tag{2.9}$$

By integrating along the streamed line from surface of the starboard reservoir to the surface of port reservoir, one has

$$\begin{aligned} \int_{star}^{port} \frac{du_f}{dt} dx = & \int_{star}^{port} \ddot{\mathbf{r}}_{p/0} \cdot \mathbf{u}_l dx - \int_{star}^{port} \frac{1}{\rho}\frac{dP}{dl} dx \\ & - \int_{star}^{port} \left\{\mathbf{a}_0 + \boldsymbol{\Omega} \times \mathbf{v}_0 + \dot{\boldsymbol{\Omega}} \times \mathbf{r}_{p/0} + 2\boldsymbol{\Omega} \times \dot{\mathbf{r}}_{p/0} + \boldsymbol{\Omega} \times \left(\boldsymbol{\Omega} \times \mathbf{r}_{p/0}\right)\right\} \cdot \mathbf{u}_l dx \\ & + \int_{star}^{port} \mathbf{g} \cdot \mathbf{u}_l dx - \int_{star}^{port} bu_f dx \end{aligned} \tag{2.10}$$

The result becomes

$$\begin{aligned} -\rho\left(2H + \frac{A_{tank}}{A_{pipe}} L\right)\ddot{h} = & \Delta P + 2h\rho g \cos\theta \cos\phi - \rho g L \cos\theta \sin\phi \\ & - \rho L\dot{v} - 2\rho H\dot{w} + 2\rho hqu - 2\rho hpv + \rho Lru - \rho Lpw \\ & - \rho(2L_Z - H)hp^2 - \rho(2L_Z - H)hq^2 \\ & + 2\rho L_X hpr - \rho L L_X pr - \rho(HL + L_Z L)qr \\ & + 2\rho L_X h\dot{q} - \rho L(L_Z + H)\dot{p} + \rho L_X L\dot{r} + bA_t(2H + L)\dot{h} \end{aligned} \tag{2.11}$$

By linearizing Equation (2.11) and multiplying it with A_t, one can derive the linear stimulator model,

$$-\rho A_t\left(2H+\frac{A_t}{A_p}L\right)\ddot{h}-2\rho A_t L_X h\dot{q}+\rho L A_t(L_Z+H)\dot{p}+\rho A_t L_X L\dot{r}+\rho A_t L\dot{v}+2\rho A_t H\dot{w}$$
$$-bA_t^2(2H+L)\dot{h}=A_t\Delta P+2A_t h\rho g-\rho A_t gL\phi \tag{2.12}$$

The stimulator roll natural frequency is

$$\omega_t=\sqrt{\frac{2g}{(2H+LA_t/A_p)}}$$

This stimulator natural frequency can also be calculated by using Rayleigh's method from Shames and Dym (1991).

2.1.2 Stimulator Force

From Newton's second law, the stimulator force generated by the motion of the fluid particle is

$$-d\mathbf{F}_s=\mathbf{a}_p dm-\mathbf{g}dm, \tag{2.13}$$

where dm is the mass of fluid particle P in the U-tube tank . Integrating Equation (2.13) along the streamline in the U-tube tank, the total stimulator force is

$$\mathbf{F_s}=X_s i+Y_s j+Z_s k,$$

where

$$-X_s=\rho g(2A_tH+A_pL)\sin\theta+(2\rho A_tH+\rho A_pL)\dot{u}-2\rho A_t hq\dot{h}-\rho A_t Lr\dot{h}-\rho(2HA_t+LA_p)rv$$
$$+\rho(2HA_t+LA_p)qw-\rho(2A_tL_xH+L_xLA_p)r^2-\rho(2A_tL_xH+L_xLA_p)q^2$$
$$+\rho A_t(2L_zH-H^2-h^2)rp+\rho L_zLA_prp+\rho A_tLhpq-\rho LhA_t\dot{r}$$
$$+\rho\{A_t(2L_zH-H^2-h^2)+L_zLA_p\}\dot{q}$$

$$
\begin{aligned}
-Y_s &= \rho A_t L\ddot{h} + \rho g\left(2A_tH + A_pL\right)\cos\theta\sin\phi + \rho\left(2A_tH + A_pL\right)\dot{v}_B + 2\rho A_t hp\dot{h} \\
&\quad + \rho A_t Lhr^2 + \rho\left\{A_t\left(2L_zH - H^2 - h^2\right) + L_zLA_p\right\}qr + \rho\left(2L_xH + L_xLA_p\right)pq \\
&\quad - \rho A_t Lhp^2 + \rho\left(2L_xA_tH + L_xLA_p\right)\dot{r} - \rho\left\{A_t\left(2L_zH - H^2 - h^2\right) + L_zLA_p\right\}\dot{p} \\
&\quad + \rho\left(2HA_t + LA_p\right)ru - \rho\left(2HA_t + LA_p\right)pw \\
-Z_s &= -2\rho A_t h\ddot{h} + \rho g\left(2A_tH + A_pL\right)\cos\theta\cos\phi + \rho\left(2A_tH + A_pL\right)\dot{w}_B + \rho A_t Lp\dot{h} \\
&\quad - \rho A_t Lhqr + \rho\left(2A_tL_xH + L_xLA_p\right)rp - \rho\left\{A_t\left(2L_zH - H^2 - h^2\right) + L_zLA_p\right\}p^2 \\
&\quad - \rho\left\{A_t\left(2L_zH - H^2 - h^2\right) + L_zLA_p\right\}q^2 - \rho\left(2HA_t + LA_p\right)qu + \rho\left(2HA_t + LA_p\right)pv \\
&\quad - 2\rho\left(L_xHA_t + L_xLA_p\right)\dot{q} + \rho LhA_t\dot{p}
\end{aligned}
\tag{2.14}
$$

2.1.3 Stimulator Moment

The moment generated by the motion of the fluid particle is

$$
-d\mathbf{M}_{st} = \mathbf{r}_p \times \mathbf{a}_p dm - \mathbf{r}_p \times \mathbf{g}dm \tag{2.15}
$$

Integrating Equation (2.15) along the streamline in the U-tube tank, the total stimulator moment is

$$
\mathbf{M}_{st} = K_s\mathbf{i} + L_S\mathbf{j} + M_s\mathbf{k},
$$

where

$$
\begin{aligned}
-K_s = &-\rho A_t LH\ddot{h} - \rho A_p L_z L\frac{A_t}{A_p}\ddot{h} - \rho A_t\left(\left(2L_Z H - H^2 - h^2\right)\dot{v} + Lhw\right) - \rho A_p L_z L\dot{v} \\
&- \rho A_t\left(\left(2L_Z H - H^2 - h^2\right)ru - \left(2L_Z H - H^2 - h^2\right)pw + Lhqu - Lhpv\right) \\
&- \rho A_p\left(L_z Lru - L_z Lpw\right) - 2\rho A_t\left(2L_Z h + 2Hh\right)p\dot{h} - \rho A_t L\left(L_Z h + Hh\right)r^2 \\
&- \frac{1}{3}\rho A_t L\left(2H^3 - 6L_z H^2 - 6L_z h^2 + 6L_z^2 H + 6Hh^2\right)qr - \rho A_t L_x\left(2L_Z H - H^2 - h^2\right)pq \\
&+ \rho A_t L\left(L_Z h - Hh\right)p^2 + \frac{1}{2}\rho A_t L^2 Hqr - \rho A_t L\left(L_Z h + Hh\right)q^2 \\
&+ \rho A_t LL_x hrp - \rho A_t L\left(L_Z h + Hh\right)p^2 + \rho A_p\left(-L_z^2 Lqr - L_z L_x Lpq + \frac{1}{12}L^3 qr\right) \\
&- \rho A_t L_x\left(2L_Z H - H^2 - h^2\right)\dot{r} + \frac{1}{3}\rho A_t\left(2H^3 - 6L_z H^2 - 6L_z h^2 + 6L_z^2 H + 6Hh^2\right)\dot{p} \\
&- \rho A_t\left(LL_x h\dot{q} - \frac{1}{2}L^2 H\dot{p}\right) + \rho A_p\left(-L_z L_x L\dot{r} + L_z^2 L\dot{p} + \frac{1}{12}L^3\dot{p}\right) \\
&- \rho g A_t\left(-\left(2L_Z H - H^2 - h^2\right)\cos\theta\sin\phi + Lh\cos\theta\cos\phi\right) - \rho g A_p\left(-L_z L\cos\theta\sin\phi\right)
\end{aligned}
$$

$$
\begin{aligned}
-L_s = &-\rho A_t 2L_x h\ddot{h} + \rho A_t\left(\left(2L_Z H - H^2 - h^2\right)\dot{u} - 2L_x H\dot{w}\right) + \rho A_p\left(L_z L\dot{u} - L_x L\dot{w}\right) \\
&+ \rho A_t\left(-\left(2L_Z H - H^2 - h^2\right)rv + \left(2L_Z H - H^2 - h^2\right)qw + 2L_x Hqu - 2L_x Hpv\right) \\
&+ \rho A_p\left(-L_z Lrv + L_z Lqw + L_x Lqu - L_x Lpv\right) + 2\rho A_t\left(-2L_Z h - 2Hh\right)q\dot{h} \\
&- 2\rho A_p\left(L_z L\frac{A_t}{A_p}r\dot{h} + L_x\frac{A_t}{A_p}Lp\dot{h}\right) - \frac{1}{2}\rho A_t L_x\left(2L_Z H - H^2 - h^2\right)r^2 \\
&+ \frac{1}{3}\rho A_t\left(L_L^3 + L_R^3\right)rp - \frac{1}{2}\rho A_t L_x\left(2L_Z H - H^2 - h^2\right)q^2 + \rho A_t L\left(L_Z h + Hh\right)pq \\
&- LL_x hqr + \frac{1}{2}\rho A_t L_x\left(2L_Z H - H^2 - h^2\right)q^2 - 2\rho A_t L_x^2 Hrp \\
&+ \frac{1}{2}\rho A_t L_x\left(2L_Z H - H^2 - h^2\right)p^2 + \rho A_p\left(-L_z L_x Lr^2 + L_z^2 Lrp - L_x^2 Lrp + L_z L_x Lp^2\right) \\
&- \rho A_t L\left(L_Z h + Hh\right)\dot{r} + \frac{1}{3} - \rho A_t\left(2H^3 - 6L_z H^2 - 6L_z h^2 + 6L_z^2 H + 6Hh^2\right)\dot{q} \\
&- \rho A_t\left(2L_x^2 H\dot{q} + LL_x h\dot{p}\right) + \rho A_p L\left(L_z^2\dot{q} + L_x^2\dot{q}\right) + \rho g A_t\left(2L_Z H - H^2 - h^2\right)\sin\theta \\
&+ 2\rho g A_t L_x H\cos\theta\cos\phi + \rho g A_p L\left(L_z\sin\theta + L_x\cos\theta\cos\phi\right)
\end{aligned}
$$

$$
\begin{aligned}
-M_s = {} & \rho A_p L_x L \frac{A_t}{A_p}\ddot{h} + \rho A_t\left(-Lh\dot{u} + 2L_x H\dot{v}\right) + \rho A_p L_x L\dot{v} \\
& + \rho A_t\left(Lhrv - \frac{1}{2}Lhqw + 2L_x Hru - 2L_x Hpw\right) \\
& + \rho A_p\left(L_x Lru - L_x Lpw\right) + 2\rho A_t\left(-LHq\dot{h} - 2L_x hp\dot{h}\right) \\
& - \rho A_t LL_x hr^2 + \rho A_t L(L_Z h + Hh)rp - \rho A_t LL_x hq^2 \\
& + \frac{1}{2}\rho A_t L^2 Hpq - \rho A_t LL_x hr^2 + \frac{1}{2}\rho A_t L_x\left(2L_Z H - H^2 - h^2\right)qr \\
& + 2\rho A_t L_x^2 Hpq - \rho A_t LL_x hp^2 + \rho A_p\left(\frac{1}{12}L^3 pq + L_z L_x Lqr + L_x^2 Lpq\right) \\
& + \rho A_t\left(\frac{1}{2}L^2 H\dot{r} + \frac{1}{4}L(L_Z h + Hh)\dot{q} + 2L_x^2 H\dot{r} - L_x\left(2L_Z H - H^2 - h^2\right)\dot{p}\right) \\
& + \rho A_p\left(\frac{1}{12}L^3\dot{r} + L_x^2 L\dot{r} - L_z L_x L\dot{p}\right) - \rho g A_t\left(Lh\sin\theta + 2L_x H\cos\theta\sin\phi\right) \\
& - \rho g A_p\left(L_x L\cos\theta\sin\phi\right)
\end{aligned}
\tag{2.16}
$$

2.2 Stimulator and Ship Roll Model

Fossen (1994) has derived dynamic equations of a ship motion in six-degree of freedom. One can combine Equations (2.14) and (2.16) with the ship dynamics model to analyze the stimulation effect on ship motion in six-degree of freedom. However, the ship motion in surge, sway, heave, pitch and yaw is usually small as compared to the ship roll motion. So the ship model is simplified to describe the ship roll motion only. Bhattacharyya (1978) described nonlinear ship roll motion with nonlinear damping and restoring force as

$$I\ddot{\phi} + B\left(\phi,\dot{\phi}\right) + C(\phi) = K_{ext}$$

For a small roll motion, it can be simplified to be a linear equation

$$I\ddot{\phi} + d_1\dot{\phi} + k_1\phi = K_{ext}, \tag{2.17}$$

where K_{ext} is the moment acting on the ship which includes environmental moment such as wave moment K_{wave}, and stimulator moment K_s.

$$K_{ext} = K_{wave} + K_s$$

After linearizing K_s shown in Equation (2.16) and substituting it into Equation (2.17) one has the linear ship model shown as

$$\left(I + \frac{1}{3}\rho A_t\left(2H^3 - 6L_zH^2 + 6L_z^2H\right) + \frac{1}{2}\rho A_tL^2H + \rho A_pL_z^2L + \rho A_p\frac{1}{12}L^3\right)\ddot{\phi}$$
$$-\left(\rho A_tLH + \rho A_tL_zL\right)\ddot{h} + d_1\dot{\phi} + \left(k_1 + \rho gA_t\left(2L_ZH - H^2\right) + \rho gA_pL_zL\right)\phi - \rho gA_tLh = K_{wave} \tag{2.18}$$

From Equations (2.12) and (2.18), one can derive a combined stimulator and ship roll model as

$$\mathbf{M}\ddot{\Theta} + \mathbf{B}\dot{\Theta} + \mathbf{K}\Theta = \mathbf{F}, \tag{2.19}$$

where

$$\mathbf{M} = \begin{bmatrix} \rho A_t\left(2H + \frac{A_t}{A_p}L\right)\frac{L^2}{4} & -\rho\frac{1}{2}L^2A_t\left(L_Z + H\right) \\ -\rho\frac{1}{2}L^2A_t\left(H + L_z\right) & \left(I + \frac{1}{3}\rho A_t\left(2H^3 - 6L_zH^2 + 6L_z^2H\right) + \frac{1}{2}\rho A_tL^2H + \rho A_pL_z^2L + \rho A_p\frac{1}{12}L^3\right) \end{bmatrix} = \begin{bmatrix} m_{hh} & m_{h\phi} \\ m_{\phi h} & m_{\phi\phi} \end{bmatrix}$$

$$\mathbf{B} = \begin{bmatrix} \frac{1}{2}bA_t^2(2H + L)L^2 & 0 \\ 0 & d_1 \end{bmatrix} = \begin{bmatrix} b_{hh} & 0 \\ 0 & b_{\phi\phi} \end{bmatrix}$$

$$\mathbf{K} = \begin{bmatrix} \frac{1}{2}\rho A_t g L^2 & -\frac{1}{2}\rho A_t g L^2 \\ -\frac{1}{2}\rho g A_t L^2 & \left(k_1 + \rho g A_t \left(2L_Z H - H^2\right) + \rho g A_p L_z L\right) \end{bmatrix} = \begin{bmatrix} k_{hh} & k_{h\phi} \\ k_{\phi h} & k_{\phi\phi} \end{bmatrix}$$

$$\Theta = \begin{bmatrix} \tau \\ \phi \end{bmatrix} \qquad \mathbf{F} = B_1 \Delta P + B_2 M_{wave} = \begin{bmatrix} -1 \\ 0 \end{bmatrix} \frac{1}{2} L A_t \Delta P + \begin{bmatrix} 0 \\ 1 \end{bmatrix} K_{wave}$$

$$\tau = \frac{h}{L/2}$$

Fluid motion in U-tube tank is driven by propeller. Generally, thrust forces of propeller depend on lift and drag forces, so thrust force is a function of propeller rotational speed and water motion in U-tube tank. Pump pressure depending on thrust forces can be considered as a pressure source when we used pressure feedback as internal loop as shown in Figure 2.2.

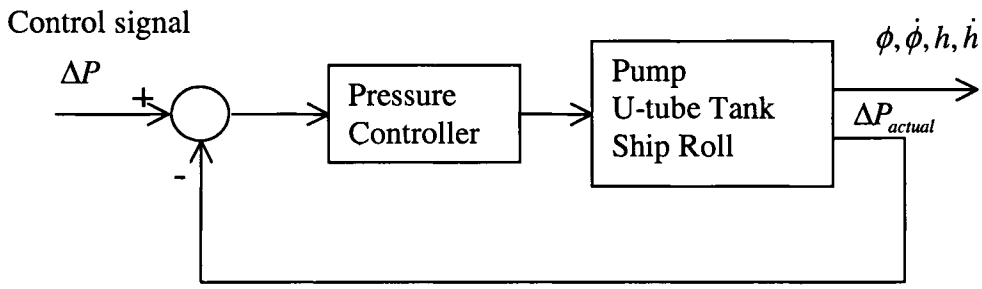

Figure 2.2 Block diagram of internal pressure loop control

2.3 Ship Roll Motion Due to Sinusoidal Stimulation

The stimulator and ship roll motion shown in Equation (2.19) can be written as

$$\begin{bmatrix} m_{hh} & m_{h\phi} \\ m_{\phi h} & m_{\phi\phi} \end{bmatrix}\begin{bmatrix} \ddot{\tau} \\ \ddot{\phi} \end{bmatrix}+\begin{bmatrix} b_{hh} & 0 \\ 0 & b_{\phi\phi} \end{bmatrix}\begin{bmatrix} \dot{\tau} \\ \dot{\phi} \end{bmatrix}+\begin{bmatrix} k_{hh} & k_{h\phi} \\ k_{\phi h} & k_{\phi\phi} \end{bmatrix}\begin{bmatrix} \dot{\tau} \\ \phi \end{bmatrix}=\begin{bmatrix} 1 & 0 \\ 0 & 1 \end{bmatrix}\begin{bmatrix} \frac{1}{2}LA_t\Delta P \\ K_{wave} \end{bmatrix} \tag{2.20}$$

When both wave moment input K_{wave} and pump pressure ΔP of the axial pump are sinusoidal functions, one has

$$\begin{aligned} K_{wave} &= K_0 e^{jw_e t+\phi_2} \\ \frac{1}{2}LA_t\Delta P &= P_0 e^{jw_e t+\phi_1} \end{aligned} \tag{2.21}$$

By substituting Equation (2.21) into Equation (2.20), the magnitude and phase shift of tank angle and ship roll angle become

$$\begin{aligned} \tau_0^2 &= \frac{A^2+C^2}{D_R^2+D_I^2} \\ \phi_h &= a\tan 2(C,A)-a\tan 2(D_I,D_R) \\ \phi_0^2 &= \frac{B^2+D^2}{D_R^2+D_I^2} \\ \phi_\phi &= a\tan 2(D,B)-a\tan 2(D_I,D_R) \end{aligned} \tag{2.22}$$

where

$$A=\frac{P_0}{k_{hh}}(1-q^2)\cos\phi_1-2q\frac{b_{\phi\phi}}{C_c}\frac{P_0}{k_{hh}}\mu\sin\phi_1-\frac{K_0}{k_{\phi\phi}}(f^2G_2-q^2G_1)\cos\phi_2$$

$$B=\frac{K_0}{k_{\phi\phi}}(f^2-q^2)\cos\phi_2-\frac{K_0}{k_{\phi\phi}}2q\frac{b_{hh}}{C_c}\sin\phi_2-\frac{P_0}{k_{hh}}\mu(f^2G_2-q^2G_1)\cos\phi_1$$

$$C=\frac{P_0}{k_{hh}}\left((1-q^2)\sin\phi_1+2q\frac{b_{\phi\phi}}{C_c}\mu\cos\phi_1\right)-\frac{K_0}{k_{\phi\phi}}(f^2G_2-q^2G_1)\sin\phi_2$$

$$D=\frac{K_0}{k_{\phi\phi}}\left((f^2-q^2)\sin\phi_2+2q\frac{b_{hh}}{C_c}\cos\phi_2\right)-\frac{P_0}{k_{hh}}\mu(f^2G_2-q^2G_1)\sin\phi_1$$

$$D_R = (f^2 - q^2)(1 - q^2) - 4q^2\mu\frac{b_{hh}}{C_c}\frac{b_{\phi\phi}}{C_c} - (f^2 G_2 - q^2 G_1)^2\mu$$

$$D_I = \left[(f^2 - q^2)2q\mu\frac{b_{\phi\phi}}{C_c} + (1 - q^2)2q\frac{b_{hh}}{C_c}\right]$$

$$\omega_t = \sqrt{\frac{k_{hh}}{m_{hh}}},\ \omega_s = \sqrt{\frac{k_{\phi\phi}}{m_{\phi\phi}}},\ \mu = \frac{m_{hh}}{m_{\phi\phi}}, f = \frac{\omega_t}{\omega_s},\ q = \frac{\omega_e}{\omega_s},\ C_c = 2m_{hh}\omega_s,$$

$$C_t = b_{hh},\ C_s = b_{\phi\phi},\ G_1 = \frac{m_{h\phi}}{m_{hh}},\ G_2 = \frac{k_{\phi h}}{k_{hh}}$$

First, we consider a single input of wave moment exciting on the ship with zero phase shift. In this case, U-tube tank acts as a passive damper. The magnitude of tank angle and ship roll angle become

$$\tau_0^2 = \frac{K_0^2}{k_{\phi\phi}^2(D_R^2 + D_I^2)}(f^2 G_2 - q^2 G_1)^2$$

$$\phi_0^2 = \frac{K_0^2}{k_{\phi\phi}^2(D_R^2 + D_I^2)}\left\{(f^2 - q^2)^2 + \left(2q\frac{b_{hh}}{C_c}\right)^2\right\} \tag{2.23}$$

The phase shift of tank angle and ship roll angle become

$$\phi_{h/w} = a\tan 2(-\sin\phi_2, -\cos\phi_2) - a\tan 2(D_I, D_R)$$

$$\phi_{\phi/w} = a\tan 2(2qb_{hh}\mu/C_c, f^2 - q^2) - a\tan 2(D_I, D_R) \tag{2.24}$$

The results are similar to those obtained from the single input single output model used by Gawad et. al. (2001). When the friction coefficient between the fluid and U-tube tank increases, the system behaves more like a one degree of freedom system.

Next, we consider a single input of pump pressure exciting on the ship with zero phase shift. The magnitude of tank angle and ship roll angle become

$$\tau_0^2 = \frac{P_0^2}{k_{hh}^2(D_R^2 + D_I^2)}\left\{(1 - q^2)^2 + \left(2q\frac{b_{\phi\phi}}{C_c}\mu\right)^2\right\}$$

$$\phi_0^2 = \frac{P_0^2}{k_{hh}^2\left(D_R^2 + D_I^2\right)}\left(f^2 G_2 - q^2 G_1\right)^2 \mu^2 \tag{2.25}$$

The phase shift of tank angle and ship roll angle become

$$\phi_{h/p} = a\tan 2\frac{2qb_{\phi\phi}\mu/C_c}{1-q^2} - a\tan 2(D_I, D_R)$$
$$\phi_{\phi/p} = a\tan 2(-\sin\phi_2, -\cos\phi_2) - a\tan 2(D_I, D_R) \tag{2.26}$$

From Equations (2.23) and (2.25), ratio of the magnitude of ship roll motion due to pump pressure and the magnitude of tank angle due to wave moment is μ.

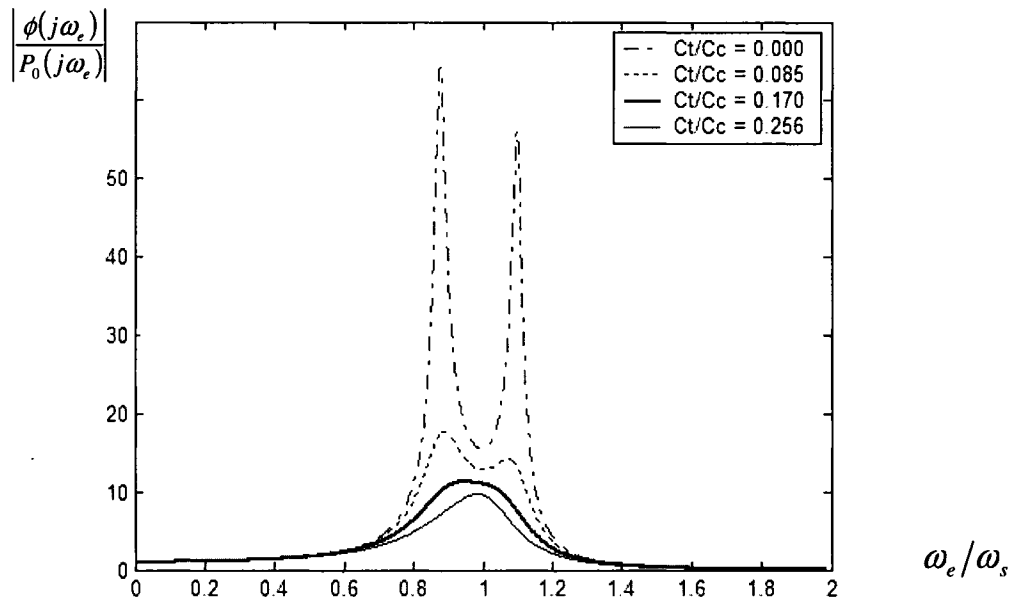

Figure 2.3 Normalized magnitude of ship roll angle due to pump pressure

Figures 2.2 and 2.3 show the magnitude and phase shift of ship roll angle due to pump pressure respectively. Figures 2.4 and 2.5 show the magnitude and phase shift of water height in U-tube tank due to pump pressure respectively. Both ship roll motion and U-tube tank water dynamics clearly show two degree of freedom at lower friction ratio.

At higher friction ratio, they become one degree of freedom. It is also noted that the higher water height is generated at lower friction coefficient.

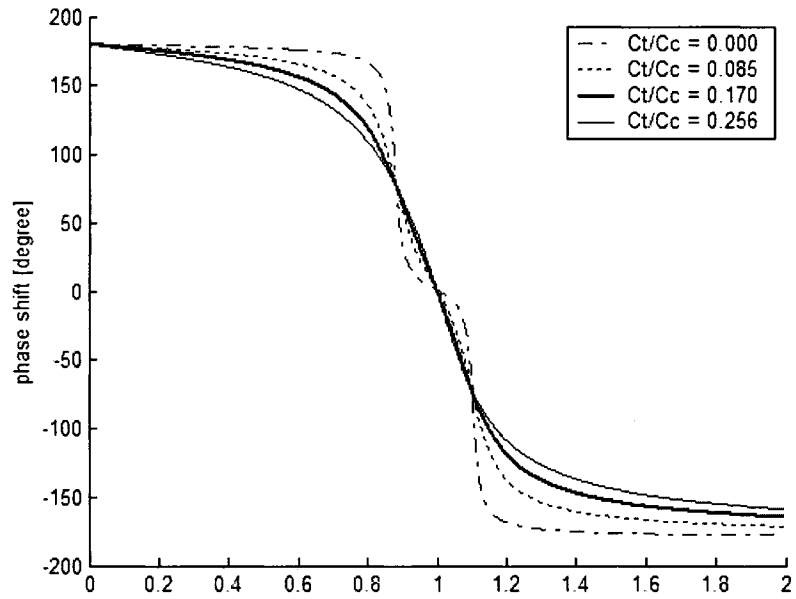

Figure 2.4 Phase angle of ship roll angle due to pump pressure

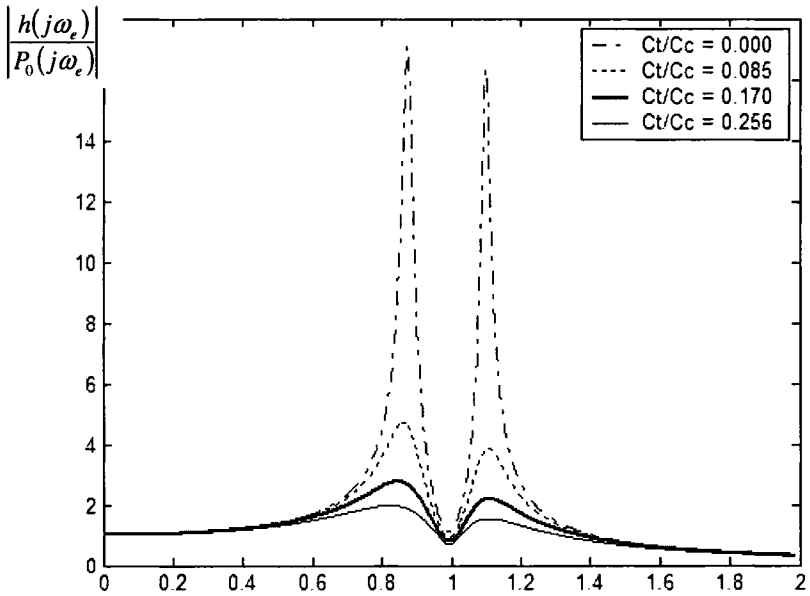

Figure 2.5 Normalized magnitude of water height due to pump pressure

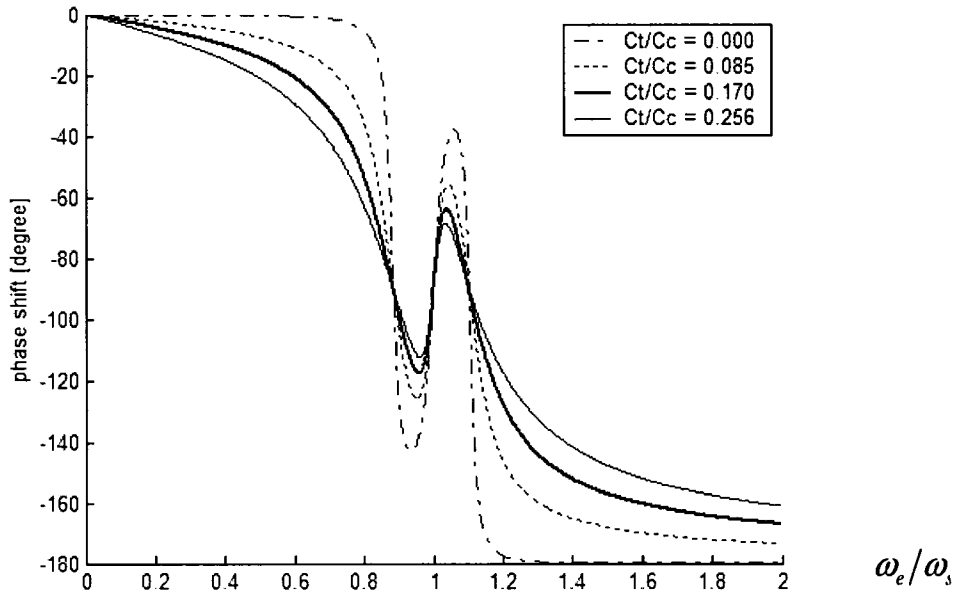

Figure 2.6 Phase angle of water height due to pump pressure

2.4 The Effect of Mass Ratio

At ship roll natural frequency, the effect of stimulator moment at different ratio of stimulator mass and ship roll inertia is considered. When ship has no motion, Figure 2.6 shows the stimulator moment per pump power as a function of the ratio of stimulator mass and ship roll inertia. From this figure the ratio of stimulator mass and ship roll inertia should be 0.02 to 0.04 for high ratio of stimulator moment and pump power. The lower ratio of stimulator mass and ship roll inertia the higher water level in the tank is required.

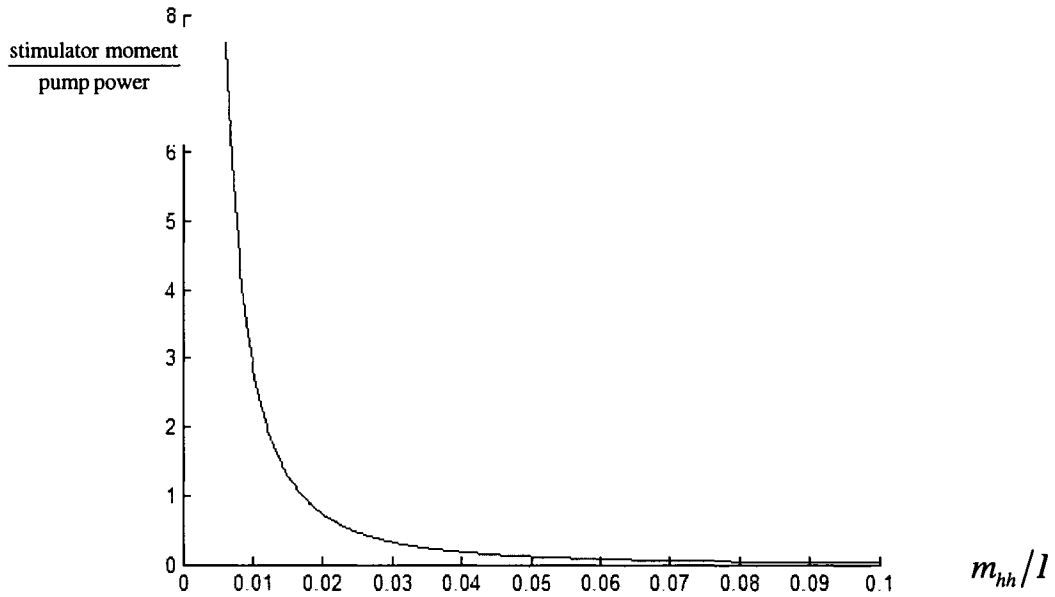

Fgure 2.7 Stimulator moment per pump power as a function of mass ratio of stimulator and ship inertia

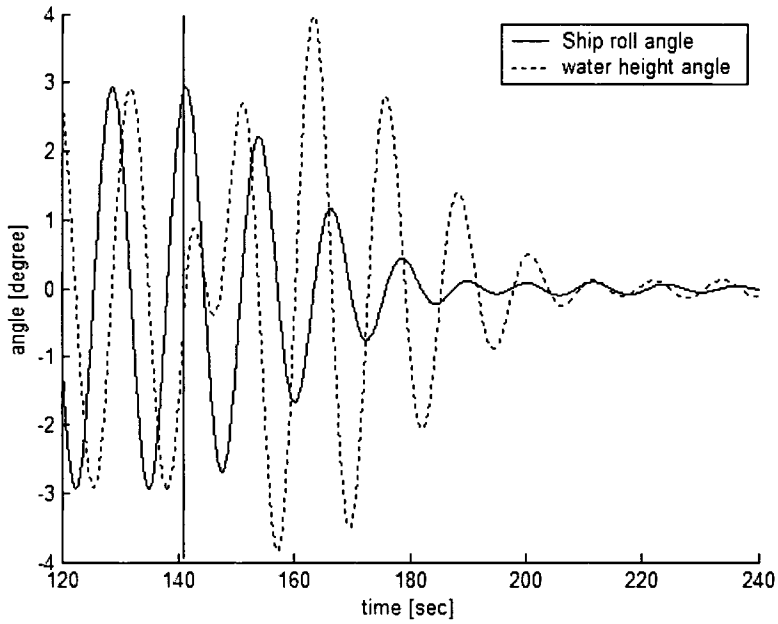

Figure 2.8 Time domain response of ship roll and tank angle (or water height) when the water pump is turned on at 0 sec. and then shut down at 141 sec.

2.5 Numerical Simulations

In this study, the numerical simulations of the coupling between ship roll motion and U-tube tank water dynamics are considered. As shown in Figure 2.7, the ship on still water starts rolling gradually by U-tube tank stimulator at the ship roll natural frequency. The water height level (or tank angle) shows a 90 degrees phase lead of the ship roll motion. That is, the moment produced by the stimulator is driving the ship's roll. At the time of shut down of the water pump (about 141 seconds), the water height drops in amplitude considerably and shifts in timing to be about 180 degrees out of phase with the roll). After the pump is stopped, water in the stimulator is moved by its inertial force and ship roll acceleration. So the tank angle amplitude becomes higher. However, the subsequent ship roll angles begin to diminish while the water height significantly increases. At this point, the ship roll angle is now leading the water height; that is, the ship's roll is now pumping the water. This energy transfer acts as an additional damping mechanism and substantially increases the natural damping characteristics of the ship. Within four or five cycles, the ship roll angle is reduced about ten times (from 3 to 0.3 degrees). Field experiments are performed and the results are similar to those shown in Figure 2.7. It is clear that U-tube tank can also be used as an effective passive damper for ship roll motion.

2.6 Conclusions

A nonlinear 6-DOF dynamic model of active tank is derived. The water motion in U-tube tank is assumed to have one-degree of freedom. This model is used to analyze the coupling between ship motion and active U-tube tank.

In order to generate effective ship roll motion, the designed U-tube stimulator should have the same natural frequency as the ship roll motion has. Otherwise, more pump power is required for pumping the water in the tank to generate the roll moment.

The ship roll motion due to sinusoidal stimulation is also derived. The friction in the tank has an effect on the ratio of bow pressure and wave moment. The lower friction

between fluid and U-tube tank is less pump pressure and higher reservoir tanks are required.

U-tube water tank can be used as an active stimulator or a passive damper for ship roll motion. It is also possible to use it as an active actuator for ship roll mitigation in high sea state environments.

CHAPTER 3

LINEAR SHIP ROLL CONTROL

Rolling is an undesirable motion for most vessels. Various active and passive systems may be used for a ship roll mitigation. Possible active systems include active flume tanks, gyroscopes, active fins, and rudders. Passive systems may consist of water tanks and bilge keels. Passive U-tube tank works well when its parameters equal to some specified values. For example, the natural fluid motion frequency in U-tube tank should be close to a ship roll natural frequency.

It has been shown that U-tube tank can be used as an active actuator for ship roll mitigation in high sea state environments. Yamagushi and Shinkai (1995) used model reference adaptive control for active U-tube tank. Chen et.al (2000) used sliding mode controller to reduce roll motion. In this study, four different control strategies are studied and compared. First the proportional and derivative (PD) control is used. U-tube tank water height and water velocity are feedback signals and the controller is tuned so that U-tube tank behaves as an optimal passive damper. The other three controllers considered are linear quadratic regulator (LQR), generalized predictive control (GPC), and deadbeat predictive control (DPC).

The GPC was introduced by Clarke et.al. (1987). GPC is a time domain method that uses a mathematical model to describe the input-output relationship of the system and to design the controller minimizing a desired cost function. Juang and Phan (1997a,b) developed a GPC by using the autoregressive with exogenous input (ARX) model to

describe input-output relationship and applied it to vibration control problems. Kvaternik et al. (2001) applied this GPC to improve aeroelastic stability in airplane.

When a ship is under loading/unloading, its moment of inertia and righting moment change. In this case, an adaptive control is needed. Chen et.al. (1992) and Juang (1994) derived a system identification algorithm which can identify a state-space model from input/output test data. Juang et.al. (1993) developed the Observer/Kalman Filter Identification (OKID) algorithm. In this study, we use OKID to update the parameters of linear ship roll model with U-tube tank. The updated parameters are then used for adaptive GPC and DPC design.

3.1 Linear Ship Roll Motion and U-tube Tank

Ship roll motion and U-tube tank in Equation (2.20) can be written as

$$\mathbf{M}\ddot{\Theta} + \mathbf{B}\dot{\Theta} + \mathbf{K}\Theta = \mathbf{F} \tag{3.1}$$

where $\mathbf{M} = \begin{bmatrix} m_{hh} & m_{h\phi} \\ m_{\phi h} & m_{\phi\phi} \end{bmatrix}$, $\mathbf{B} = \begin{bmatrix} b_{hh} & 0 \\ 0 & b_{\phi\phi} \end{bmatrix}$, $\mathbf{K} = \begin{bmatrix} k_{hh} & k_{h\phi} \\ k_{\phi h} & k_{\phi\phi} \end{bmatrix}$

$$\mathbf{F} = B_1 P + B_2 K_{wave} = \begin{bmatrix} 1 \\ 0 \end{bmatrix} \frac{1}{2} L A_t P + \begin{bmatrix} 0 \\ 1 \end{bmatrix} K_{wave}$$

$$m_{hh} = \rho A_t \left(2H + \frac{A_t}{A_p} L \right) \frac{L^2}{4}, \qquad m_{h\phi} = m_{\phi h} = -\rho \frac{1}{2} L^2 A_t (H + L_z)$$

$$m_{\phi\phi} = \left(I + \frac{1}{3} \rho A_t \left(2H^3 - 6L_z H^2 + 6L_z^2 H \right) + \frac{1}{2} \rho A_t L^2 H + \rho A_p L_z^2 L + \rho A_p \frac{1}{12} L^3 \right)$$

$$b_{hh} = \frac{1}{2} b A_t^2 (2H + L) L^2, \quad b_{\phi\phi} = d_1$$

$$k_{hh} = \frac{1}{2} \rho A_t g L^2, \quad k_{h\phi} = k_{\phi h} = -\frac{1}{2} \rho A_t g L^2, \quad k_{\phi\phi} = \left(k_1 + \rho g A_t \left(2L_Z H - H^2 \right) + \rho g A_p L_z L \right)$$

$$\Theta = \begin{bmatrix} \tau \\ \phi \end{bmatrix}, \ \tau = \frac{h}{L/2}.$$

Equation (3.1) can be written as

$$\begin{bmatrix} \dot{\Theta} \\ \ddot{\Theta} \end{bmatrix} = \begin{bmatrix} 0_{2\times 2} & I_{2\times 2} \\ -\mathbf{M}^{-1}\mathbf{K} & -\mathbf{M}^{-1}\mathbf{B} \end{bmatrix} \begin{bmatrix} \Theta \\ \dot{\Theta} \end{bmatrix} + \frac{1}{2} \begin{bmatrix} 0_{2\times 2} \\ \mathbf{M}^{-1} \end{bmatrix} \begin{bmatrix} LA_t P \\ 0 \end{bmatrix} + \begin{bmatrix} 0_{2\times 2} \\ \mathbf{M}^{-1} \end{bmatrix} \begin{bmatrix} 0 \\ K_{wave} \end{bmatrix} \tag{3.2}$$

$y = [0 \quad 1 \ \vdots \ 0 \quad 0] \begin{bmatrix} \Theta \\ \dot{\Theta} \end{bmatrix}$, when ship roll is the only measured variable.

$$\text{or} \quad \dot{\mathbf{x}} = \mathbf{A}_c\mathbf{x} + \mathbf{B}_c\mathbf{u} + \mathbf{B}_{dc}\mathbf{d} \tag{3.3}$$

$$\mathbf{y} = \mathbf{C}_c\mathbf{x} + \mathbf{D}_c\mathbf{u} + \mathbf{D}_{dc}\mathbf{d}.$$

It can be transformed to a discrete time model

$$\begin{aligned} \mathbf{x}(k+1) &= \mathbf{A}\mathbf{x}(k) + \mathbf{B}\mathbf{u}(k) + \mathbf{B}_d\mathbf{d}(k) \\ \mathbf{y}(k) &= \mathbf{C}\mathbf{x}(k) + \mathbf{D}\mathbf{u}(k) + \mathbf{D}_d\mathbf{d}(k) \end{aligned} \tag{3.4}$$

where $\mathbf{x}(k) \in \mathbf{R}^n$, $\mathbf{y}(k) \in \mathbf{R}^m$, $\mathbf{u}(k) \in \mathbf{R}^r$.

3.2 Passive U-tube Tank

For ship roll motion, the U-tube water tank can increase the ship roll damping by generating moment in opposite direction of wave moment to reduce its motion. Total moment acting on the ship roll motion becomes

$$\begin{aligned} & K_{wave} - k_{\phi h}\tau - m_{\phi h}\ddot{\tau} - (k_{\phi\phi} - k_1)\phi - (m_{\phi\phi} - I)\ddot{\phi} \\ &= K_{wave} + \frac{1}{2}\rho g A_t L^2 \tau + \rho \frac{1}{2} L^2 A_t (H + L_z)\ddot{\tau} - \left(\rho g A_t (2L_Z H - H^2) + \rho g A_p L_z L\right)\phi \\ & - \left(\frac{1}{3}\rho A_t (2H^3 - 6L_z H^2 + 6L_z^2 H) + \frac{1}{2}\rho A_t L^2 H + \rho A_p L_z^2 L + \frac{1}{12}\rho A_p L^3\right)\ddot{\phi}. \end{aligned}$$

The water tank moment generated by the passive U-tube tank has four components which include $\frac{1}{2}\rho g A_t L^2 \tau$ generated by the difference of the water weight of one side to the weight of the other, $\rho \frac{1}{2} L^2 A_t (H + L_z)\ddot{\tau}$ generated by water acceleration in U-tube tank, $-\left(\rho g A_t (2L_Z H - H^2) + \rho g A_p L_z L\right)\phi$ generated gravitational force due to ship roll, and $-\left(\frac{1}{3}\rho A_t (2H^3 - 6L_z H^2 + 6L_z^2 H) + \frac{1}{2}\rho A_t L^2 H + \rho A_p L_z^2 L + \frac{1}{12}\rho A_p L^3\right)\ddot{\phi}$ generated by ship roll acceleration.

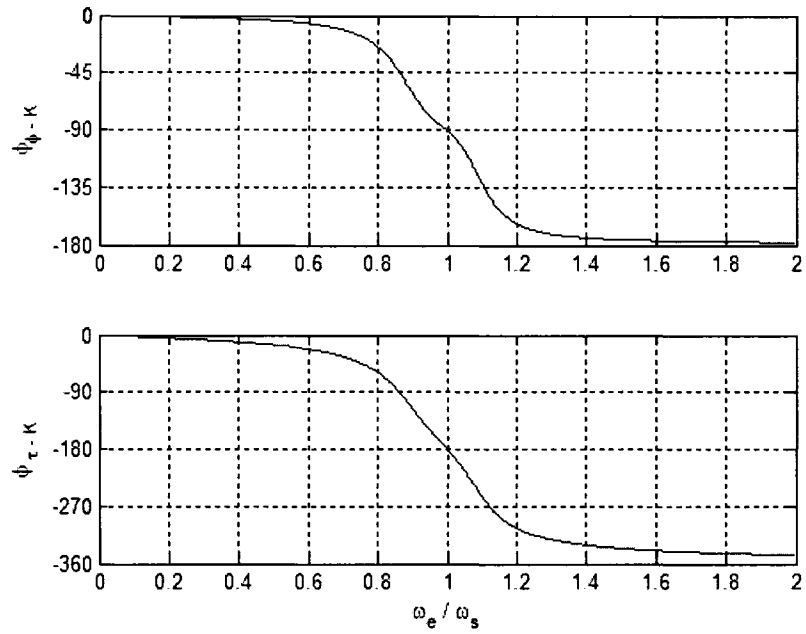

Figure 3.1 Upper graph: phase shift of ship roll angle with respect to wave moment. Lower graph: phase shift of water height with respect to wave moment.

Phase shift of ship roll angle and water height with respect to wave moment are shown in Figure 3.1. At low frequency, U-tube tank moment is generated by ship roll angle and water height. At the ship roll natural frequency, the ship roll angle has 90 degrees phase lag with respect to the wave moment and water height has 180 degrees

phase shift with respect to wave moment. U-tube tank moment is generated by water height and water height acceleration.

The water tank moment, $(1/2)\rho L^2 A_t L_z \ddot{\tau} - 2\rho g A_t L_Z H\phi - \rho g A_p L_z L\phi + 2\rho A_t L_z H^2 \ddot{\phi} - 2\rho A_t L_z^2 H\ddot{\phi} - \rho A_p L_z^2 L\ddot{\phi}$, generated by the passive U-tube tank depends on its level L_z in the ship. At the ship roll natural frequency, U-tube tank moment generated due to L_z is $\left(f^2 \mu \omega_{\phi\phi}^2 k_1 \tau / g\right) L_z$. The wave moment changes its direction if U-tube tank is placed above the ship center of gravity ($L_z < 0$). The effectiveness of this passive U-tube tank on the ship roll motions is greater when its location in the ship is higher. At low frequency, U-tube tank moment generated is $-\left(4f^2 \mu H \phi k_1 / L^2\right) L_Z - \left(2f^2 \mu A_p \phi k_1 / (LA_t)\right) L_Z$. The wave moment changes its direction if U-tube tank is placed below the ship center of gravity ($L_z > 0$). If U-tube tank is placed on a higher level, it is more effective as a damper, but it reduces the ship stability.

U-tube tank can be designed to minimize the maximum values of the amplitude of roll motion in the frequency domain by solving

$$\min_{\xi_2, f}\left(\max_{q \in R^+} \left| \frac{\phi_0}{\phi_{st}} \right| \right)$$

where $\frac{\phi_0^2}{\phi_{st}^2} = \frac{\phi_0^2}{K_0^2 / k_{\phi\phi}^2} = \frac{1}{\left(D_R^2 + D_I^2\right)} \left\{ \left(f^2 - q^2\right)^2 + \left(2qf\xi_{hh}\right)^2 \right\}$

$$D_R = \left(f^2 - q^2\right)\left(1 - q^2\right) - 4q^2 f \xi_{hh} \xi_{\phi\phi} - \left(f^2 - q^2 G_1\right)^2 \mu$$

$$D_I = \left[2\left(f^2 - q^2\right) q \xi_{\phi\phi} + 2\left(1 - q^2\right) qf \xi_{hh}\right]$$

$$\omega_t = \sqrt{\frac{k_{hh}}{m_{hh}}},\ \omega_s = \sqrt{\frac{k_{\phi\phi}}{m_{\phi\phi}}},\ \mu = \frac{m_{hh}}{m_{\phi\phi}},\ f = \frac{\omega_t}{\omega_s},\ q = \frac{\omega_e}{\omega_s},\ \xi_{hh} = \frac{b_{hh}}{2m_{hh}\omega_{hh}},$$

$$\xi_{\phi\phi} = \frac{b_{\phi\phi}}{2m_{\phi\phi}\omega_{\phi\phi}},\ G_1 = \frac{m_{h\phi}}{m_{hh}} = \frac{2(H+L_z)}{(2H+A_tL/A_p)}.$$

The adjustable parameters of U-tube tank are U-tube tank natural frequency and damping ratio of fluid motion in U-tube tank. Analytical method can be applied by following the procedure shown in Den Hartog (1988). However, a numerical method is used due to its simplicity. The result is shown in Figure 3.2. The optimal frequency ratio is close to one. The damping ratio of water motion in U-tube tank depends on the damping ratio of ship roll motion, $\xi_{\phi\phi}$ and mass ratio, μ. As compared to the damping ratio of water motion in U-tube tank, the optimal frequency ratio is more sensitive to changes of the mass ratio. Frequency response of ship roll with U-tube tank at optimal frequency ratio and varied damping ratio of water motion is shown in Figure 3.3, where $\phi_{st} = K_{wave}/k_{\phi\phi}$. Frequency response of ship roll with U-tube tank at optimal damping ratio and varied natural frequency ratio is shown in Figure 3.4. U-tube tank has the best performance when its natural frequency is close to the ship roll natural frequency.

3.3 Proportional and Derivative (PD) Controller

In this section, a simple PD controller is considered. U-tube tank water height h and the water height velocity $\dot{h}$ are the feedback signals. From the water height h, one can calculate the tank angle $\tau = h/(L/2)$. The PD control becomes

$$\Delta P = -k_1\tau - k_2\dot{\tau} \tag{3.5}$$

where k_1 and k_2 are the feedback gains. One can adjust the feedback gains so that U-tube tank has the optimal natural frequency and damping ratio shown in Figure 3.3. In this way, U-tube tank behaves as an optimal passive damper. In this study, we

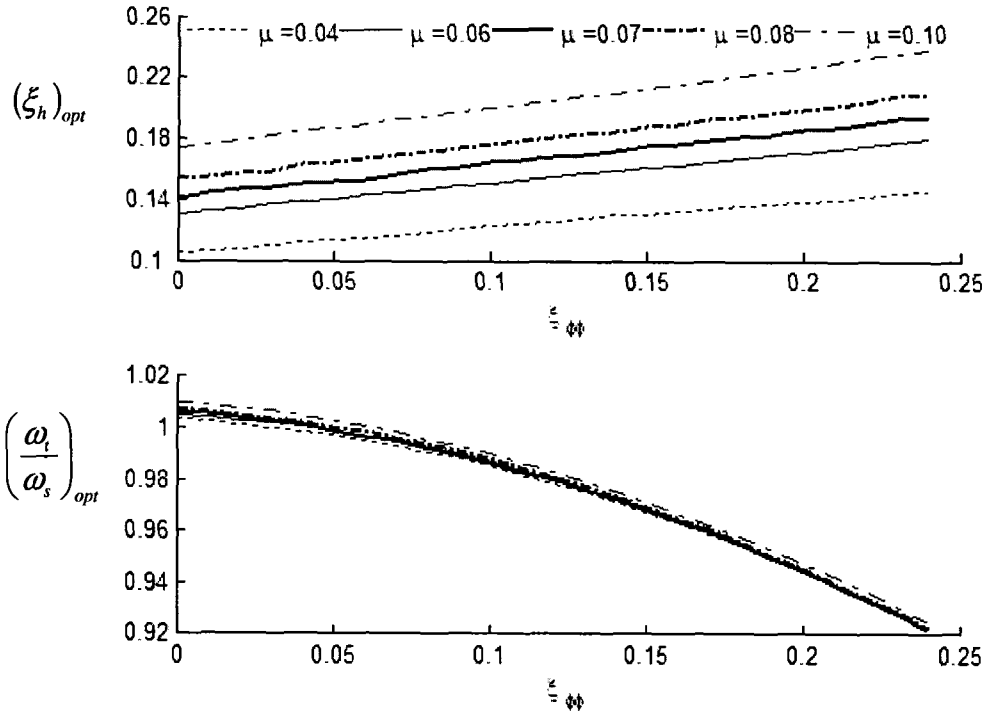

Figure 3.2 Optimal natural frequency ratio and damping ratio of water in U-tube tank

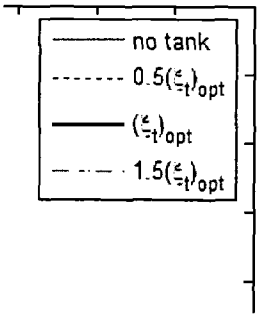

Figure 3.3 Ship roll angle at optimal frequency ratio with different value of water motion damping ratio.

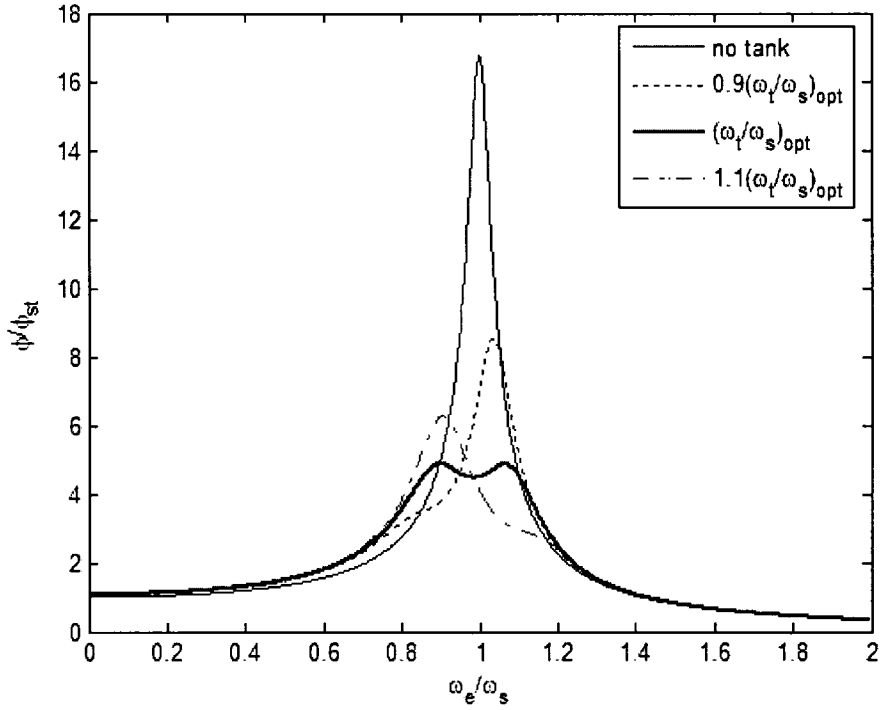

Figure 3.4 Ship roll angle at optimal value of water motion damping ratio with different value of natural frequency.

represent the optimal passive U-tube tank with PD controller because we use PD controller with U-tube tank to get the optimal U-tube tank.

3.4 Linear Quadratic Regulator (LQR)

In this section, we use full-states feedback LQR control. LQR finds the control signal $\mathbf{u}(k) = -\mathbf{K}\mathbf{x}(k)$ such that the quadratic cost function of system state and input

$$J = \sum_{k=0}^{\infty} \mathbf{x}^T(k)\mathbf{Q}\mathbf{x}(k) + \mathbf{u}^T(k)\mathbf{R}\mathbf{u}(k)$$

Define value function $V : \mathbf{R}^n \rightarrow \mathbf{R}$,

$$V = \min \sum_{k=0}^{\infty} \left(\mathbf{x}^T(k)\mathbf{Q}\mathbf{x}(k) + \mathbf{u}^T(k)\mathbf{R}\mathbf{u}(k) \right)$$

subjected to $\mathbf{x}(0)$ and $\mathbf{x}(k+1) = \mathbf{A}\mathbf{x}(k) + \mathbf{B}\mathbf{u}(k)$.

Hamilton-Jacobi equation

$$V(x_0) = \min\left(\mathbf{x}_0^T \mathbf{Q}\mathbf{x}_0 + w^T(k)\mathbf{R}w + V\left(A\mathbf{x}_0 + Bw\right) \right)$$

or

$$\mathbf{z}^{\mathrm{T}}\mathbf{P}z = \min\left(\mathbf{x}_0^T \mathbf{Q}\mathbf{x}_0 + \mathbf{w}^{\mathrm{T}}(\mathbf{k})\mathbf{R}\mathbf{w} + \left(\mathbf{A}\mathbf{x}_0 + \mathbf{B}\mathbf{w}\right)^{\mathrm{T}} \mathbf{P}\left(\mathbf{A}\mathbf{x}_0 + \mathbf{B}\mathbf{w}\right) \right)$$

minimizing w is $\mathbf{w}^* = -\left(\mathbf{R} + \mathbf{B}^{\mathrm{T}}\mathbf{P}\mathbf{B}\right)^{-1}\mathbf{B}^{\mathrm{T}}\mathbf{P}\mathbf{A}\mathbf{x}_0$

so Hamilton-Jacobi equation is

$$\begin{aligned} \mathbf{z}^{\mathrm{T}}\mathbf{P}\mathbf{z} &= \mathbf{x}_0^{\mathrm{T}}\mathbf{Q}\mathbf{x}_0 + \mathbf{w}^{*\mathrm{T}}(\mathbf{k})\mathbf{R}\mathbf{w}^* + \left(\mathbf{A}\mathbf{x}_0 + \mathbf{B}\mathbf{w}^*\right)^{\mathrm{T}}\mathbf{P}\left(\mathbf{A}\mathbf{x}_0 + \mathbf{B}\mathbf{w}^*\right) \\ &= \mathbf{x}_0^T\left(\mathbf{Q} + \mathbf{A}^{\mathrm{T}}\mathbf{P}\mathbf{A} - \mathbf{A}^{\mathrm{T}}\mathbf{P}\mathbf{B}\left(\mathbf{R} + \mathbf{B}^{\mathrm{T}}\mathbf{P}\mathbf{B}\right)^{-1}\mathbf{B}^{\mathrm{T}}\mathbf{P}\mathbf{A}\right)\mathbf{x}_0 \end{aligned}$$

This equation must be hold for all $\mathbf{x}_0$, so we can conclude that P satisfies the algebraic Ricatti's Equation

$$\mathbf{P} = \mathbf{Q} + \mathbf{A}^{\mathrm{T}}\mathbf{P}\mathbf{A} - \mathbf{A}^{\mathrm{T}}\mathbf{P}\mathbf{B}\left(\mathbf{R} + \mathbf{B}^{\mathrm{T}}\mathbf{P}\mathbf{B}\right)^{-1}\mathbf{B}^{\mathrm{T}}\mathbf{P}\mathbf{A},$$

and the optimal input constant gain vector is

$$K = -\left(R + B^T PB\right)^{-1} B^T PA$$

and $\mathbf{R}$, P are symmetric positive definite, $\mathbf{Q}$ is symmetric positive semi-definite.

3.5 Generalized Predictive Control (GPC)

Juang and Phan (1997a, b) developed a GPC algorithm by using autoregressive with exogenous input (ARX) model as a simple model represents the input-output relationship. It can be used to form a multi-step output prediction equation over a finite

prediction horizon while subject to controls imposed over a finite control horizon. The control to be imposed at the next time step is determined by minimizing the deviation of the predicted controlled plant outputs from the desired outputs, subject to a penalty on control effort.

Ship roll motion and U-tube tank can be represented by p^{th}-order of ARX model

$$\begin{aligned}\mathbf{y}(k) &= \boldsymbol{\alpha}_1\mathbf{y}(k-1)+\boldsymbol{\alpha}_2\mathbf{y}(k-2)+\cdots+\boldsymbol{\alpha}_p\mathbf{y}(k-p)\\ &\quad+\boldsymbol{\beta}_0\mathbf{u}(k)+\boldsymbol{\beta}_1\mathbf{u}(k-1)+\boldsymbol{\beta}_2\mathbf{u}(k-2)+\cdots+\boldsymbol{\beta}_p\mathbf{u}(k-p)\end{aligned} \tag{3.6}$$

where order of ARX model $p \geq \dfrac{\text{number of system order (n)}}{\text{number of system outputs (m)}}$.

From Equation (3.6), system output can be written in multi-step output prediction as

$$\mathbf{y}_{h_p}(k) = \boldsymbol{\tau}_c\mathbf{u}_{h_c}(k)+\mathbf{B}\mathbf{u}_p(k-p)+\mathbf{A}\mathbf{y}_p(k-p) \tag{3.7}$$

where

$$\mathbf{y}_{h_p}(k) = \begin{bmatrix}\mathbf{y}(k) & \mathbf{y}(k+1) & \cdots & \mathbf{y}(k+h_c-1) & \mathbf{y}(k+h_c) & \cdots & \mathbf{y}(k+h_p-1)\end{bmatrix}^T$$

$$\mathbf{y}_p(k-p) = \begin{bmatrix}\mathbf{y}(k-1) & \mathbf{y}(k-2) & \cdots & \mathbf{y}(k-p+1) & \mathbf{y}(k-p)\end{bmatrix}^T$$

$$\mathbf{u}_{h_c}(k) = \begin{bmatrix}\mathbf{u}(k) & \mathbf{u}(k+1) & \cdots & \mathbf{u}(k+h_c-1)\end{bmatrix}^T$$

$$\mathbf{u}_p(k-p) = \begin{bmatrix}\mathbf{u}(k-1) & \mathbf{u}(k-2) & \cdots & \mathbf{u}(k-p+1) & \mathbf{u}(k-p)\end{bmatrix}^T$$

$$\mathbf{A} = \begin{bmatrix} \boldsymbol{\alpha}_1 & \boldsymbol{\alpha}_2 & \cdots & \boldsymbol{\alpha}_{p-1} & \boldsymbol{\alpha}_p \\ \boldsymbol{\alpha}_1^{(1)} & \boldsymbol{\alpha}_2^{(1)} & \cdots & \boldsymbol{\alpha}_{p-1}^{(1)} & \boldsymbol{\alpha}_p^{(1)} \\ \vdots & \vdots & \cdots & \vdots & \vdots \\ \boldsymbol{\alpha}_1^{(h_c-1)} & \boldsymbol{\alpha}_2^{(h_c-1)} & \cdots & \boldsymbol{\alpha}_{p-1}^{(h_c-1)} & \boldsymbol{\alpha}_p^{(h_c-1)} \\ \boldsymbol{\alpha}_1^{(h_c)} & \boldsymbol{\alpha}_2^{(h_c)} & \cdots & \boldsymbol{\alpha}_{p-1}^{(h_c)} & \boldsymbol{\alpha}_p^{(h_c)} \\ \vdots & \vdots & \vdots & \vdots & \vdots \\ \boldsymbol{\alpha}_1^{(h_p-1)} & \boldsymbol{\alpha}_2^{(h_p-1)} & \cdots & \boldsymbol{\alpha}_{p-1}^{(h_p-1)} & \boldsymbol{\alpha}_p^{(h_p-1)} \end{bmatrix}, \quad \mathbf{B} = \begin{bmatrix} \boldsymbol{\beta}_1 & \boldsymbol{\beta}_2 & \cdots & \boldsymbol{\beta}_{p-1} & \boldsymbol{\beta}_p \\ \boldsymbol{\beta}_1^{(1)} & \boldsymbol{\beta}_2^{(1)} & \cdots & \boldsymbol{\beta}_{p-1}^{(1)} & \boldsymbol{\beta}_p^{(1)} \\ \vdots & \vdots & \cdots & \vdots & \vdots \\ \boldsymbol{\beta}_1^{(h_c-1)} & \boldsymbol{\beta}_2^{(h_c-1)} & \cdots & \boldsymbol{\beta}_{p-1}^{(h_c-1)} & \boldsymbol{\beta}_p^{(h_c-1)} \\ \boldsymbol{\beta}_1^{(h_c)} & \boldsymbol{\beta}_2^{(h_c)} & \cdots & \boldsymbol{\beta}_{p-1}^{(h_c)} & \boldsymbol{\beta}_p^{(h_c)} \\ \vdots & \vdots & \vdots & \vdots & \vdots \\ \boldsymbol{\beta}_1^{(h_p-1)} & \boldsymbol{\beta}_2^{(h_p-1)} & \cdots & \boldsymbol{\beta}_{p-1}^{(h_p-1)} & \boldsymbol{\beta}_p^{(h_p-1)} \end{bmatrix},$$

$$\boldsymbol{\tau}_c = \begin{bmatrix} \boldsymbol{\beta}_0 & 0 & \cdots & 0 \\ \boldsymbol{\beta}_0^{(1)} & \boldsymbol{\beta}_0 & \cdots & 0 \\ \vdots & \vdots & \ddots & \vdots \\ \boldsymbol{\beta}_0^{(h_c-1)} & \boldsymbol{\beta}_0^{(h_c-2)} & \cdots & \boldsymbol{\beta}_0 \\ \boldsymbol{\beta}_0^{(h_c)} & \boldsymbol{\beta}_0^{(h_c-1)} & \cdots & \boldsymbol{\beta}_0^{(1)} \\ \vdots & \vdots & \cdots & \vdots \\ \boldsymbol{\beta}_0^{(h_p-1)} & \boldsymbol{\beta}_0^{(h_p-2)} & \cdots & \boldsymbol{\beta}_0^{(h_p-h_c)} \end{bmatrix}$$

$$\boldsymbol{\beta}_0^{(q)} = \boldsymbol{\beta}_1^{(q-1)} + \boldsymbol{\alpha}_1^{(q-1)}\boldsymbol{\beta}_0, \qquad \boldsymbol{\alpha}_{l-1}^{(q)} = \boldsymbol{\alpha}_l^{(q-1)} + \boldsymbol{\alpha}_1^{(q-1)}\boldsymbol{\alpha}_{l-1}$$

$$\boldsymbol{\beta}_{l-1}^{(q)} = \boldsymbol{\beta}_l^{(q-1)} + \boldsymbol{\alpha}_1^{(q-1)}\boldsymbol{\beta}_{l-1}. \; l = 1,2,3,\ldots p, \text{ and } q = 1,2,3,\ldots,h_p - 1.$$

The predictive control law is obtained by minimizing the deviation of the predicted controlled response, $\mathbf{y}_{h_p}$, from the specified target response, $\mathbf{y}_T$, over a prediction horizon h_p. Let $\boldsymbol{\varepsilon} = \mathbf{y}_T - \mathbf{y}_{h_p}$, and the cost function to be minimized is

$$J = \boldsymbol{\varepsilon}^T \mathbf{R}\boldsymbol{\varepsilon} + \mathbf{u}_{h_c}^T \mathbf{Q}\mathbf{u}_{h_c} \tag{3.8}$$

Two weighting matrices are included in the cost function: **Q** (symmetric and positive definite) is the weighting matrix for the control effort, and **R** (symmetric and positive semi-definite) is the weighting matrix for the relative differences between the target and predicted response. For simple selection of weighting, we choose the weighting matrices **Q** and **R** to be diagonal matrices. Minimizing J by choosing $\mathbf{u}_{h_c}(k)$ gives

$$\mathbf{u}_{h_c}(k) = -\left(\boldsymbol{\tau}_c{}^{+}\mathbf{R}\boldsymbol{\tau} + \mathbf{Q}\right)^{+} \boldsymbol{\tau}_c{}^{T}\mathbf{R}\left(-\mathbf{y}_T(k) + \mathbf{B}\mathbf{u}_p(k-p) + \mathbf{A}\mathbf{y}_p(k-p)\right)$$

as the control sequence to be applied to the system over next h_c time steps. However, only the first r values are applied to the r control inputs and the remainders are discarded. So

$$\mathbf{u}(k) = \text{the first } r^{th} \text{rows } \left[-\left(\boldsymbol{\tau}_c{}^{+}\mathbf{R}\boldsymbol{\tau} + \mathbf{Q}\right)^{+} \boldsymbol{\tau}_c{}^{T}\mathbf{R}\left(-\mathbf{y}_T(k) + \mathbf{B}\mathbf{u}_p(k-p) + \mathbf{A}\mathbf{y}_p(k-p)\right)\right] \tag{3.9}$$

Then the control sequence is updated at the next time step. The GPC has a limit

$$h_p \geq p, \quad h_p \geq h_c$$

The lower value of control horizon, h_c, is chosen the more control effort is used.

3.6 Deadbeat Predictive Control (DPC)

For deadbeat predictive control, the system outputs in Equation (3.7) from time step $k+h_c+1$ to $k+h_p$ are set to zero and matrices $\boldsymbol{\tau}_c$, **B**, and **A** are considered only from row $(h_c+1)m$ to $h_p m$ for deriving the control signal.

3.7 Adaptive Predictive Control

When a ship is under loading or unloading, its dynamics changes. In this case, system identification is needed to update the ship dynamics for the control design.

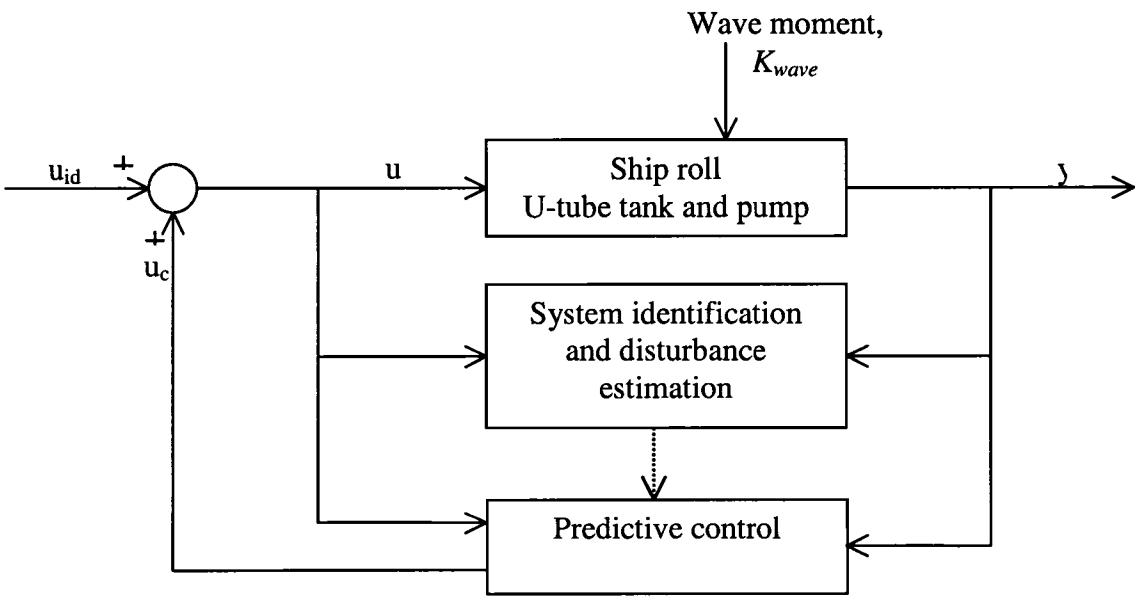

Figure 3.5 Block diagram of predictive control with system identification.

The structure of adaptive GPC or DPC is shown in Figure 3.5. The controller includes system identification and GPC or DPC. System identification provides updated system parameters for GPC or DPC controller design. When system identification is performed, the random input signal u_{id} is added to control signal u_c. So, the full spectrum of ship dynamics is stimulated. In this application, it is difficult to put a random input signal to drive the water pump. So, the pulse input with random amplitude is applied as the stimulation input for system identification.

From Equation (3.4), one has

$$\begin{aligned} \mathbf{x}(k+1) &= \mathbf{A}\mathbf{x}(k) + \mathbf{B}\mathbf{u}(k) + \mathbf{B}_d\mathbf{d}(k) + \mathbf{G}\mathbf{y}(k) - \mathbf{G}\mathbf{y}(k) \\ &= (\mathbf{A}+\mathbf{G}\mathbf{C})\mathbf{x}(k) + (\mathbf{B}+\mathbf{G}\mathbf{D})\mathbf{u}(k) - \mathbf{G}\mathbf{y}(k) \\ &= \overline{\mathbf{A}}\mathbf{x}(k) + \overline{\mathbf{B}}\mathbf{v}(k) + \mathbf{B}_d\mathbf{d}(k) \\ \mathbf{y}(k) &= \mathbf{C}\mathbf{x}(k) + \mathbf{D}\mathbf{u}(k) + \mathbf{D}_d\mathbf{d}(k) \end{aligned} \tag{3.10}$$

where $\overline{\mathbf{A}} = \mathbf{A}+\mathbf{G}\mathbf{C}$, $\overline{\mathbf{B}} = [\mathbf{B}+\mathbf{G}\mathbf{D} \quad -\mathbf{G}]$, $\mathbf{v}(\mathbf{k}) = \begin{bmatrix} \mathbf{u}(\mathbf{k}) \\ \mathbf{y}(\mathbf{k}) \end{bmatrix}$.

The matrix $\mathbf{G}$ is an $n \times m$ arbitrary matrix chosen to make the eigenvalues of $\overline{\mathbf{A}}$ to any desired values. This ensures that $\mathbf{C}\overline{\mathbf{A}}^k\overline{\mathbf{B}} = 0$ for $k \geq p$.

The system output at time step k can be written in term of past input, output, disturbance, and initial state as

$$\mathbf{y}(k) = \mathbf{C}\overline{\mathbf{A}}^k\mathbf{x}(0) + \sum_{i=0}^{k-1}\mathbf{C}\overline{\mathbf{A}}^{k-1-i}\overline{\mathbf{B}}\mathbf{v}(i) + \sum_{i=0}^{k-1}\mathbf{C}\overline{\mathbf{A}}^{k-1-i}\mathbf{B}_d\mathbf{d}(i) + \mathbf{D}_d\mathbf{d}(k) + \mathbf{D}\mathbf{u}(k) \tag{3.11}$$

or $$\mathbf{y}(k) = \mathbf{C}\overline{\mathbf{A}}^k\mathbf{x}(0) + \sum_{i=0}^{k-1}\mathbf{C}\overline{\mathbf{A}}^{k-1-i}\overline{\mathbf{B}}\mathbf{v}(i) + \mathbf{D}\mathbf{u}(k) + \eta(k)$$

where $\eta(k) = \sum_{i=0}^{k-1}\mathbf{C}\overline{\mathbf{A}}^{k-1-i}\mathbf{B}_d\mathbf{d}(i) + \mathbf{B}_d\mathbf{d}(k)$.

Goodzeit and Phan (2000) showed that disturbance input could be represented by some basis function such as sine and cosine function, polynomial function or exponential function. In our problem, the disturbance is assumed to be regular beam seas and can be represented by sine and cosine basis function. Based on linear system property, the output signal at steady state is also sinusoidal with a different magnitude and phase shift due to the sinusoidal nature of the disturbance (i.e. wave moment) with frequency ω_i

$$\eta_i(k\Delta t) = (\dot{\eta}_i(0)/\omega_i)\sin(k\omega_i\Delta t) + \eta_i(0)\cos(k\omega_i\Delta t)$$

or $\eta_i(k) = \alpha_i^d \sin(k\omega_i - p) + \beta_i^d \cos(k\omega_i - p)$, when Δt is omitted.

When there are L different wave frequencies encountered with a ship, Equation (3.11) becomes

$$\mathbf{y}(k) = \mathbf{C}\overline{\mathbf{A}}^k\mathbf{x}(0) + \sum_{i=0}^{k-1}\mathbf{C}\overline{\mathbf{A}}^{k-1-i}\overline{\mathbf{B}}\mathbf{v}(i) + \mathbf{D}\mathbf{u}(k) + \sum_{i=1}^{L}\begin{bmatrix}\alpha_i^d & \beta_i^d\end{bmatrix}\psi_i(k-p)$$

where $\psi_i(k) = \begin{bmatrix}\sin\omega_i k \\ \cos\omega_i k\end{bmatrix}$.

For $k = p, p+1, p+2, \ldots, l-1$, it can be written in the matrix form

$$\overline{\mathbf{y}} = init + \overline{\mathbf{Y}}\overline{\mathbf{V}} + \overline{\mathbf{Y}}^d\psi \qquad (3.12)$$

where $\overline{\mathbf{y}} = [\mathbf{y}(p) \quad \mathbf{y}(p+1) \quad \cdots \quad \mathbf{y}(l-1)]$

$$init = \left[\mathbf{C}\overline{\mathbf{A}}^p\mathbf{X}(0) \;\; \mathbf{C}\overline{\mathbf{A}}^{p+1}\mathbf{X}(0) \;\cdots\; \mathbf{C}\overline{\mathbf{A}}^{l-p-1}\mathbf{X}(0)\right]$$

$$\overline{\mathbf{Y}} = [\mathbf{D} \;\; \mathbf{C}\overline{\mathbf{B}} \;\; \mathbf{C}\overline{\mathbf{A}}\overline{\mathbf{B}} \;\cdots\; \mathbf{C}\overline{\mathbf{A}}^{(p-1)}\overline{\mathbf{B}}]$$

$$\overline{\mathbf{Y}}^d = [\begin{bmatrix}\alpha_1^d & \beta_1^d\end{bmatrix} \begin{bmatrix}\alpha_2^d & \beta_2^d\end{bmatrix} \begin{bmatrix}\alpha_3^d & \beta_3^d\end{bmatrix} \cdots \begin{bmatrix}\alpha_L^d & \beta_L^d\end{bmatrix}]$$

$$\overline{\mathbf{V}}=\begin{bmatrix} \mathbf{u}(p) & \mathbf{u}(p+1) & \cdots & \mathbf{u}(l-1) \\ \mathbf{v}(p-1) & \mathbf{v}(p) & \cdots & \mathbf{v}(p-2) \\ \mathbf{v}(p-2) & \mathbf{v}(p-1) & \cdots & \mathbf{v}(p-3) \\ \vdots & \vdots & \vdots & \vdots \\ \mathbf{v}(0) & \mathbf{v}(1) & \cdots & \mathbf{v}(l-p-1) \end{bmatrix}, \psi=\begin{bmatrix} \psi_1(0) & \psi_1(1) & \cdots & \psi_1(l-p-1) \\ \psi_2(0) & \psi_2(1) & \cdots & \psi_2(l-p-1) \\ \psi_3(0) & \psi_3(1) & \cdots & \psi_3(l-p-1) \\ \vdots & \vdots & \vdots & \vdots \\ \psi_L(0) & \psi_L(1) & \cdots & \psi_L(l-p-1) \end{bmatrix}$$

where $\mathbf{D}, \mathbf{C}\overline{\mathbf{B}}, \mathbf{C}\overline{\mathbf{A}}\overline{\mathbf{B}}, \cdots, \mathbf{C}\overline{\mathbf{A}}^{(p-1)}\overline{\mathbf{B}}$ are called observer Markov parameters.

The first term in Equation (3.12) represents the effect of the preceding *p-1* time steps due to initial states. When $\overline{\mathbf{A}}^{p}$ is sufficiently small and all the states in **x** are bounded, Equation (3.12) can be approximated by neglecting the first term on the right-hand side,

$$\underset{m\times l}{\overline{\mathbf{y}}} = \underset{m\times[(m+r)p+r]}{\overline{\mathbf{Y}}} \overset{[(m+r)p+r]\times l}{\overline{\mathbf{V}}} + \overline{\mathbf{Y}}^{d}\psi . \tag{3.13}$$

From observer Markov parameters $\overline{\mathbf{Y}}$, one can realize the system parameters **[A,B,C,D]** by using eigenvalues realization. If the disturbance does not exist, Equation (3.13) becomes Equation (3.6).

3.8 Numerical Simulations

In order to study the effect of the ship roll mitigation by using different controllers, numerical simulations are performed. Ship parameters used in the simulation include ship linear damping $d_1 = 4.87\times10^{8}\ \mathrm{N\cdot m\cdot s\cdot rad^{-1}}$, ship moment of inertia $I = 1.9275\times10^{9}\ \mathrm{kg\text{-}m^2}$, and ship roll natural frequency $\omega_s = 0.5\ rad/\sec$. U-tube tank parameters are $A_p = 6.22\ \mathrm{m^2}$, $\mathrm{L} = 17.1\ \mathrm{m}$, $\mathrm{H} = 4.88\ \mathrm{m}$, $\mathrm{L_z} = 1.83\ \mathrm{m}$, and $\mathrm{A_t} = 17.11\ \mathrm{m^2}$.

Figure 3.6 shows frequency responses of ship roll mitigation by using active U-tube tank with PD, LQR, GPC, and DPC. For LQR, the state weighting matrix $\mathbf{R} = 10^{14} \times \mathbf{I}_4$ and control effort weighting matrix $\mathbf{Q} = 1$. For ship roll angle and water height feedback, GPC has the deviation of predicted response weighting matrix

$$\mathbf{R} = 10^{14} \begin{bmatrix} 0 & & \\ & 1 & 0 \\ & \ddots & \\ & 0 & 0 \\ & & 1 \end{bmatrix}_{2hc \times 2hc} \quad \text{and } \mathbf{Q} = 1.$$

For predictive control, GPC and DPC have control horizon $h_c = 25$. For ship roll angle feedback, GPC has deviation of predicted response weighting matrix $\mathbf{R} = 10^{14}\mathbf{I}_{hc \times hc}$, and control effort weighting matrix $\mathbf{Q} = 1$. Both GPC and DPC have control horizon $h_c = 50$.

From controller design, for ship roll feedback and $h_c = 50$, we will have DPC as

$$\begin{aligned} u(k) = & -1.5996\times10^{-1}\ u(k\text{-}1) + 1.6676u(k\text{-}2) - 5.3846e\times10^{-2}\ u(k\text{-}3) - 1.7555u(k\text{-}4) \\ & - 4.9422\times10^{9}\ \phi(k\text{-}1) + 1.4438\times10^{10}\ \phi(k\text{-}2) - 1.4101\times10^{10}\ \phi(k\text{-}3) + 4.6059\times10^{9}\ \phi(k\text{-}4) \end{aligned}$$

, for ship roll feedback and $h_c = 50$, we will have GPC as

$$\begin{aligned} u(k) = & -2.2029\times10^{-1}\ u(k\text{-}1) + 2.2026u(k\text{-}2) + 8.2552e\times10^{-2}\ u(k\text{-}3) - 2.1745u(k\text{-}4) \\ & - 6.5885\times10^{9}\ \phi(k\text{-}1) + 1.8736\times10^{10}\ \phi(k\text{-}2) - 1.7859\times10^{10}\ \phi(k\text{-}3) + 5.7052\times10^{9}\ \phi(k\text{-}4) \end{aligned}$$

, for ship roll and water height feedback and $h_c = 25$, we will have DPC as

$$\begin{aligned} u(k) = & -5.3668\times10^{-1}\ u(k\text{-}1) - 2.9047e\times10^{-2}\ u(k\text{-}2) \\ & - 6.6394\times10^{6}\ h(k\text{-}1) + 4.0560\times10^{6}\ h(k\text{-}2) \\ & - 4.7209\times10^{8}\ \phi(k\text{-}1) + 4.7456\times10^{8}\ \phi(k\text{-}2) \end{aligned}$$

, for ship roll and water height feedback and $h_c = 25$, we will have GPC as

$$u(k) = -1.8500\times10^{-1}\ u(k\text{-}1) - 9.5337e\times10^{-2}\ u(k\text{-}2) - 2.7080\times10^{6}\ h(k\text{-}1) + 2.2912\times10^{6}\ h(k\text{-}2) - 7.0738\times10^{8}\ \phi(k\text{-}1) + 7.1088\times10^{8}\ \phi(k\text{-}2)$$

The performance of LQR and GPC depends on the selected weighting matrices $\mathbf{Q}$ and $\mathbf{R}$ and the performance of DPC relies on the control horizon and predicted horizon. Figure 3.6 shows that all active controllers are effective in ship roll mitigation. Time histories of ship roll and pump pressure (i.e. control effort) are shown in Figure 3.7 and 3.8 respectively. The PD control has the worst performance. It is noted that DPC and GPC used ship roll angle feedback have high control effort at the beginning.

For DPC with ship roll angle and water height feedback, Figure 3.9 shows the effect of control horizon to the ship roll amplitude at different frequency. The lower control horizon is used, the more ship roll amplitude is reduced.

For performance comparison, the ratio of ship roll amplitude reduced from passive tank and control pressure, $\frac{\phi_{OL}(q)-\phi_{CL}(q)}{|u_{CL}(q)|}$ is considered, the results are shown in Figure 3.10. The higher ratio the better performance we can get from the controller. From Figure 3.10, at low frequency, GPC with ship roll feedback has the best performance. At frequency ratio between 0.95 and 1.8, GPC with ship roll feedback and both DPC with ship roll and DPC with ship roll and water height feedback are higher performance than LQR and GPC with ship roll and water height feedback.

For overall performance, $\int_{q}\frac{|\phi_{OL}(q)-\phi_{CL}(q)|}{|u_{CL}(q)|}dq$ is used for criterion comparison, the order of performance from highest to lowest performance is GPC (ship roll feedback) 578 m^2/N, LQR 504 m^2/N, DPC (with ship roll and water height feedback) 500 m^2/N,

DPC (with ship roll feedback) 499 m^2/N, and GPC (water height and ship roll feedback) 484 m^2/N. The GPC with ship roll feedback has the best result; performances of both DPC (with ship roll feedback and with ship roll and water height feedback) are closely to LQR. DPC is easiest to implement then DPC is selected for adaptive predictive control.

When a ship is under loading or unloading, its dynamics change. U-tube tank is no longer operating at the desired performance and the ship roll performance is degraded. In this case, system identification is needed to update the ship parameters for the controller. In order to stimulate the full spectrum of ship dynamics, a random input signal u_{id} is added to the control signal u_c. The GPC and DPC are redesigned with identified system parameters. Figure 3.11 shows the performance of adaptive DPC with control horizon $h_c = 25$ by using two feedback signals (i.e. ship roll and water height angle). At time $t = 0$ sec, the ship roll period is reduced by 40% to be 7.5 sec. During the time period from 0 to 200 sec, the ship roll is controlled by DPC with ship roll and water height angle feedback. The DPC controller is designed from original ship roll parameters (with the ship roll period 12.5 sec). During the time period from 200 to 700 sec, a random pulse input u_{id} is applied without any control input and ship parameters are identified. Figure 3.12 shows the input P and output τ and ϕ used for system identification. Then the controller is updated at time $t = 700$ sec. During the time period from 700 to 1000 sec, the updated DPC controller gain is applied to ship roll mitigation. The control horizon is 50, ARX order is 120 and system order is four.

Figure 3.13 shows performance of the adaptive DPC by using only one feedback signal (i.e. ship roll angle) is shown in Figures 3.13 and 3.14. The control horizon is 70, ARX order is 200 and system order is four. In Figure 3.14, the stimulation signal used for

system identification has a higher frequency with smaller amplitude. From Figures 3.11 and 3.13, ship roll mitigation is improved about 40% after updating the controller with system identification.

Figure 3.15 shows the performance of adaptive GPC with ship roll feedback, control horizon $h_c = 50$, $\mathbf{R} = 10^{14}\mathbf{I}_{hc \times hc}$, and $\mathbf{Q} = 1$. The ship roll amplitude is almost the same for before and after updating the controller, but after updating controller system is more stability.

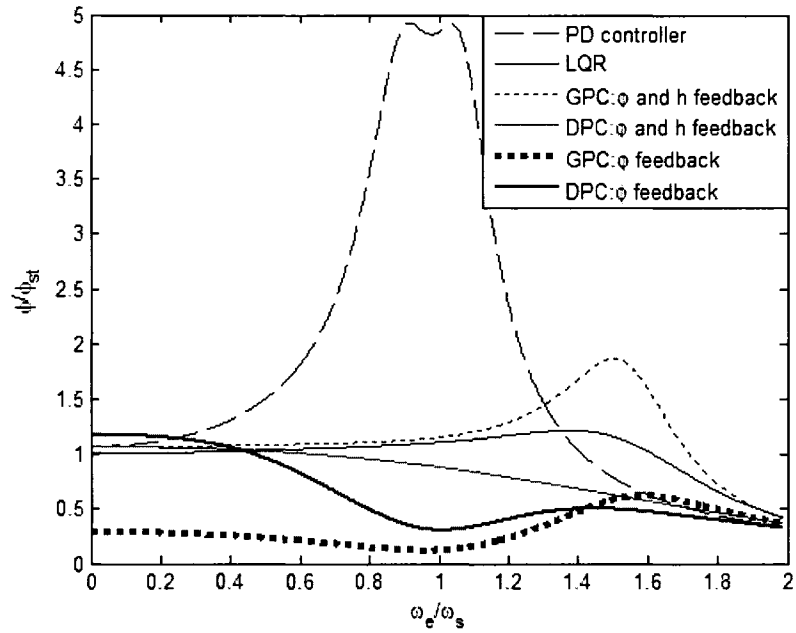

Figure 3.6 Frequency response of ship roll angle by using U-tube tank with different controllers.

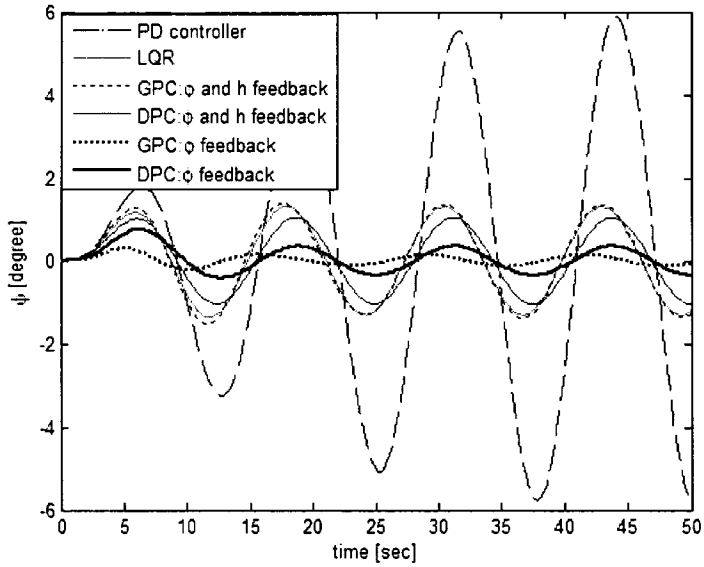

Figure 3.7 Time history of ship roll angle with PD, LQR, GPC, and DPC.

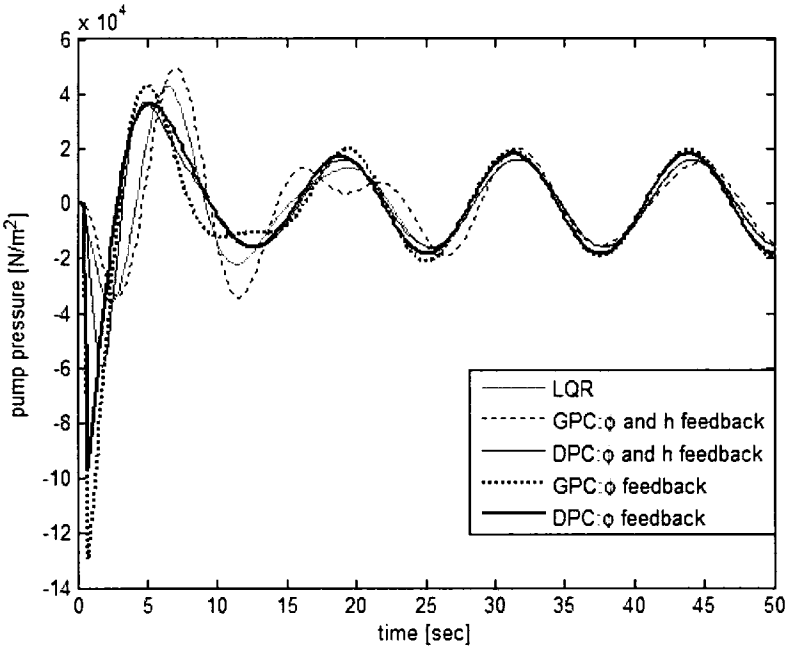

Figure 3.8 Time history of pump pressure with LQR, GPC, and DPC.

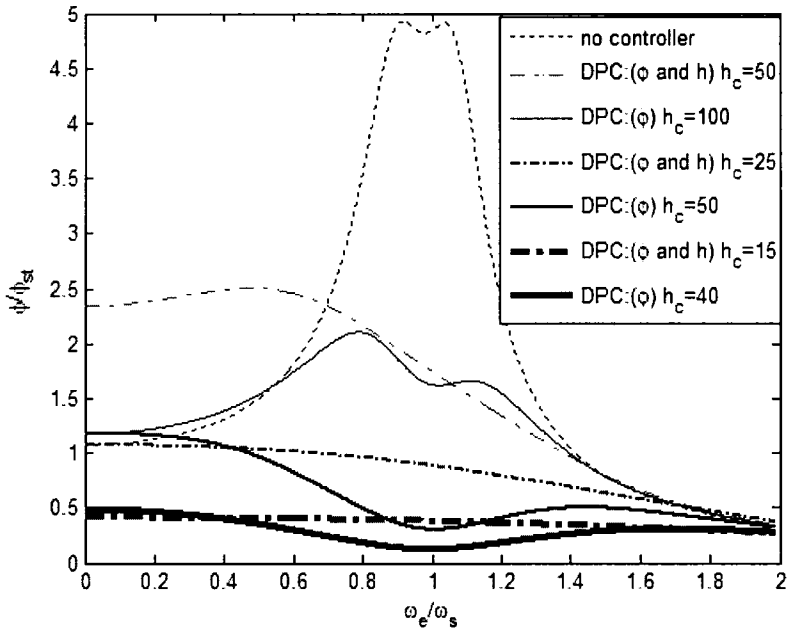

Figure 3.9 Frequency response of ship roll with different control horizon of DPC.

$$\frac{\phi_{OL}-\phi_{CL}}{|u_{CL}|}$$

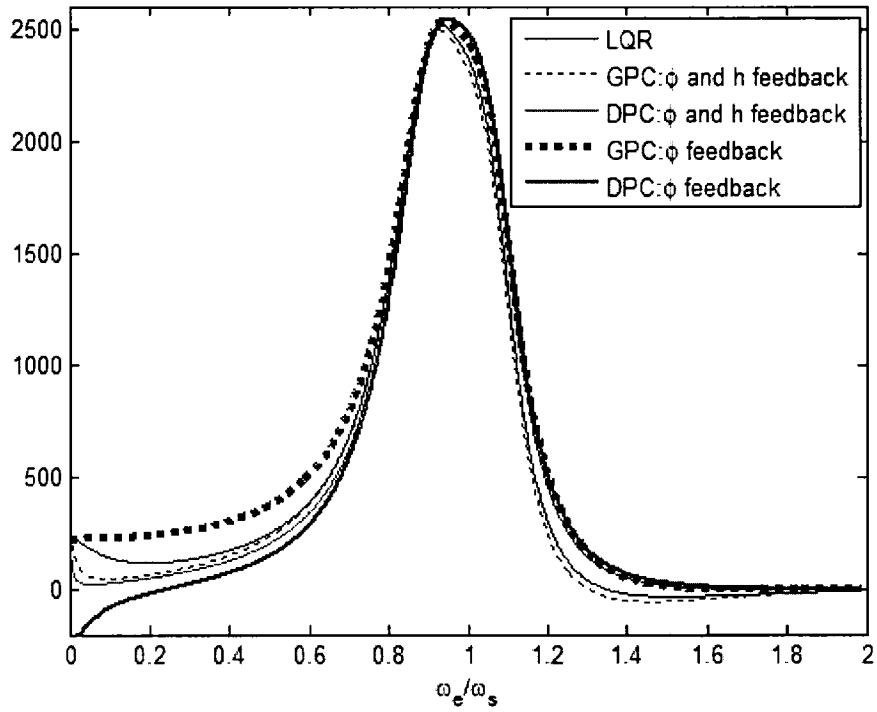

Figure 3.10 The ratio of ship roll amplitude reduced from passive tank and control pressure

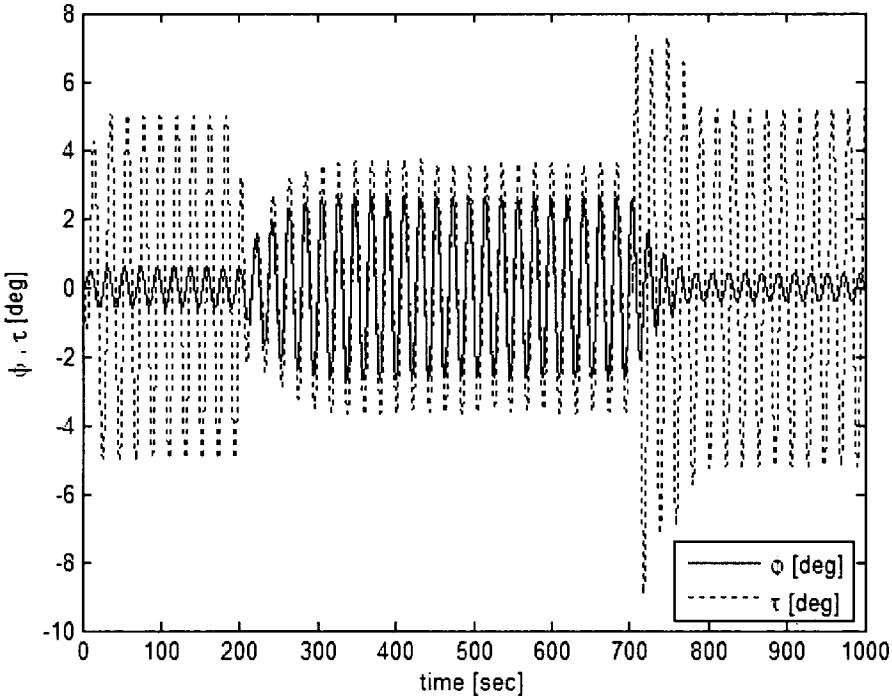

Figure 3.11 Time history of ship roll and water height due to regular beam seas with DPC (ship roll and water height angle feedback) before, during, and after system identification.

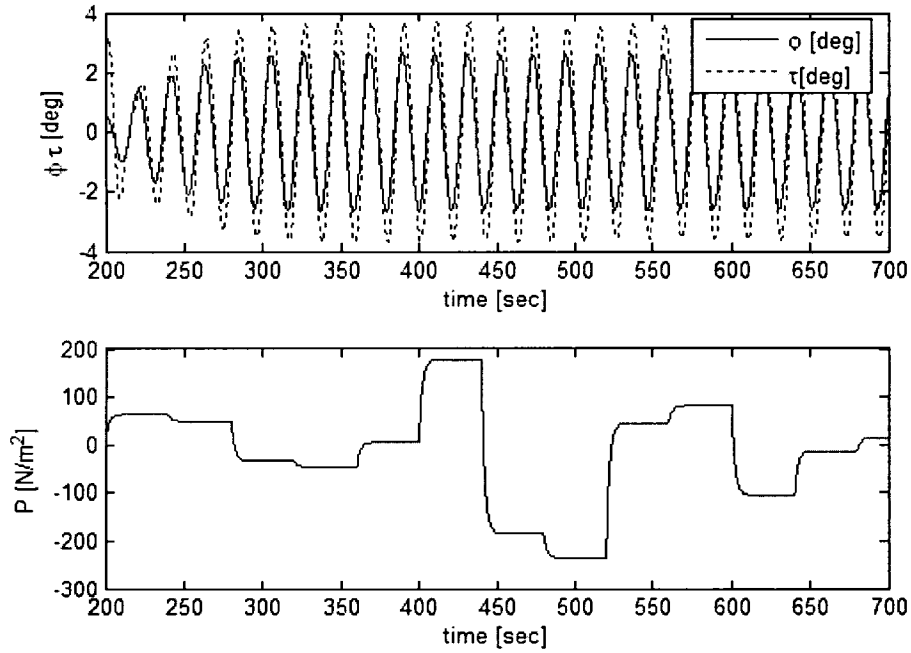

Figure 3.12 Time history of ship roll and water height angle and identification input used for system identification under regular beam sea. Time history of ship roll and water height angle and identification input used for system identification under regular beam sea. Time history of ship roll and water height angle and identification input used for system identification under regular beam sea.

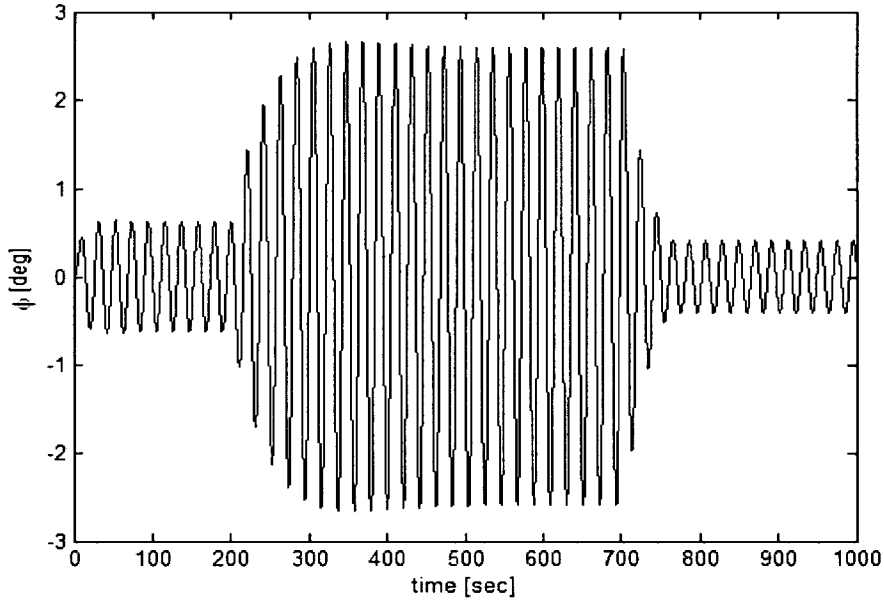

Figure 3.13 Time history of ship roll and water height due to regular beam seas with DPC (ship roll angle feedback) before, during, and after system identification.

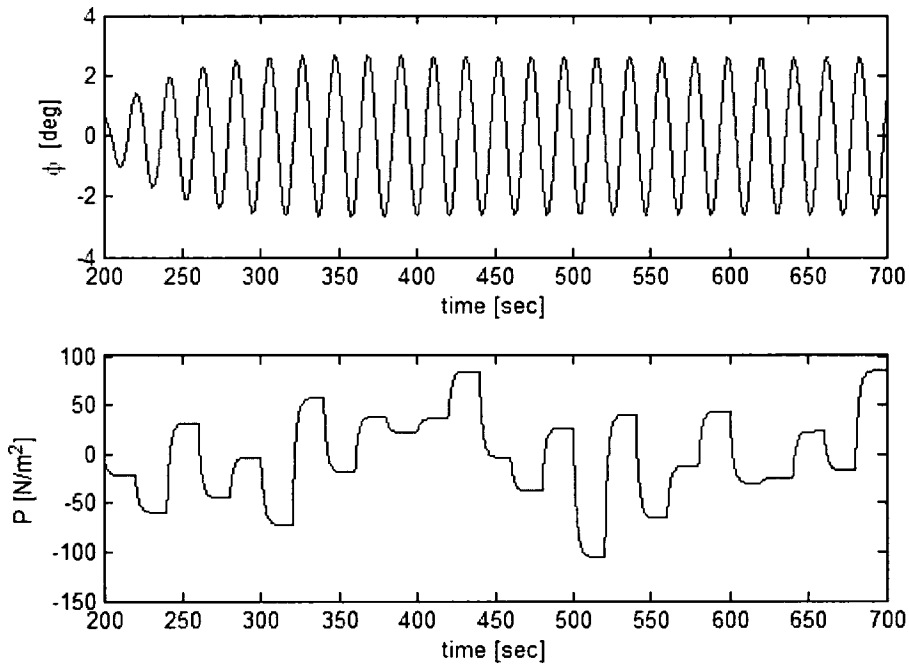

Figure 3.14 Time history of ship roll angle and identification input used for system identification under regular beam sea.

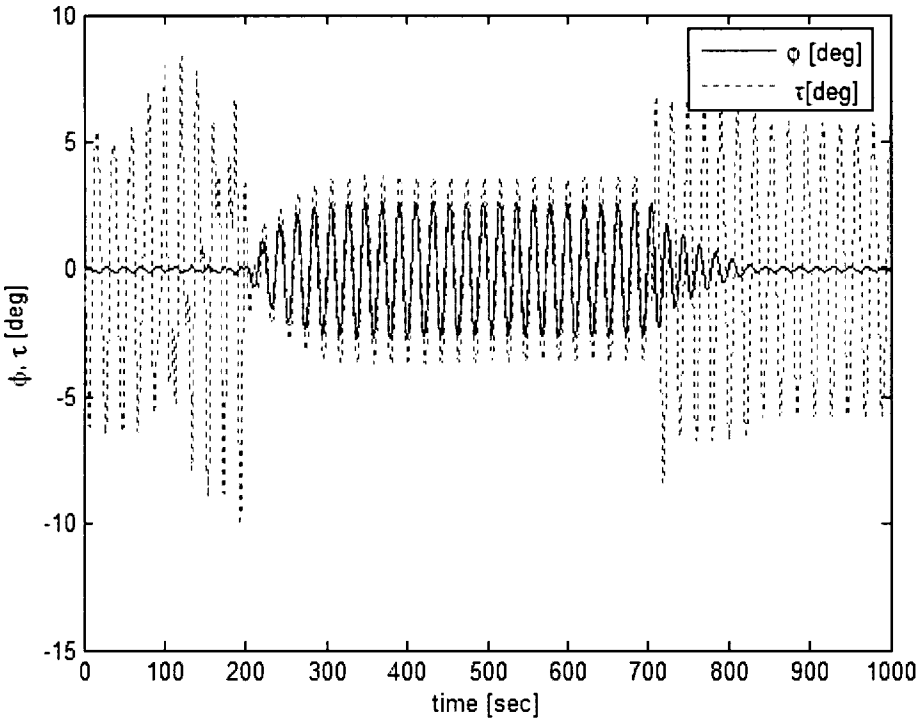

Figure 3.15 Time history of ship roll and water height due to regular beam seas with GPC (ship roll feedback) before, during, and after system identification.

3.9 Conclusions

In this study, the ship roll mitigation is studied by using a U-tube water tank with four dynamic controllers. The U-tube water tank can be used as an optimal passive damper if a PD controller is used by properly tuning its controller gains.

From numerical simulations, active controllers like LQR, GPC and DPC can greatly enhance the ship roll mitigation. The GPC achieves the best performance and can be easily implemented since it only requires one feedback signal (i.e. ship roll) to be measured. When ship dynamics change, a system identification algorithm is proposed and the performance of ship roll mitigation using adaptive GPC and DPC is demonstrated.

CHAPTER 4

NONLINEAR SHIP ROLL CONTROL

Linear ship roll motion with U-tube tank was studied in Chapters 2 and 3. It is reasonable for a small ship roll motion. Large amplitude ship roll motions would be nonlinear; these can be caused by wave action and load effects. These results will be represented by nonlinear damping moment and the nonlinear restoring moment. A coupling motion with other directions or with flooded water on deck can cause nonlinear ship roll motion as well. For water on deck, Murashigae et al. (1999) showed that a ship can exhibit undesirable nonlinear roll motion even in waves of moderate amplitude.

For nonlinear ship roll motion, conventional linear control cannot prevent a ship from capsizing. In this study, a nonlinear controller was considered for nonlinear ship roll motion generated by wave action and load. One of the nonlinear controllers is feedback linearization. Feedback linearization deals with techniques for transforming original system models into equivalent models of a simpler form. Then the nonlinear control signal is derived for desired performance. Applicability of this method is quite limited because it depends on an exact knowledge of nonlinear plant. To disregard this limitation, a neural network and fuzzy system are applied to represent unknown nonlinear function. He et al. (1998) used a neural network to represent the nonlinear function. Wang (1993), and Spooner and Pasinno (1996) applied a fuzzy system as a direct and indirect adaptive controller. Chen et al. (1996) and Park (2003) employed a fuzzy system as an indirect adaptive controller, and Yang and Ren (2003) applied a fuzzy system as a direct adaptive controller.

In this study, feedback linearization and an adaptive fuzzy robust controller were applied to nonlinear ship roll mitigation.

4.1 Nonlinear Ship Roll and U-tube Tank

Ship motion can be written as

$$I_{44}\ddot{\phi} = F_{total}$$

, where total moment F_{total} is the combination of hydrodynamic moments $F_{hdtotal}(\dot{\phi},\ddot{\phi})$, hydrostatic moments $F_{hs}(\phi)$, wave moments F_w, wind moments, and U-tube tank moments K_{stim}. Hydrodynamic moments depend on ship motion and can be represented by $F_{hdtotal}(\dot{\phi},\ddot{\phi}) = -m_{44}(\omega)\ddot{\phi} - b_{44}\dot{\phi} - b_{44q}|\dot{\phi}|\dot{\phi}$. Hydrostatic moments depend on hull shape and can be approximated by polynomial function $F_{hs}(\phi) = -\Delta(c_1\phi - c_3\phi^3)$. Wave moments can be represented by $F_w = M_{wo}\cos(\omega t)$. Ship roll motion can be written as

$$(I_{44} + m_{44}(\omega))\ddot{\phi} = F_{hd}(\dot{\phi}) + F_{hs}(\phi) + F_w + K_{stim} \tag{4.1}$$

, where $F_{hd}(\dot{\phi},\ddot{\phi}) = -b_{44}\dot{\phi} - b_{44q}|\dot{\phi}|\dot{\phi}$

From Equation (2.11), water motion in stimulator

$$\begin{aligned} & m_{h\phi}\ddot{\phi} - \rho m_{hh}\ddot{h} \\ &= \Delta P + 2\rho g h\cos\phi - \rho g L\sin\phi - \rho(2L_Z - H)h\dot{\phi}^2 + bA_t(2H + L)\dot{h} \\ &= \Delta P + F_{shh}(h,\dot{h},\phi,\dot{\phi}) \end{aligned} \tag{4.2}$$

, where

$$F_{shh}(h,\dot{h},\phi,\dot{\phi}) = 2\rho g h\cos\phi - \rho g L\sin\phi - \rho(2L_Z - H)h\dot{\phi}^2 + bA_t(2H + L)\dot{h}$$

$$m_{h\phi} = \rho L(L_Z + H)$$

$$m_{hh} = \rho\left(2H + \frac{A_{tank}}{A_{pipe}}L\right).$$

From Equation (2.16), moment generated by U-tube tank

$$\begin{aligned} K_{stim} &= -\rho A_t\left(\frac{1}{3}\left(2H^3 - 6L_zH^2 - 6L_zh^2 + 6L_z^2H + 6Hh^2\right) + \frac{1}{2}L^2H + \frac{A_p}{A_t}L_z^2L + \frac{1}{12}\frac{A_p}{A_t}L^3\right)\ddot{\phi} \\ &\quad + \rho A_t(LH + L_zL)\ddot{h} + 4\rho A_t(L_Z + H)h\dot{\phi}\dot{h} + 2\rho A_t LHh\dot{\phi}^2 \\ &\quad - \rho g A_t\left(2L_ZH - H^2 - h^2\right)\sin\phi + \rho g A_t Lh\cos\phi - \rho g A_p L_z L\sin\phi \\ &= -\left(m_{s44} + 2\rho A_t(H - L_z)h^2\right)\ddot{\phi} + m_{\phi h}\ddot{h} + F_{s4r}\left(h, \dot{h}, \phi, \dot{\phi}\right) \end{aligned} \tag{4.3}$$

, where

$$\begin{aligned} F_{s4r}\left(h, \dot{h}, \phi, \dot{\phi}\right) &= 4\rho A_t(L_Z + H)h\dot{\phi}\dot{h} + 2\rho A_t LHh\dot{\phi}^2 - \rho g A_t\left(2L_ZH - H^2 - h^2\right)\sin\phi \\ &\quad + \rho g A_t Lh\cos\phi - \rho g A_p L_z L\sin\phi \end{aligned}$$

$$m_{s44} = \rho A_t\left(\frac{1}{3}\left(2H^3 - 6L_zH^2 + 6L_z^2H\right) + \frac{1}{2}L^2H + \frac{A_p}{A_t}L_z^2L + \frac{1}{12}\frac{A_p}{A_t}L^3\right)$$

$$m_{\phi h} = \rho A_t(LH + L_zL)$$

From Equation (4.1)-(4.3), coupling of ship roll motion and U-tube tank can be written as

$$-m_{hh}\ddot{h} + m_{h\phi}\ddot{\phi} = \Delta P + F_{shh}\left(h, \dot{h}, \phi, \dot{\phi}\right)$$

$$-m_{\phi h}\ddot{h} + m_{\phi\phi}\ddot{\phi} = F_{hd}\left(\dot{\phi}\right) + F_{hs}(\phi) + F_w + F_{s4r}\left(h, \dot{h}, \phi, \dot{\phi}\right)$$

or $$\ddot{h} = f_h\left(h, \dot{h}, \phi, \dot{\phi}\right) + g_{\phi\phi}\Delta P - g_{h\phi}F_w$$

$$\ddot{\phi} = f_\phi\left(h, \dot{h}, \phi, \dot{\phi}\right) + g_{\phi h}\Delta P - g_{hh}F_w \tag{4.4}$$

, where $m_{\phi\phi} = \left(I_{44} + m_{44}(\omega) + m_{s44} + 2\rho A_t(H - L_z)h^2\right)$

$$m_{eq} = -m_{hh}m_{\phi\phi} + m_{h\phi}m_{\phi h}$$

$$g_{\phi\phi} = \frac{m_{\phi\phi}}{m_{eq}}, g_{\phi h} = \frac{m_{\phi h}}{m_{eq}}, g_{h\phi} = \frac{m_{h\phi}}{m_{eq}}, g_{hh} = \frac{m_{hh}}{m_{eq}}$$

$$f_h(h,\dot{h},\phi,\dot{\phi}) = -g_{h\phi}F_{hd}(\dot{\phi}) - g_{h\phi}F_{hs}(\phi) + g_{\phi\phi}F_{shh}(h,\dot{h},\phi,\dot{\phi}) - g_{h\phi}F_{s4r}(h,\dot{h},\phi,\dot{\phi})$$
$$= +g_{h\phi}b_{44}\dot{\phi} + g_{h\phi}b_{44q}|\dot{\phi}|\dot{\phi} + g_{h\phi}\Delta c_1\phi - g_{h\phi}\Delta c_3\phi^3$$
$$-4g_{h\phi}\rho A_t(L_Z + H)h\dot{\phi}\dot{h} - \rho(2g_{h\phi}A_tLH - g_{\phi\phi}(2L_Z - H))h\dot{\phi}^2$$
$$-g_{h\phi}\rho g A_t h^2 \sin\phi + \rho g(g_{h\phi}A_pL_zL - g_{\phi\phi}L + g_{h\phi}A_t(2L_ZH - H^2))\sin\phi$$
$$+\rho g(2g_{\phi\phi} - g_{h\phi}A_tL)h\cos\phi + g_{\phi\phi}bA_t(2H + L)\dot{h}$$

$$= a_1\dot{\phi} + a_2|\dot{\phi}|\dot{\phi} + a_3\phi - a_4\phi^3 - a_5h\phi\dot{h} - a_6h\dot{\phi}^2 - a_7h^2\sin\phi + a_8\sin\phi + a_9h\cos\phi + a_{10}\dot{h}$$

$$f_\phi(h,\dot{h},\phi,\dot{\phi}) = -g_{hh}F_{hd}(\dot{\phi}) - g_{hh}F_{hs}(\phi) + g_{\phi h}F_{shh}(h,\dot{h},\phi,\dot{\phi}) - g_{hh}F_{s4r}(h,\dot{h},\phi,\dot{\phi})$$

$$= a_{11}\dot{\phi} + a_{12}|\dot{\phi}|\dot{\phi} + a_{13}\phi - a_{14}\phi^3 - a_{15}h\phi\dot{h} - a_{16}h\dot{\phi}^2 - a_{17}h^2\sin\phi + a_{18}\sin\phi + a_{19}h\cos\phi + a_{20}\dot{h}$$

They can be written in first order system differential equation as

$$z_2 = \dot{z}_1 = \dot{h}$$
$$\dot{z}_2 = \ddot{h} = f_h(z_1,z_2,z_3,z_4) + g_{\phi\phi}\Delta P - g_{h\phi}F_w$$
$$z_4 = \dot{z}_3 = \dot{\phi}$$
$$\dot{z}_4 = \ddot{\phi} = f_\phi(z_1,z_2,z_3,z_4) + g_{\phi h}\Delta P - g_{hh}F_w$$

, or $$\dot{\mathbf{z}} = \begin{bmatrix} z_2 \\ f_h(z_1,z_2,z_3,z_4) \\ z_4 \\ f_\phi(z_1,z_2,z_3,z_4) \end{bmatrix} + \begin{bmatrix} 0 \\ g_{\phi\phi} \\ 0 \\ g_{\phi h} \end{bmatrix}\Delta P + \begin{bmatrix} 0 \\ g_{h\phi} \\ 0 \\ g_{hh} \end{bmatrix}F_w = \mathbf{f}(\mathbf{z}) + \mathbf{g}(\mathbf{z})\Delta p + \mathbf{g_d}(\mathbf{z},t)F_w \quad (4.5)$$

$$y = \phi = h(\mathbf{z})$$

In this study, we are not considering the disturbance term for wave moment, F_w, for controller design.

4.2 Ship Roll Motion Phase Plane

For no bias of a ship and no viscous damping, phase plane of ship roll and roll rate are shown in Figure 4.1

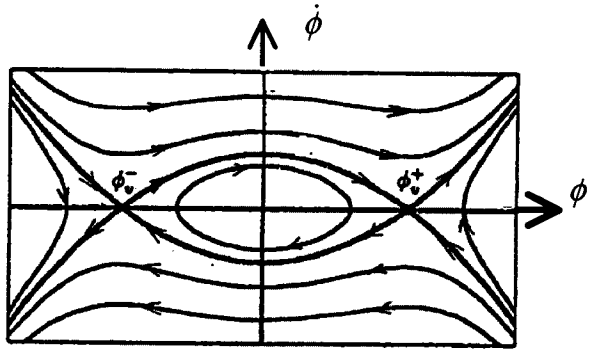

Figure 4.1 Phase plane of ship roll motion without damping: From jiang et. al. (1996)

It has two fixed points of saddle type which are referred to as "the angle of vanishing stability" and one fixed point of the center type between the saddles, representing the upright equilibrium position. It has a heteroclinic cycle connecting the two saddle points and also encircling the center. Two saddle points are located at $(\phi_v, 0)$, where $\phi_v^{\pm} = \pm\sqrt{\frac{a_{13}}{a_{14}}}$. The safe region is defined as the one bounded by the heteroclinic cycle. This is because every initial condition located in those regions will lead to bounded oscillatory motion. Outside those regions, the motion will be unbounded, corresponding to capsize.

4.3 Feedback Linearization

4.3.1 Basic theory

The central idea of the approach is to algebraically transform a nonlinear system into a fully or partially linear system as a controllable canonical form shown by Slotine

and Li (1991). A single-input, single-output nonlinear system is described by the state space representation

$$\dot{\mathbf{z}} = \mathbf{f}(\mathbf{z}) + \mathbf{g}(\mathbf{z})u$$
$$y = h(\mathbf{z})$$

Differentiating y with respect to time, one obtains

$$\dot{y} = \nabla h(\mathbf{f} + \mathbf{g}u) = L_{\mathbf{f}} h(\mathbf{x}) + L_{\mathbf{g}} h(\mathbf{x})u$$

, where $L_{\mathbf{f}} h(\mathbf{x})$, $L_{\mathbf{g}} h(\mathbf{x})$ represent the Lie derivative of h with respect to $\mathbf{f}, \mathbf{g}$ respectively.

If $L_{\mathbf{g}} h(\mathbf{x})u \neq 0$ for all $\mathbf{x}$ in a region Ω then the input transformation

$$u = \frac{1}{L_{\mathbf{g}} h(\mathbf{x})}\left(-L_{\mathbf{f}} h(\mathbf{x}) + v\right)$$

results in a linear differential relation between y and v

$$\dot{y} = v$$

If $L_{\mathbf{g}} h(\mathbf{x})u = 0$ for all $\mathbf{x}$ in a region Ω we can differentiate $\dot{y}$ to obtain

$$\ddot{y} = L_{\mathbf{f}^2} h(\mathbf{x}) + L_{\mathbf{g}} L_{\mathbf{f}} h(\mathbf{x})u$$

If $L_{\mathbf{g}} L_{\mathbf{f}} h(\mathbf{x})$ is again zero, we shall differentiate again and again, until for some integer

$$L_{\mathbf{g}} L_{\mathbf{f}}^{r-1} h(\mathbf{x}) \neq 0$$

Then the control law

$$u = \frac{1}{L_{\mathbf{g}} L_{\mathbf{f}}^{r-1} h}\left(-L_{\mathbf{f}}^{r-1} h + v\right)$$

yields the linear multiple-integrator relation

$$y^{(r)} = v$$

The number of differentiations of y required for input u to appear is called relative degree of system.

When $r < n$ the nonlinear system can be transformed, using $h, L_f h, \ldots, L_f^{r-1} h$ as a part of new states, into a so-called "normal form." The normal form of system can be written as

$$\frac{d}{dt}\begin{bmatrix} x_1 \\ \cdots \\ \cdots \\ x_{r-1} \\ x_r \end{bmatrix} = \begin{bmatrix} x_2 \\ \cdots \\ \cdots \\ x_r \\ a(\mathbf{x},\boldsymbol{\eta}) + b(\mathbf{x},\boldsymbol{\eta})u \end{bmatrix}$$
$$\dot{\boldsymbol{\eta}} = w(\mathbf{x},\boldsymbol{\eta}) \qquad (4.6)$$
$$y = x_1$$

, where

$$\mathbf{x} = [h \;\; L_f h \;\; \ldots \;\; L_f^{r-1} h]^T$$
$$\boldsymbol{\eta} = [\eta_1 \;\; \eta_2 \cdots \;\; \eta_{n-r}]^T$$

$$a(\mathbf{x},\boldsymbol{\eta}) = L_f^r h(\mathbf{x}) = L_f^r h[\phi^{-1}(\mathbf{x},\boldsymbol{\eta})]$$
$$b(\mathbf{x},\boldsymbol{\eta}) = L_g L_f^{r-1} h(\mathbf{x}) = L_g L_f^r h[\phi^{-1}(\mathbf{x},\boldsymbol{\eta})]$$

The first r equations of the normal form have a companion form, while the last $n-r$ equations are not directly related to the system input u.

To show that the nonlinear system can indeed be transformed into the normal form, we have to show that the component of $\mathbf{x}$ are independent (and thus eligible to serve as a subset of state vector), and thus $(n-r)$ other variables η_i can be found to complete the new state vector.

For latter, find $(n-r)$ more functions η_i such that the set of functions $\varsigma_i, \eta_j (i=1,\ldots,r;\ j=1,\ldots n-r)$ are independent of each other in Ω. The $(n-r)$ independent functions $\lambda_k (k=1,\ldots,n-r)$ such that

$$L_{\mathbf{g}} \lambda_k(\mathbf{x}) = 0, \qquad \forall \mathbf{x} \in \Omega$$

4.3.2 Ship Roll Motion with U-tube Tank

In this section, ship roll and U-tube tank feedback linearization is considered. From equation of motion in Equation (4.5), it has $L_{\mathbf{g}} h(\mathbf{x}) = 0$, and $L_{\mathbf{g}} L_{\mathbf{f}} h(\mathbf{x}) = g_{\phi h} \neq 0$ then this system has relative degree 2 and has normal forms as controllable part

$$\begin{bmatrix} \dot{x}_1 \\ \dot{x}_2 \end{bmatrix} = \begin{bmatrix} \dot{\phi} \\ \ddot{\phi} \end{bmatrix} = \begin{bmatrix} x_2 \\ f_\phi(\mathbf{x}, \boldsymbol{\eta}) + g_{\phi h} \Delta P \end{bmatrix} \tag{4.7}$$

, and an uncontrollable part

$$\begin{aligned} \dot{\eta}_1 &= \dot{h} = -\frac{1}{g_{\phi h}} \eta_2 + \frac{g_{\phi\phi}}{g_{\phi h}} x_2 \\ \dot{\eta}_2 &= -g_{\phi h} \ddot{h} + g_{\phi\phi} \ddot{\phi} = \frac{1}{m_{eq}} \left(F_{hd}(\dot{\phi}) + F_{hs}(\phi) + F_w + F_{s4r}(h, \dot{h}, \phi, \dot{\phi}) \right) \end{aligned} \tag{4.8}$$

Transformation matrix between normal forms and physical form is

$$\begin{bmatrix} x_1 \\ x_2 \\ \eta_1 \\ \eta_2 \end{bmatrix} = \begin{bmatrix} 1 & 0 & 0 & 0 \\ 0 & 1 & 0 & 0 \\ 0 & 0 & 1 & 0 \\ 0 & -g_{\phi\phi} & 0 & g_{\phi h} \end{bmatrix} \begin{bmatrix} \phi \\ \dot{\phi} \\ h \\ \dot{h} \end{bmatrix} \tag{4.9}$$

Jacobian matrix of transformation matrix is non-singular for any states, **z**. Thus this state transformation is valid globally.

The normal form has zero dynamics system as

$$\dot{\eta}_1 = -\frac{1}{g_{\phi h}}\eta_2$$
$$\dot{\eta}_2 = g_{\phi\phi}\ddot{h} = -\frac{1}{m_{eq}}\left(F_{hd}(0) + F_{hs}(0) + F_{s4r}(h,\dot{h},0,0)\right) = -\frac{1}{m_{eq}}\rho g A_t L \eta_1 \tag{4.10}$$

, which is marginal stability. It will oscillate with frequency $\sqrt{\frac{g}{H+L_z}}$ rad/sec. The oscillation affects the ship roll motion, so the uncontrollable part is not need to be stabilized it by changing the coordinate of the controllable part. Control signal for feedback linearization is

$$u(\mathbf{x}) = \frac{1}{g_{\phi h}}\left[-f_{\phi}(\mathbf{x},\boldsymbol{\eta}) - v\right] \tag{4.11}$$

, where v as the controllable part has the linear characteristic we need. A schematic diagram of ship roll feedback linearization is shown in Figure 4.2.

If we need to avoid the non-minimum phase due to marginal stable of uncontrollable part by changing coordinate of controllable part. One we can change to new states as

$$x_1 = \phi + k_L \sin(h)$$
$$x_2 = \dot{x}_1 = \dot{\phi} + k_L \dot{h}\cos(h)$$
$$\dot{x}_2 = \ddot{\phi} + k_L \ddot{h}\cos(h) - k_L \dot{h}^2 \sin(h) = f_{\phi} + g_{\phi h}\Delta P + k_L\left(f_h + g_{\phi\phi}\Delta P\right)\cos(h) - k_L \dot{h}^2 \sin(h)$$

$$\dot{\eta}_1 = \frac{\eta_2 - g_{\phi\phi}x_2}{-g_{\phi h} - g_{\phi\phi}k_L \cos x_1}$$

$$
\begin{aligned}
\dot{\eta}_2 &= -m_{\phi h}\ddot{h} + m_{\phi\phi}\ddot{\phi} \\
&= F_{hd}(\dot{\phi}) + F_{hs}(\phi) + F_w + F_{s4r}(h,\dot{h},\phi,\dot{\phi}) \\
&= -b_{44}\dot{\phi} - b_{44q}|\dot{\phi}|\dot{\phi} - \Delta c_1\phi + \Delta c_3\phi^3 + 4g_{h\phi}\rho A_t(L_Z + H)h\dot{\phi}\dot{h} + 2\rho g_{h\phi}A_t LHh\dot{\phi}^2 \\
&\quad + g_{h\phi}\rho g A_t h^2 \sin\phi - \rho g\left(A_p L_z L + A_t\left(2L_Z H - H^2\right)\right)\sin\phi + \rho g A_t Lh\cos\phi + F_w \\
&= -a_{01}\dot{\phi} - a_{02}|\dot{\phi}|\dot{\phi} - a_{03}\phi + a_{04}\phi^3 + a_{05}h\dot{\phi}\dot{h} + a_{06}h\dot{\phi}^2 + a_{07}h^2\sin\phi - a_{08}\sin\phi + a_{09}h\cos\phi + F_w
\end{aligned}
$$

, where $\dot{\phi} = \dfrac{-g_{\phi h}x_2 - k_L\cos x_1\eta_2}{-g_{\phi h} - g_{\phi\phi}k_L\cos x_1}$, $\dot{h} = \dfrac{\eta_2 - g_{\phi\phi}x_2}{-g_{\phi h} - g_{\phi\phi}k_L\cos x_1}$, $h = \eta_1$, $\phi = x_1 - k_L\sin(h)$

Control signal for feedback linearization is

$$
u(\mathbf{x}) = -\frac{1}{g_{\phi h} + g_{\phi\phi}k_L\cos(h)}\left(f_\phi + k_L\cos(h)f_h - k_L\dot{h}^2\sin(h) - v\right)
$$

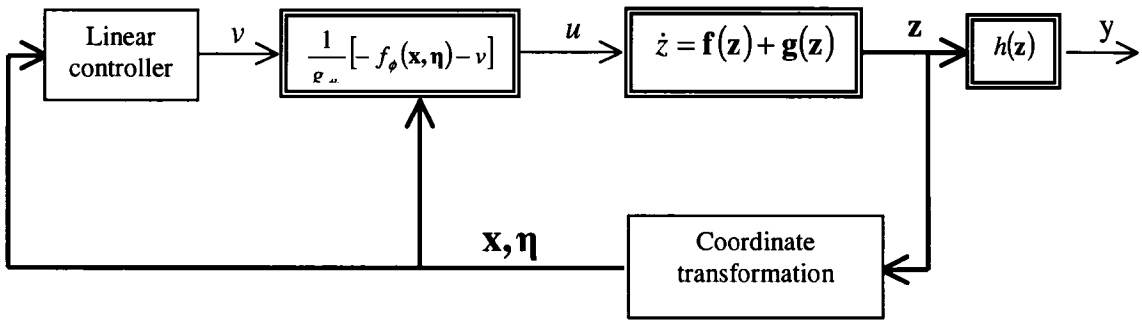

Figure 4.2 Block diagram of ship roll and U-tube tank with feedback linearization

4.4 Adaptive Fuzzy Control

4.4.1 Problem formulation

Consider system order n^{th}

$$
\begin{aligned}
&\dot{x}_i = x_{i+1}, 1 \le i \le n-1 \\
&\dot{x}_n = f(\mathbf{x}) + g(\mathbf{x})u + d(\mathbf{x},t) \\
&y = x_1
\end{aligned}
\tag{4.12}
$$

Let $v = \left[y_d \;\; y_d^{(1)} \;\; y_d^{(2)} \;\cdots\; y_d^{(n-1)}\right]^T$, and $e = \mathbf{x} - v$ then system equation can be

$$\begin{aligned} \dot{e}_i &= e_{i+1} \qquad\qquad ,1 \le i \le n-1 \\ \dot{e}_n &= f(\mathbf{x}) + g(\mathbf{x})u - y_d^{(n)}(t) + d(\mathbf{x},t) \end{aligned} \tag{4.13}$$

Using the pole-placement approach, we consider a term $\mathbf{kx}$, where $\mathbf{k} = [k_1 \;\; k_2 \;\; \cdots \;\; k_{n-1}]$, the k_i are chosen such that $s^n + k_{n-1}s^{n-1} + k_2 s + k_1 = 0$ is a stable polynomial, which leads to exponentially stable dynamics

$$x^n + k_{n-1}x^{n-1} + k_2 x^2 + k_1 x = 0$$

$$\dot{\mathbf{e}} = \mathbf{Ae} + \mathbf{B}\{g(\mathbf{x})u + f(\mathbf{x}) - y_d^{(n)} + \mathbf{k}^{\mathrm{T}}\mathbf{e} + d(\mathbf{x},t)\}$$

, where

$$\mathbf{A} = \begin{bmatrix} 0 & 1 & 0 \cdots & 0 \\ 0 & 0 & 1 \cdots & 0 \\ \vdots & \vdots & \vdots & \vdots \\ -k_1 & -k_2 & -k_3 \cdots & -k_n \end{bmatrix}; \quad \mathbf{b} = \begin{bmatrix} 0 \\ 0 \\ \cdots \\ 1 \end{bmatrix}$$

Because A is stable, positive-definite solution $\mathbf{P} = \mathbf{P}^T$ of Lyapunov equation

$$\mathbf{A}^{\mathrm{T}}\mathbf{P} + \mathbf{PA} + \mathbf{Q} = 0 \tag{4.14}$$

always exists and $\mathbf{Q} > 0$ is specified by the designer.

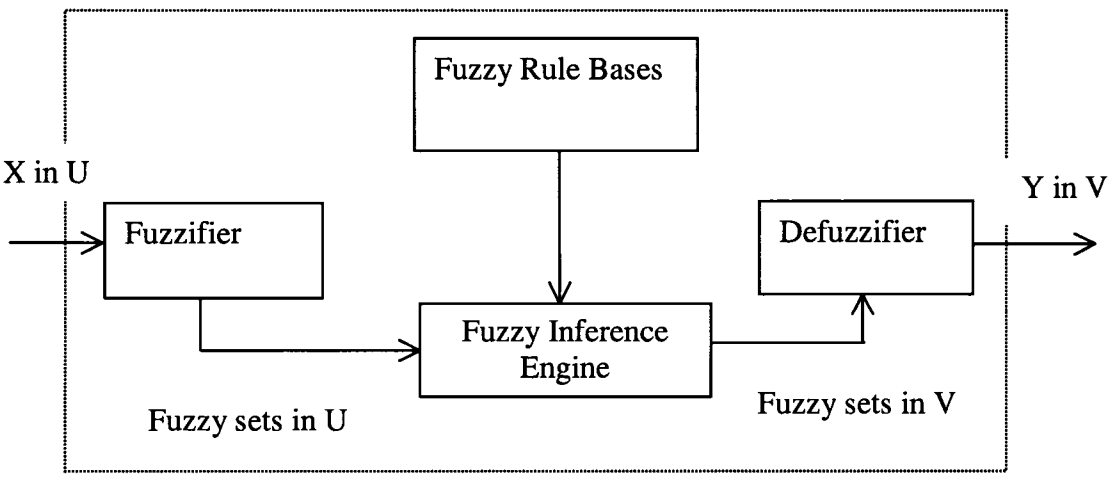

Figure 4.3 Basic configuration of fuzzy system

4.4.2 Structure of Fuzzy System

Fuzzy system is considered in this study shown in Figure 4.3. The fuzzy system performs a mapping from $U \in R^n$ to $V \in R$.

(a) Fuzzifier

Fuzzy logic systems have been proved to be universal approximators. They can be uniformly approximate any continuous functions defined on compact domains to any degree of accuracy.

Consider a fuzzy system to uniformly approximate function $y = f(\mathbf{x})$, where $\mathbf{x} = [x_1\ x_2\ x_3 \cdots x_n]^T \in U$ is the input vector.

The domain of x_i is defined on $\theta_i = [a_i, b_i]$. The domain of x is

$$\Theta = \theta_1 \times \theta_2 \times \cdots \times \theta_n = [a_1, b_1] \times [a_2, b_2] \times \cdots \times [a_n, b_n]$$

In order to construct a fuzzy system, the interval $[a_i, b_i]$ is divided into N_i subintervals

$$a_i = C_0^i < C_1^i < \cdots C_{N_i-1}^i < C_{N_i}^i = b_i$$

On each interval $\theta_i, 1 \le i \le n$, $N_i + 1, N_i > 0$ continuous input fuzzy sets, denoted by $A_j^l, 0 \le j \le N_i$, are define to fuzzify x_i. The membership function of A_j^l is denoted by $\mu_{A_j^l}(x_j)$, which can be represented by triangular, trapezoid, generalized bell or Gaussian type and so on.

(b) Fuzzy rule bases

Generally, fuzzy systems can be constructed by $K, K > 1$ fuzzy rules. **Fuzzy rule base** is a set of fuzzy IF-THEN rules collected from field experts, which represent the knowledge of how to describe the plant or how to control the plant.

$$Rule^{(l)}: IF\ \ x_1\ is\ A_1^l\ \text{AND}\ \ldots\ \text{AND}\ x_n\ is\ A_n^l\ Then\ y_i\ is\ G^l,\ \ l=1,2,\ldots,\text{M}$$

, where G^l is a function of $a_0^l + a_1^l x_1 + \cdots + a_n^l x_n$ for the Takagi-Sugino (T-S) type fuzzy system, $\mathbf{x} = [x_1\ x_2\ x_3 \cdots x_n]^T \in U$, y are the input and output of the fuzzy system, $A_1^l, A_2^l, \ldots, A_s^l$ are fuzzy sets of the input, G^l is the output fuzzy set, and $l = 1,2,\ldots.M$ is the number of fuzzy rule.

(d) Fuzzy inference engine

Fuzzy inference engine, fuzzy logic principles are used to combine the fuzzy *IF-THEN* rules in the fuzzy rule base into a mapping from the fuzzy set in $U = U_1 \times U_2 \times \cdots \times U_n$ to a fuzzy set in V. Fuzzy implication rules are used to represent *IF-THEN* rules before combining them together. For product-operation rule of fuzzy implication

$$\mu_{F_1^l \times F_2^l \times \cdots \times F_n^l \to G^l}(x, y) = \mu_{F_1^l \times F_2^l \times \cdots \times F_n^l \to G^l}(x)\mu_{G^l}(y)$$

Compositional rule of inference

$$\mu_{A_x \circ R^{(l)}}(y) = \sup_{x \in U}\left(\mu_{A_x}(x)\mu_{F_1^l}(x_1)\mu_{F_2^l}(x_2)\cdots\mu_{F_n^l}(x_n)\mu_{G^l}(y)\right)$$

A_x is an arbitrary fuzzy set in U. If A_x is fuzzy singleton with support x then

$$\mu_{A_x \circ R^{(l)}}(\bar{y}) = \sup_{x \in U}\left(\mu_{A_x}(x)\mu_{F_1^l}(x_1)\mu_{F_2^l}(x_2)\cdots\mu_{F_n^l}(x_n)\mu_{G^l}(\bar{y})\right) = \prod_{i=1}^{n}\mu_{F_1^i}(x)\mu_{G^l}(\bar{y}) = \prod_{i=1}^{n}\mu_{F_1^i}(x)$$

, where $\bar{y}$ is the point in R which $\mu_{G^l}(y)$ achieve its maximum value.

(e) Defuzzifier

By using a center-averaged defuzzifier, the output of fuzzy system

$$\hat{y}(x)=\frac{\sum_{l=1}^{M}\bar{y}^{l}\mu_{A_x\circ R^{(l)}}(\bar{y})}{\sum_{l=1}^{M}\mu_{A_x\circ R^{(l)}}(\bar{y})}=\frac{\sum_{l=1}^{M}\bar{y}^{l}\left(\prod_{i=1}^{n}\mu_{F_i^l}(x_i)\right)}{\sum_{l=1}^{M}\left(\prod_{i=1}^{n}\mu_{F_i^l}(x_i)\right)}$$

or $$\hat{f}(x,A_x)=\sum_{i=1}^{K}y_i\xi_i(x)=\xi(x)A_x\bar{x} \qquad (4.15)$$

, where $\mathbf{x}=[x_1\ x_2\ x_3\cdots x_n]^T$, $\bar{\mathbf{x}}=[1\ \ x^T]^T$, and

$\xi_i(\mathbf{x})=\dfrac{\left(\prod_{i=1}^{n}\mu_{F_i^l}(x_i)\right)}{\sum_{l=1}^{K}\left(\prod_{i=1}^{n}\mu_{F_i^l}(x_i)\right)}$, which is called a fuzzy base function and

$$\xi(\mathbf{x})=[\xi_1(\mathbf{x})\ \ \xi_2(\mathbf{x})\ \ \ldots\ \ \xi_K(\mathbf{x})]$$

$$A_x=\begin{bmatrix} a_0^1 & a_1^1 & \cdots & a_n^1 \\ a_0^2 & a_1^2 & \cdots & a_n^2 \\ \vdots & \vdots & \cdots & \vdots \\ a_0^K & a_1^K & \cdots & a_n^K \end{bmatrix}$$

$a_j^i, j=0,1,\ldots,n, i=0,1,\ldots,K$ are unknown constants.

Lemma 1. Suppose that the input universe of discourse U is a compact set in R^r. Then for any given real continuous function $f(\mathbf{x})$ on U and $\forall\varepsilon>0$, there exist the fuzzy systems $\hat{f}(x,A_x)$ such that

$$\sup_{x\in U}\left\|f(x)-\hat{f}(x,A_x)\right\|<\varepsilon.$$

Proof. The proof was given by Wang (1997)

For any n-dimensional continuous function $f(\mathbf{x})$, if N_i+1 is input fuzzy sets for each variable x_i are used, there will be $K=\prod_{i=1}^{n} N_i+1$ *IF-THEN* fuzzy rules in the T-S fuzzy systems. In such a way, we will get a total of $(n+1)\prod_{i=1}^{n} N_i+1$ parameters to describe the T-S fuzzy systems $\hat{f}(\mathbf{x},\mathbf{A}_x)$ which is used to approximate the function $f(\mathbf{x})$.

4.4.3 Direct Adaptive Fuzzy Control

In direct adaptive control, the parameters of the controller are directly adjusted to reduce some norm of the output error between the plant and the reference model. We need to find $f(\mathbf{x})$ for finding the control law to create stability. For $f(\mathbf{x})$ is an unknown continuous function, T-S fuzzy system $\hat{f}(\mathbf{x},\mathbf{A}_z)$ with input vector x.

$$\begin{aligned} f(\mathbf{x}) &= \hat{f}(x,A_z)+\varepsilon \\ &= \xi(x)A_x\bar{x}+\varepsilon = \xi(x)A_z^0+\xi(x)A_z'e+\xi(x)A_z'v+\varepsilon \end{aligned}$$

Substitute into system equation (4.12)

$$\dot{e}=Ae+B\left\{g(x)u+\xi(x)A_z^0+\xi(x)A_z'e+\xi(x)A_z'v+\varepsilon-y_d^{(n)}+k^Te+\Delta(x,t)\right\} \quad (4.16)$$

Let $c_\theta=\|A_z'\|=\lambda_{\max}^{1/2}\left(A_z'^TA_z'\right)$, such that $A_z'=c_\theta A_z^m$ and $\|A_z'\|\le 1$

$$\dot{e}=Ae+B\left\{g(x)u+\xi(x)A_z^0+\xi(x)A_z'v+\varepsilon-y_d^{(n)}+k^Te+\Delta(x,t)\right\}+c_\theta B\xi(x)A_z^me \quad (4.17)$$

The adaptive controller is designed by using the small gain theorem. The above equation can be written into two subsystems as

$$\begin{aligned} \dot{e} &= Ae+B\left\{g(x)u+\xi(x)A_z^0+\xi(x)A_z'v+\varepsilon-y_d^{(n)}+k^Te+\Delta(x,t)\right\}+c_\theta B\xi(x)w \\ \hat{z} &= H(e)=e \end{aligned} \quad (4.18)$$

$$w = K(\hat{z}) = A_z^m e \tag{4.19}$$

, and their connection is shown in Figure 4.4. Controller $u = U(e)$ should be made to satisfy input to state practically stable (ISpS).

Assumption 1: There exists an unknown positive constant p^* such that $\forall(t,x) \in R_+ \times R^n$

$$\Delta(t,x) \leq p^* \phi(x)$$

where $\phi(x)$ is a known nonnegative smooth function.

Assumption 2: The sign of $g(x)$ is known, and there exists a constant $b_{\min} > 0$ such that $|g(x)| > b_{\min}, \forall x \in R^n$.

Theorem 1 (Uniformly Ultimately Bounded 1): Consider system (4.16); suppose that Assumptions 1 and 2 are satisfied and the $f(x)$ can be approximated by the T-S fuzzy system. If we pick $\gamma < 1$, which is the gain of $\sum_{\tilde{z}w}$ there exists a positive constant ρ and $\lambda_{\min}(Q) > 2$ in Equation (4.14), and then a tracking-based robust adaptive fuzzy control scheme is proposed as follows:

$$u = -\hat{\lambda} \vartheta(x) B^T P e \tag{4.20}$$

, where

$$\vartheta(x) = \left(\frac{1}{4\gamma^2} \xi(x) \xi^T(x) + \frac{1}{4\rho^2} \psi^2(x) \right) \tag{4.21}$$

, and adaptation law for $\hat{\lambda}$ is now chosen as

$$\dot{\hat{\lambda}} = \Gamma\left(\vartheta(x) e^T P B B^T P e - \sigma(\lambda - \lambda_0) \right) \tag{4.22}$$

Proof. The proof was given by Yang and Zhou (2003)

$$b_{\min} = \min(g(x))$$

$$d_1 = \frac{1}{2} b_{\min} \sigma(\lambda - \lambda_0)^2 + \rho^2$$

$$c_1 = \min\left(\frac{\lambda_{\min}(Q) - 2}{\lambda_{\max}(P)}, \sigma\Gamma \right)$$

The solutions of composite closed loop system are uniformly bounded, and imply that for any $\mu_1 > \left(\frac{d_1}{c_1} \right)^{1/2}$, there exists a constant $T > 0$ such that $\|e_1(t)\| < \mu_1$ for all $t \geq t_0 + T$. The value μ_1 can be made arbitrary small if the design parameters λ_0, σ, ρ are chosen approximately.

Theorem 2 (Uniformly Ultimately Bounded 2): Consider the system (4.16), suppose that assumption 1 is satisfied and the $f(x)$ can be approximated by the T-S fuzzy system. If we pick $\gamma < 1$ and $\lambda_{\min}(Q) > 1$ in (4.14), then the control scheme (4.23) with adaptive law (4.24) is an adaptive fuzzy robust tracking control which can make all the solutions $\left(e(t), \lambda, \hat{\theta}\right)$ of the derived closed loop system uniformly ultimately bounded. Furthermore, given any $\mu > 0$ and bounds on c and θ, we can tune our controller parameters such that the output error $e(t) = y(x) - y_d(x)$ satisfies $\lim_{t \to \infty} |e(t)| < \mu$.

Control law

$$\begin{aligned} u &= u_{equ} + u_s \\ &= -\left[\frac{\lambda}{2\gamma^2} \xi(x) \xi^T(x) B^T P e \right] - \hat{\theta} \psi(x) \tanh\left(\frac{\hat{\theta} \psi(x) B^T P e}{\varepsilon} \right) \end{aligned} \tag{4.23}$$

adaptation parameters

$$\dot{\lambda} = \Gamma_1\left[\frac{1}{2\gamma^2} e^T PB\xi(x)\xi^T(x)B^T Pe - \sigma_1(\lambda - \lambda_0)\right]$$
$$\dot{\hat{\theta}} = \Gamma_2\left[\psi(x)\left\|B^T Pe\right\| - \sigma_2(\hat{\theta} - \hat{\theta}_0)\right] \tag{4.24}$$

, where $\psi(x) = 1 + \|x\| + \|\xi(x)\|$

$$\|\mathbf{x}\| = \mathbf{x}^T\mathbf{x}.$$

Proof. The proof was given by Yang and Ren (2003)

$$b_{\min} = \min(g(x))$$
$$c = b_{\min}^{-1} c_\theta^2 \text{ estimating } \lambda$$
$$d_1 = b_{\min}\left(\sigma_1(c - \lambda_0)^2 + \sigma_2(\theta - \theta_0)^2 + 2\varepsilon\right)$$
$$c_1 = \min\left(\frac{\lambda_{\min}(Q) - 1}{\lambda_{\max}(P)}, \sigma_1\Gamma_1, \sigma_1\Gamma_1\right)$$

The solutions of composite closed loop system are uniformly bounded, and imply that for any $\mu_1 > \left(\frac{d_1}{c_1}\right)^{1/2}$, there exists a constant $T > 0$ such that $\|e_1(t)\| < \mu_1$ for all $t \geq t_0 + T$. The value μ_1 can be made arbitrary small if the design parameters $\lambda_0, \theta_0, \varepsilon, \sigma_1, \sigma_2$ are chosen approximately.

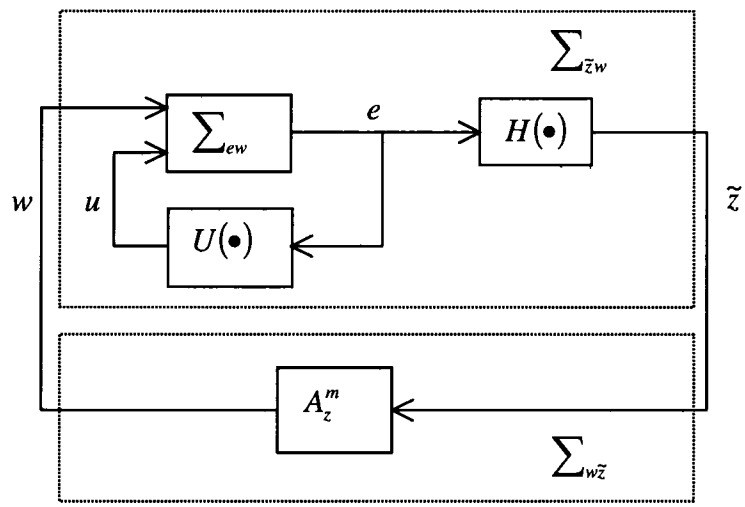

Figure 4.4 Feedback connection of fuzzy system

4.4.4 Indirect Adaptive Fuzzy Control

If plant parameters and structure are exactly known, the technique of feedback linearization gives the control input as

$$u = \frac{1}{g(x)}\left(-f(x) + y_d^{(n)} - k^T e\right)$$

For unknown nonlinear system function $f(x), g(x)$, they can be represented by fuzzy system, then control law will be

$$u_c = \frac{1}{\hat{g}(x,\theta_g)}\left(-\hat{f}(x,\theta_f) + y_d^{(n)} - k^T e\right) \tag{4.25}$$

$\hat{f}(x,A_x), \hat{g}(x,B_x)$ can be represented by fuzzy system.

$$\hat{f}(x,A_x) = \sum_{i=1}^{K} y_i \xi_i(x) = \xi(x) A_x \bar{x}$$

$$\hat{g}(x,B_x) = \sum_{i=1}^{K} y_i \eta_i(x) = \eta(x) B_x \bar{x}$$

This controller must have no estimated $\hat{g}(x,B_x) = 0$. The adaptation will be adjusted to the parameters of matrix A_x and B_x.

4.5 Numerical Simulations

In a numerical simulation, Patti-B 238 t fishing boat is a studied model, which parameters are given by Hsieh et al. (1994), Jiang et al. (2000) as shown in Table 4.1. Optimal U-tube tank parameters of the fishing boat have $L = 5$ m, $H = 2$ m, $A_t = 2$ m^2, and $A_p = 0.19$ m^2. For fuzzy system, linguistic variables are ship roll and ship roll rate, and linguistic values are positive, zero, and negative. *IF-THEN* rules for adaptive fuzzy control are

rule1: IF x_1 is N and x_2 is N and x_3 is N and x_4 is N

THEN $y = a_0^1 + a_1^1 x_1 + a_2^1 x_2 + a_3^1 x_3 + a_4^1 x_4$

rule2: IF x_1 is N and x_2 is N and x_3 is N and x_4 is Z

THEN $y = a_0^2 + a_1^2 x_1 + a_2^2 x_2 + a_3^2 x_3 + a_4^2 x_4$

$\vdots$

rule81: IF x_1 is P and x_2 is P and x_3 is P and x_4 is P

THEN $y = a_0^{81} + a_1^{81} x_1 + a_2^{81} x_2 + a_3^{81} x_3 + a_4^{81} x_4$

Membership functions have values between zero and one. Membership functions shown in Figure 4.5 are positive (P), zero (Z), and negative (N) which correspond with j = 1, 2, and 3 respectively.

$$\mu_{ij}(x) = \begin{cases} 1 & , x < c_{ij} \\ \exp\left(-0.5(x_i - c_{ij})/\sigma^2\right) & , \text{otherwise} \end{cases} \quad , \text{for left}$$

$$\mu_{ij}(x) = \exp\left(-\frac{0.5(x_i - c_{ij})}{\sigma^2}\right) \quad , \text{for center} \tag{4.26}$$

$$\mu_{ij}(x) = \begin{cases} \exp\left(-0.5(x_i - c_{ij})/\sigma^2\right) & , \text{otherwise} \\ 1 & , x > c_{ij} \end{cases} \quad , \text{for right}$$

, where $\mu_{ij}(x)$ are membership function of inputs x_i, c_{ij} is constant values of membership function of state x_i. $c_{1j} = c_{2j} = (-1 + 0.5(j-1)) \times \pi/6$, $c_{3j} = c_{4j} = (-1 + 0.5(j-1)) \times 1$, j = 1, 2, 3.

Simulations are compared among no U-tube tank, passive U-tube tank, feedback linearization, and direct adaptive fuzzy controller with Equation (4.23) under 0.6 rad/s of wave moment frequency. All initial states of a ship are zero. Wave moment amplitudes are 5.0860×10^4 N-m, 7.8601×10^4 N-m, and 1.7292×10^5 N-m have time history of ship roll as shown in Figure 4.6, 4.8, and 4.10 respectively, and phase trajectory of

ship roll and roll rate as shown in Figures 4.7, 4.9, and 4.11 respectively. A ship without U-tube tank will be capsized at 5.0860×10^4 N - m , a ship with optimal U-tube tank will be capsized at 8.6461×10^4 N - m . At encountered wave amplitude 7.8601×10^4 N - m , adaptation parameters for adaptive fuzzy controller λ and θ are shown in Figures 4.12 and 4.13 respectively.

For direct adaptive fuzzy controller Equation (4.20), numerical simulation results are shown in Figures 4.14 and 4.15. The adaptation gain λ is shown in Figure 4.16.

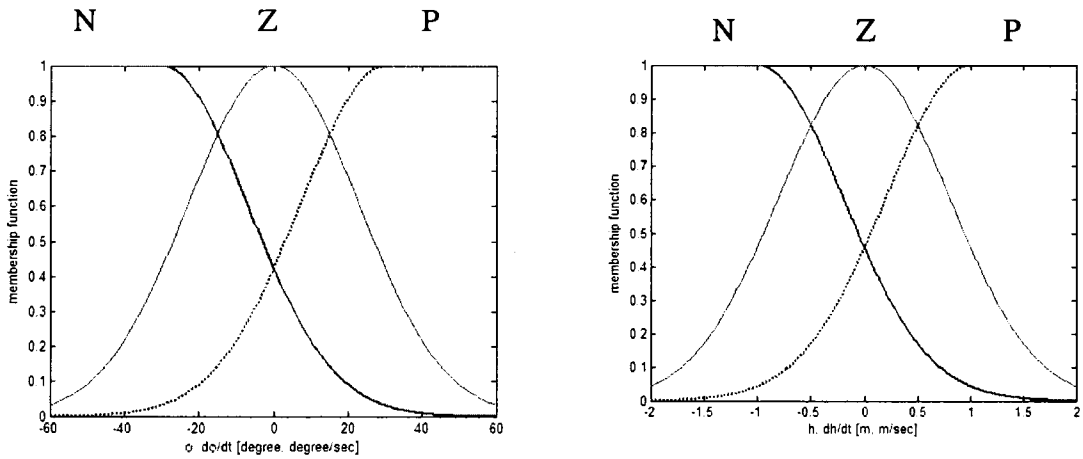

Figure 4.5 Membership function

From numerical simulations, show that U-tube tank increases ship roll damping and improves ability of a ship to survive in rough seas. Comparing with passive U-tube tank, an adaptive fuzzy controller does not significantly help a ship to survive in severe seas, partly because it must have some time to adjust its own parameters.

Ship roll motion damping increases 100 percent with an optimal U-tube tank versus a ship without a U-tube tank; it increases 20 percent with adaptive fuzzy control versus a passive U-tube tank; and it increases 20 percent with linearization feedback with known nonlinear functions versus adaptive fuzzy control.

Table 4.1 Parameters for Patti-B, a 22.9 m, 238 t fishing boat Jiang et al. (2000),

Parameter	Numerical value	Parameter	Numerical value
$I_{44}+m_{44}(\omega)$	1.468×10^{6} kg - m^2	Δ	2.366×10^{6} N
$b_{44}(\omega)$	3.206×10^{3} kg - m^2 - s^{-1}	$b_{44}(\omega)$	9.882×10^{4} kg - m^2
c_1	0.2138 m	c_3	0.6713 m

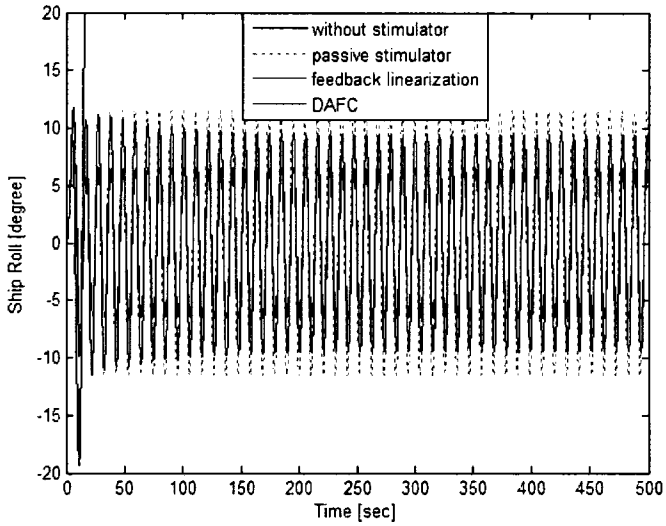

Figure 4.6 Time history of ship roll motion with wave amplitude 5.0860×10^{4} N - m

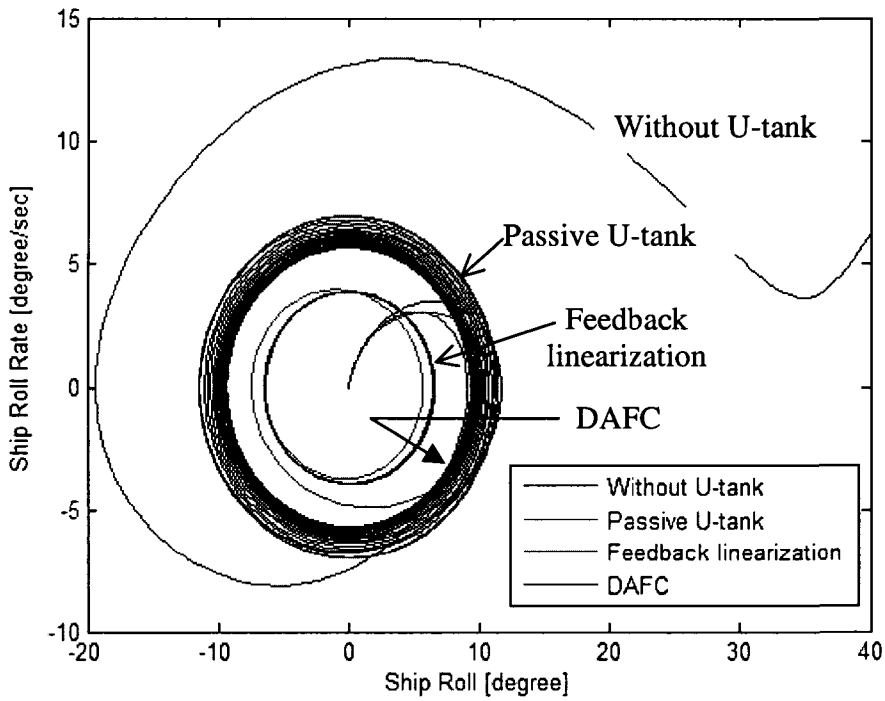

Figure 4.7 Phase trajectory of ship roll and roll rate with wave amplitude 5.0860×10^{4} N - m

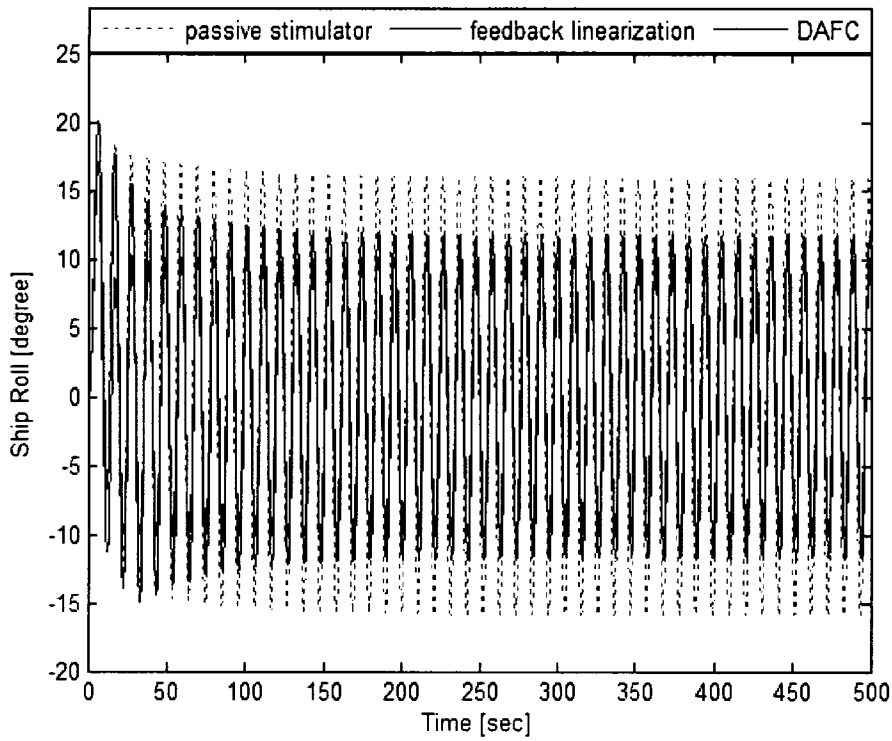

Figure 4.8 Time history of ship roll motion with wave amplitude 7.8601×10^4 N - m

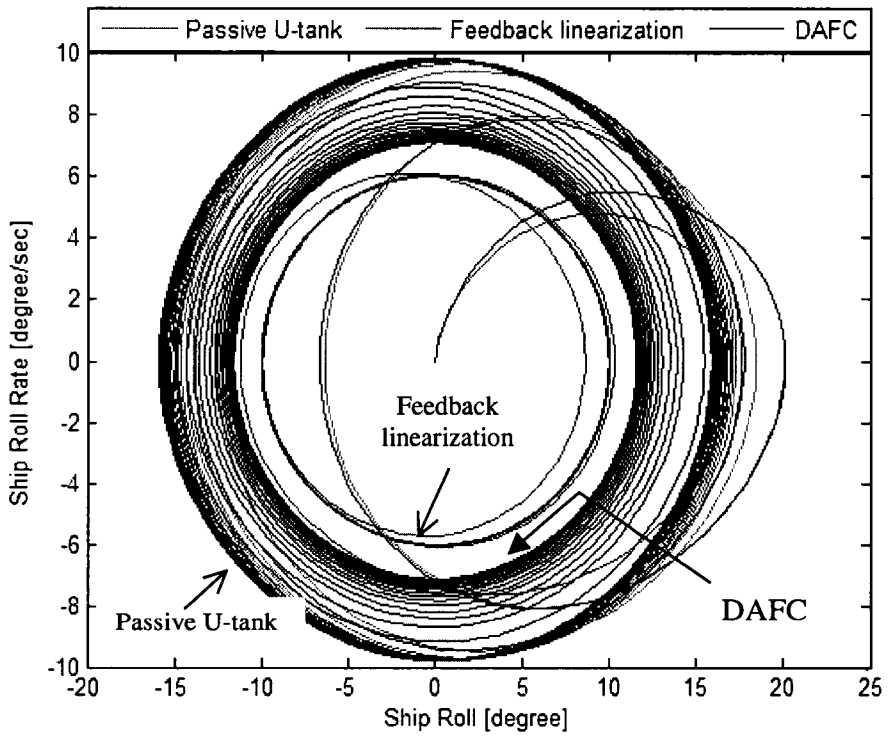

Figure 4.9 Phase trajectory of ship roll and roll rate with wave amplitude 7.8601×10^4 N - m

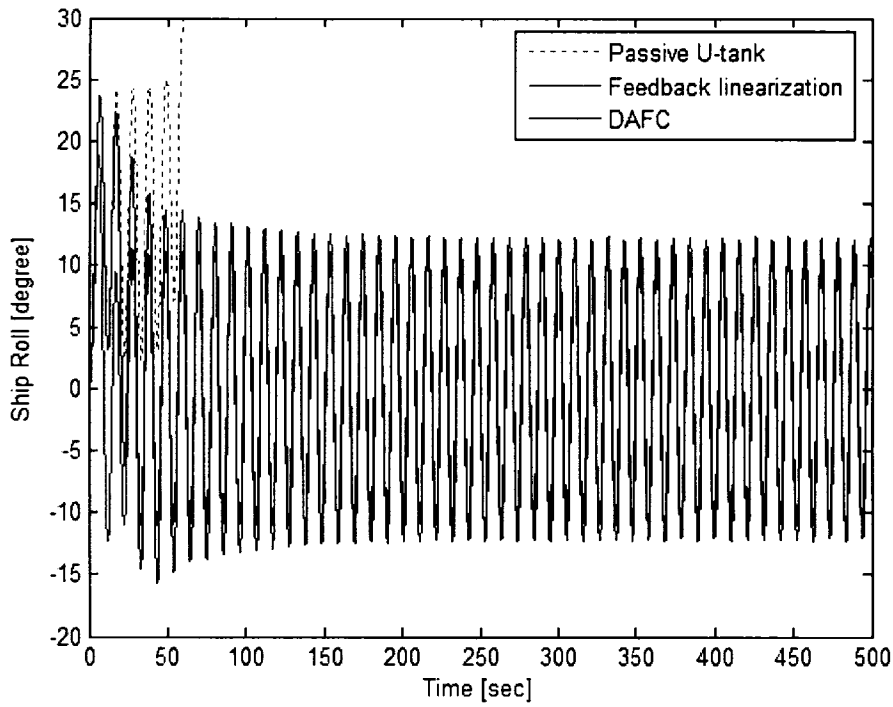

Figure 4.10 Time history of ship roll motion with wave amplitude 8.6461×10^4 N - m

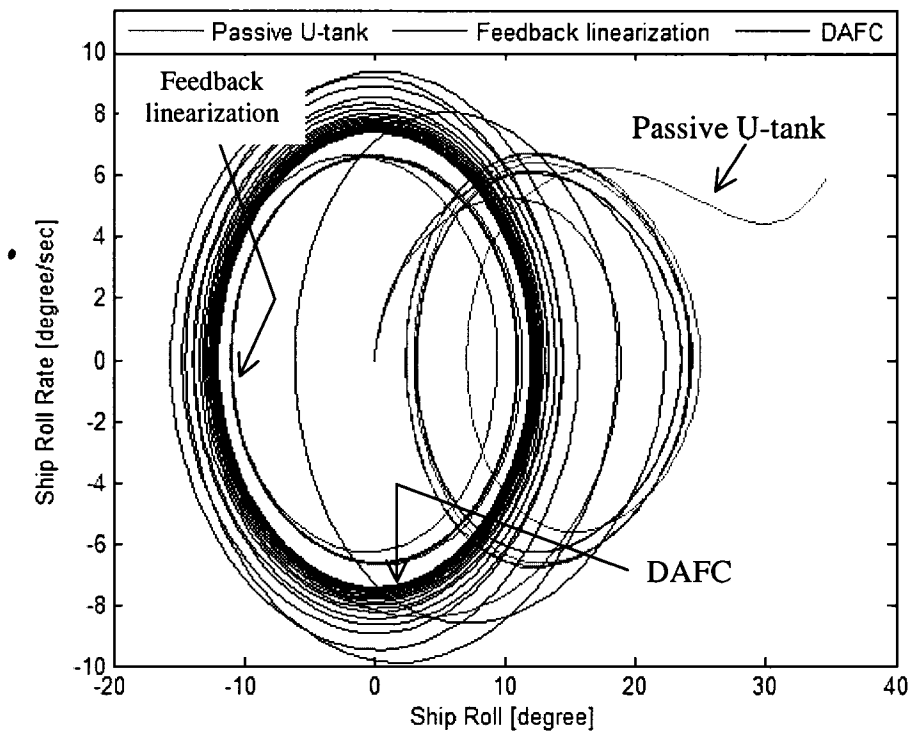

Figure 4.11 Phase trajectory of ship roll and roll rate with wave amplitude 8.6461×10^4 N - m

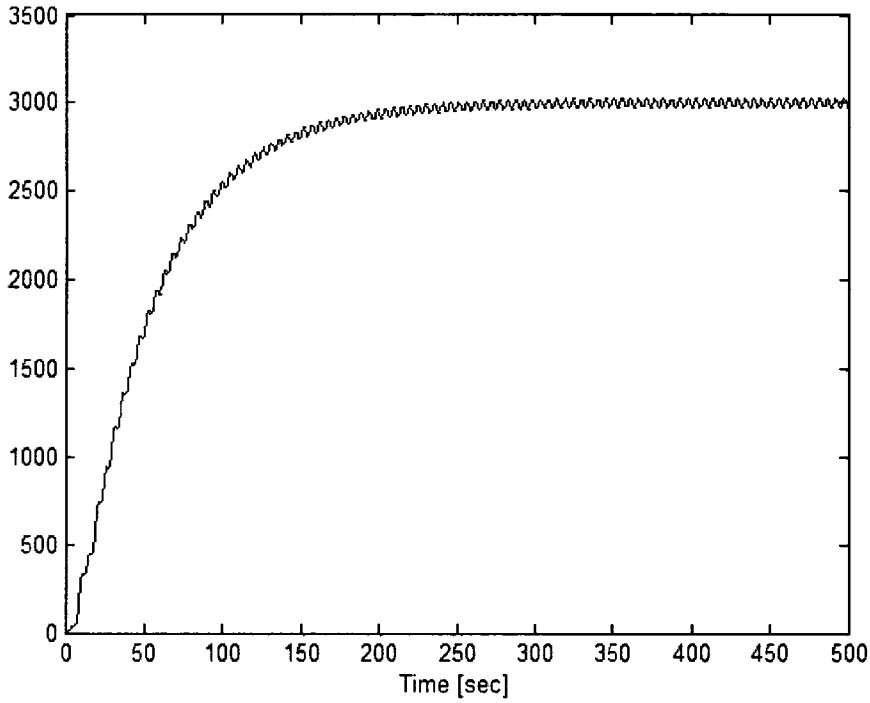

Figure 4.12 Adaptation parameter of λ at wave magnitude 7.8601×10^4 N - m

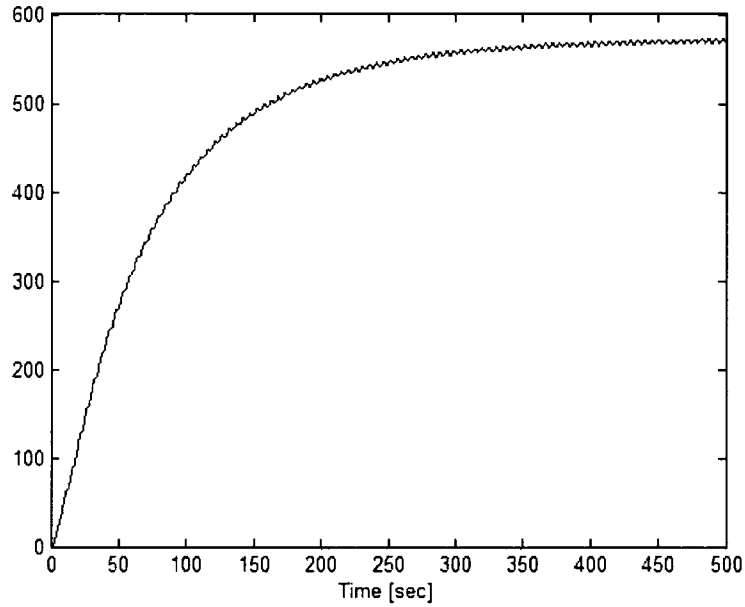

Figure 4.13 Adaptation parameter of θ at wave magnitude 7.8601×10^4 N - m

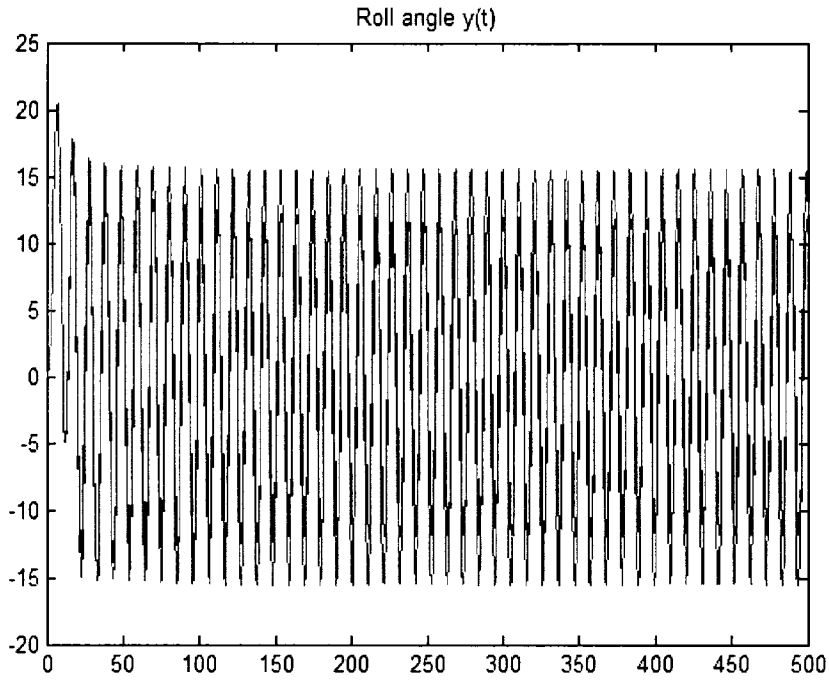

Figure 4.14 Time history of ship roll motion with wave amplitude 7.8601×10^4 N - m for DAFC with Equation (4.20)

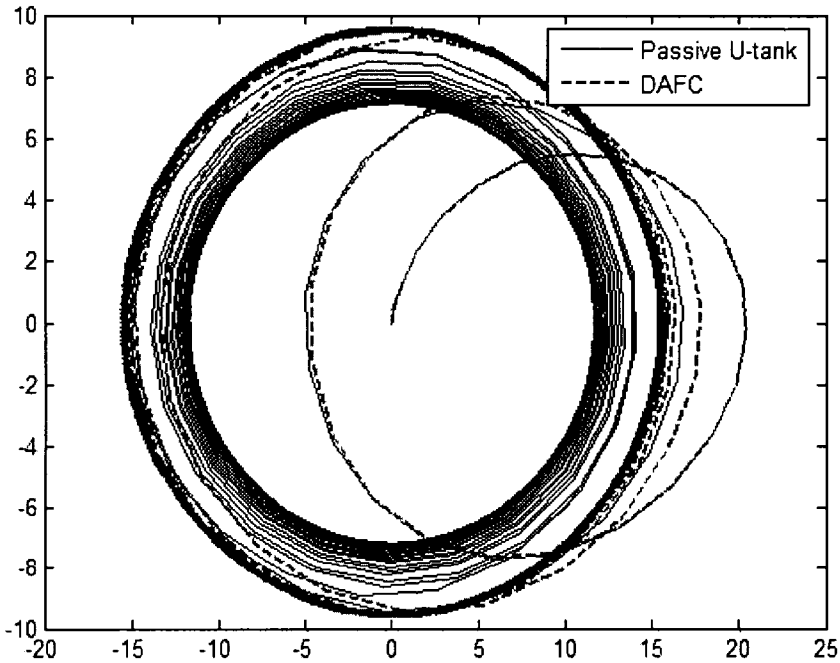

Figure 4.15 Phase trajectory of ship roll and roll rate with wave amplitude 7.8601×10^4 N - m for DAFC with Equation (4.20)

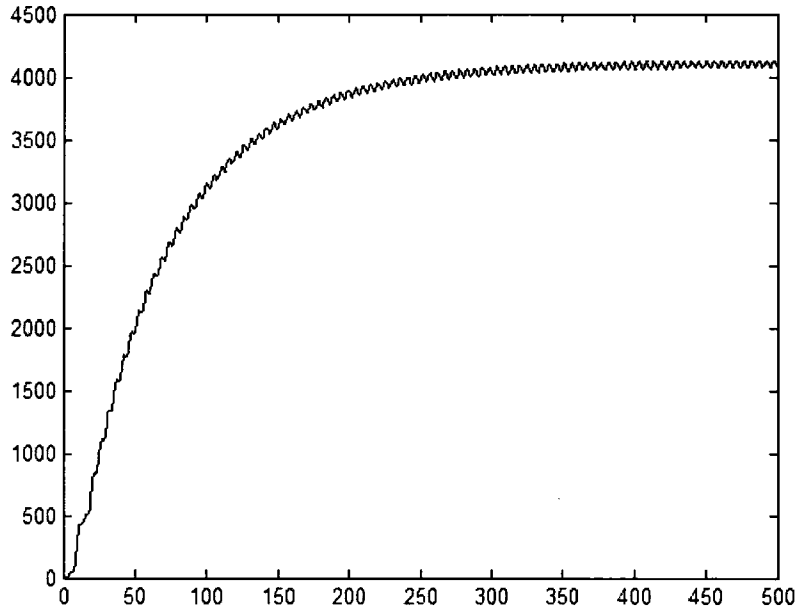

Figure 4.16 Adaptation parameter of λ at wave magnitude 7.8601×10^4 N - m for DAFC with Equation (4.20)

4.6 Conclusions

The nonlinear coupling of ship roll and U-tube tank was studied. A passive U-tube tank helps to reduce ship roll and capsizing. Two types of direct adaptive fuzzy system give close results. To compare with passive U-tube tank, the direct adaptive fuzzy controllers do not show significantly to protect ship capsizing.

For large external moment, ship roll will oscillate around some roll equilibrium. This effect depends on the friction coefficient between fluid motion in the U-tube tank and the U-tube tank's natural frequency.

In the transient states, when ship roll is stimulated, it can cause capsizing immediately. This result comes from the limitation of fuzzy adaptive controller design considerations.

CHAPTER 5

CONCLUSIONS

5.1 Conclusion

A nonlinear, six degrees of freedom of ship roll stimulator, U-tube tank mathematical model was derived and verified with experimental results.

Optimal passive U-tube tanks were considered especially the natural frequency of water motion in U-tube tank and friction between the water and U-tube tank. One can get the optimal passive U-tube tank by using a PD controller. It can increase ship roll damping by 40 percent.

For a linear active U–tube tank, LQR and predictive control are effective in reducing ship roll motion, but predictive control is easier to implement. If ship roll parameters change, an adaptive predictive controller gives better results.

For a passive nonlinear U-tube tank, not only does the U-tube tank increase ship roll damping, but it also reduces ship capsizing in rough seas. For an active U-tube tank, when nonlinear function and system parameters are known, feedback linearization is applied to ship roll mitigation. For an unknown mathematical model exactly adaptive fuzzy control is applied. Feedback linearization significantly reduces ship capsizing from optimal passive U-tube tank.

5.2 Further Extension of the Research

Water slamming on the cover of a U-tube tank will give a large impulsive force to the ship roll motion.

In real application, semi-active U-tube control (by using an air valve to control the water flow in the U-tube tank as shown in Figure 5.1) was one of the interesting topics. An air valve control is cheaper and consumes less energy than an active U-tube tank.

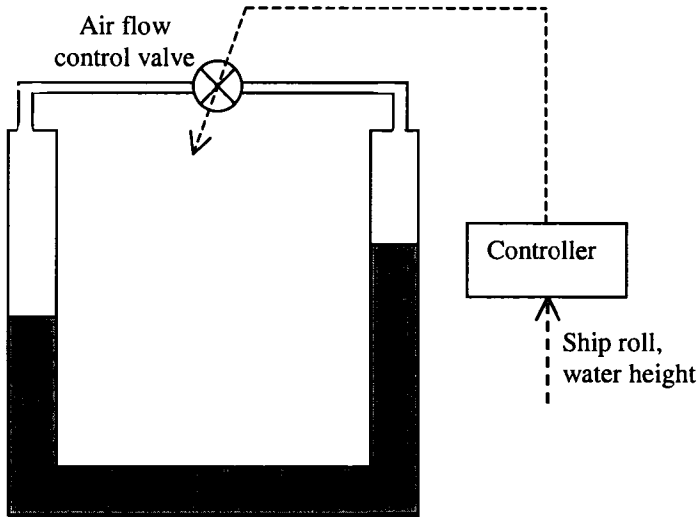

Figure 5.1 Schematic diagram of semi-active U-tube tank

Verification of the selected controller with an experimental set up should be done.

The effect of a U-tube tank on ship motion, especially the ship's turning ability should be studied.

The use of a U-tube tank with other stabilizers should be studied.

Although only 1-DOF beam sea model is analyzed in this study, one should be noted that the current approach can be applied to 3-DOF beam sea model developed by Chen et al. (1999).

REFERENCES

1 Abkowitz M. (1969). Stability and motion control of ocean vehicles. Cambridge, Massachusetts, The MIT press.

2 Amerogen J.V., Van Der Klugt P.G.M., Van Nauta Lemke H.R., (1990). Rudder roll stabilization for ships, Automatica, Vol.26. No.24, pp.679-690.

3 Bhattacharyya, R. 1978. Dynamic of marine vehicles. John Wiley and Son, NewYork.

4 Bird, J.D. and Lucero, L.L., (1999) Ship Roll Stimulation, Craft Engineering Associates, Inc., Hampton, Virginia.

5 Burns R.S. (1991), An optimal control system for pitch, heave, and roll stabilization of surface vessels,

6 Chen C.W., Huang J.K., Phan M., and Juang J.N., 1992. Integrated system identification and state estimation for control of flexible space structures. Journal of Guidance, Control and Dynamics, Vol.15, No.1, 88-95.

7 Chen S., Shaw S.W., Troesch A.W., 1999. Systematic approach to modeling nonlinear multi-DOF ship motions in regular seas. Journal of ship research, Vol.43 No.1, pp 25-37.

8 Chen S., Shaw S.W.,Khalil H., Troesch A.W., 2000. Robust stabilization of large amplitude ship rolling in beams sea. Transaction of ASME Vol.22, pp 108-113.

9 Chen S.L. and Shaw S.W. (1996). A fast manifold approach to Melnikov functions for slowly varying oscillators, International Journal of Bifurcation and Chaos pp.

10 Chen S.L.and Hsu W.C. (2003). Fuzzy sliding mode control for ship roll stabilization. Asian Journal of Control, Vol.5 No.2, pp. 187-194.

11 Chen B.S., Li C.H., Chang Y.C. (1996). H-infinity tracking design of uncertain nonlinear SISO systems: Adaptive fuzzy IEEE Trans. Fuzzy Syst., Vol.4 No.1, pp.32-43.

12 Clarke D.W., Motadi C., and Tuffs P.S., 1987. Generalized predictive controls-parts I and II. Automatica, Vol.23, No.2, 137-160.

13 Den Hartog J.P., 1985. Mechanical vibrations. Dover Publications Inc., New York, Reprint.

14 Falazano J.M., Shaw S.W., Troesch A.W., (1992). Application of global methods for analysis dynamical systems to ship rolling motion and capsizing. International of Bifurcation and Chaos Vol.2 No.1 pp101-115.

15 Fossen, T. I., 1994, Guidance and control of ocean vehicles, John Wiley and Sons.

16 Gawad A.F.A., Ragab S.A., Nafeh A.H., and Mook D.T., 2001. Roll stabilization by anti-roll passive tanks. Ocean Engineering, 457-469.

17 Ge S.S., Hang C.C., and Zhang T., (1999). Adaptive Neural Network Control of Nonlinear Systems by State and Output Feedback, IEEE Transactions on Systems, Man, and Cybernetics, Vol. 29, No. 6, pp. 818-828.

18 Goodzeit N.E. and Phan M.Q., 2000. System and disturbance identification for feedforward-feedback control applications. Journal of Guidance, Control and Dynamics, Vol. 23, No. 2, 260–268.

19 Guo C., Simaan M.A., Sun Z.(2003). Neuro-fuzzy intelligent controller for ship roll motion stabilization. Proceeding of the 2003 IEEE International Symposium on Intelligent control Houston, Texas. 2003.

20 He S., Reif K., and Unbehauen R., (1998). A neural approach for control of nonlinear systems with feedback linearization, IEEE Transactions on Neural Networks, Vol. 9, No.6, pp 1409-1421.

21 Hickey N.A., Grimble M.J., Johnson M.A., Katebi M.R., and Melville R.. (1997) Robust fin roll stabilization of surface ships. Proceeding of the 36th Conference on Decision and Control, San Diego, California, 1997.

22 Hsieh S.R., Trosch A.W., and Shaw S.W., (1994). A nonlinear probabilistic method for predicting capsizing in random beam seas. Proceeding of the Royal Society of London. Series A, pp 1-17.

23 Hua J., Wang W.H., and Chang J.R. (1999). A representation of GM-variation in waves by Volterra system. Journal of Marine Science and Technology, Vol.7 No.2, pp94-100.

24 Jiang C., Tresch A.W., and Shaw S.W. (2000). Capsize criteria for ship models with memory-dependent hydrodynamics and random excitation. Phil Trans. R. Soc. London A pp.1761-1791.

25 Juang J.N., 1994. Applied system identification. Prentice Hall, 1994.

26 Juang J.N., Phan M., Horta M., and Longman R.W., 1993. Identification of Observer/Kalman filter Markov parameters: theory and experiments. Journal of Guidance, Control and Dynamics, Vol. 16, No. 2, 320–329.

27 Juang J.N., and Phan M.Q., 1997a. Deadbeat predictive controllers. NASA TM112862.

28 Juang J.N., and Phan M.Q., 1997b. Recursive deadbeat controller design. NASA TM112862.

29 Kim Y., 2002. A numerical study on sloshing flows coupled with ship motion – The anti-rolling tank problem. Journal of Ship Research. Vol.46, 52-62.

30 Kvaternik R.G., Piatak D.J., Nixon M.W., Langston C.W., Singleton J.D., Benett R.L., and Brown R.K., 2001. An experimental evaluation of generalized predictive control for Tiltrotot aeroelastic stability augmentation in airplane mode of flight. American Helicopter Society 57th Annual Forum, Wasington DC.

31 Lewis, E.V., 1989, Principles of naval architecture, 2nd revision, The Society of Naval Architects and Marine Engineers.

32 Lewis F.L., 1986. Optimal control. A Wiley Inter-Science publication.

33 Lloyd A.R.J.M., 1989. Sea keeping-ship behavior in rough weather. Ellis Horwood Limited, Chichester.

34 Nejim S. (2000). Rudder roll damping systems for ships using fuzzy logic control.

35 Neves M.A.S., Pe´rez N., Valerio L.(1999), Stability of small fishing vessels in longitudinal waves. Ocean Engineering. pp. 1389–1419

36 Neves M. A. S., Pe´rez N., Lorca O., (2003). Analysis of roll motion and stability of a fishing vessel in head seas. Ocean Engineering. pp. 921–935

37 Oh I.G., Nayfeh H., and Mook D.T., (1993). Theoretical and experimental study of the nonlinearity coupled heave, pitch, and roll motions of a ship in longitudinal waves. ASME. Nonlinear Vibrations. pp 105-125.

38 Park J-H., Seo S-J., and Park G-T., (2003). Robust adaptive fuzzy controller for nonlinear system using estimation of bounds for approximation errors, Fuzzy Sets and Systems, pp. 19-36.

39 Phairoh T., and Huang J.K., 2005. Modeling and analysis of ship roll tank stimulator systems. Ocean Engineering, 1037-1053.

40 Phairoh T., and Huang J.K., 2005. Adaptive Ship Roll Mitigation by Using a U-tube Tank, accepted Ocean Engineering.

41 Roberts J. (1982). A stochastic theory for nonlinear ship rolling in irregular seas. Journal of Ship Research. pp 299-245.

42 Roberts G.N. and Barboza T.L. (1988). Analysis of warship roll stabilization by controlled anti-roll tanks with the aid of digital simulation.

43 Sastry S. and Bodson M., (1989). Adaptive control: Stability, convergence, and robustness, Prentice-Hall International Editions NJ.

44 Slotine J.J. and Li W., (1991). Applied nonlinear control, Prentice Hall-International Editions NJ.

45 Shames I.H., and Dym C.L., (1991). Energy and finite element methods in structural mechanics. Taylor and Francis.

46 Shao Z.J., Wang H., Zhu Y.K., and Qian J.X. (1994). Multivariable optimal control with adaptation mechanism in rudder/fin stabilization system.

47 Robert G.N., Sharif M.T., Sutton R., and Agrawal A. (1997). Robust control methodology applied to design of a combined steering/stabilizer system for warships. IEE Proc. Control Theory Appl. Vol.144, No.2 pp.128-136.

48 Spooner J.T., and Pasinno K.M., (1996). Stable adaptive control using fuzzy systems and neural networks, IEEE. Trasaction on Fuzzy system, Vol.4, No.3, pp.339-359.

49 Sontag E.D. (1995). On the input-to-state stability property. Eur. J. Control. pp24-36.

50 Stoustrup J., Niemann H.H., Blanke M. (1994) Roll damping by rudder control – A new H-infinity approach.

51 Sutton R., Roberts G.N., and Dearden S.R. (1989). Design study of a fuzzy controller for ship roll stabilization. Electronics and Communication Engineering Journal, pp 159-166.

52 Tanguay H., and Lebret G. (2004). Fin rudder stabilization of ships: a gain scheduling control meyhodology, Proceeding of the 2004 American Control Conference Boston, Massachusetts, 2004.

53 Thompson J.M.T. (1989). Chaotic phenomena triggering the escape from potential well. Proceeding of the Royal Society of London. Series A, pp 195-225.

54 Thompson J.M.T. and Soliman M.S. (1990). Fractal control boundaries of driven oscillators and their relevance to safe engineering design. Proceeding of the Royal Society of London. Series A, pp 1-13.

55 Thompson J.M.T., Rainey R.C.T., and Soliman M.S. (1990). Ship stability criteria based on chaotic transients from incursive fractals. Proceeding of the Royal Society of London. Series A, pp 149-167.

56 Wang L-X., (1994). Adaptive fuzzy systems and control: Design and stability analysis, Prentice-Hall Englewood Cliffs N.J.

57 Webster W.C., (1967), Analysis of the control of activated antiroll tanks, Proceedings from the Annual Meeting of The Society of Naval Architects and Marine Engineers, New York, NY. pp. 296-325.

58 Webster B.N., Birmingham R.W., Jones E.B., and Roskilly A.P. (2003). The application of artificial intelligence to roll stabilization for a range of loading and operating conditions, International Journal of Marine Engineering.

59 Yalla S.K., Kareem A., and Kantor J.C. (2001). Semi-active tuned liquid column dampers for vibration control of structures, Engineering Structures, pp. 469–1479.

60 Yamagushi S., and Shinkai A., 1995. An advanced adaptive control system for activated anti-rolling tank. International Journal of Offshore and Polar Engineering, 17-22.

61 Yang Y., Zhou C., and Jia X., (2002). Robust adaptive fuzzy control and its application to ship roll stabilization, Information Sciences, pp. 177-194.

62 Yang Y. and Ren J., (2003). Adaptive fuzzy robust tracking controller design vi small gain approach and its application, IEEE Transactions on Fuzzy Systems, Vol. 11, No. 6, pp783-795.

63 Yim S.C.S., Nakhata T., Bartel W.A., and Huang E.T., (2005). Couple nonlinear barge motions, part I:Deterministic models development, identification and calibration, ASME Journal of Offshore Mechanics and Arctic Engineering, Vol. 27 pp. 1-10.

64 Zhang H., Jiang D., Liang L., Huang S., and Li G. (2004) Modeling and simulation of passive controlled anti-rolling tank, Proceding of 5th World Congress on Intelligent Control and Automation, June 15-19, 2004.

APPENDIX A

ISS and SMALL GAIN THEOREM

Definition A1 (Uniformly Ultimately Bounded) It is said that the solution of system $\dot{x} = f(x,u)$ with $y = h(x)$ is uniformly ultimately bounded if for any U, a compact subset of R^n, and all $x_0(t_0) = x_0 \in U$, there exists an $\varepsilon > 0$ and a number $T(\varepsilon, x_0)$ such that $\|x(t)\| < \varepsilon$ for all $t \geq t_0 + T$.

Definition A2 (Class K-function) A class K-function γ is a continuous, strictly increasing from R_+ into R_+ and $\gamma(0) = 0$. It is of class K_∞ if additionally $\gamma(s) \to \infty$ as $s \to \infty$. A function $\beta : R_+ \times R_+ \to R_+$ is a class of KL if $\beta(\cdot, t)$ is a class K for every $t \geq 0$ and $\beta(s,t) \to 0$ as $t \to \infty$.

Definition A3 (Input to State practically Stable, ISpS) For system $\dot{x} = f(x,u)$, it is said to be input-to-state practically stable (ISpS) if there exist a function γ of class K, called the nonlinear L_∞ gain, and a function β of class KL such that, for any initial condition x(0), each measurable essentially bounded control u(t) defined for all $t \geq 0$ and a nonnegative constant d, the associated solution x(t) is defined on [0,∞) and satisfies:

$$\|x(t)\| \leq \beta(\|x(0)\|, t) + \gamma(\|u_t\|_\infty) + d \qquad \text{(A1)}$$

When d = 0 in Equation (1), the ISpS property becomes the input-to-state stability (ISS) property.

Definition A4 (Input to State practically Stable Lyapunov function) A C^1 function V is said to be an ISpS-Lyapunov function for system $\dot{x} = f(x,u)$ if there exist functions α_1, α_2 of class K_∞ such that

$$\alpha_1(\|x(t)\|) \le V(x) \le \alpha_2(\|x(t)\|), \quad \forall x \in R^n, \tag{A2}$$

and there exist functions α_3, α_4 of class K and a constant d > 0 such that

$$\frac{\partial V}{\partial x}(x) f(x,u) \le -\alpha_3(\|x(t)\|) + \alpha_4(\|u\|) + d \tag{A3}$$

When Equation (A3) holds with d = 0, V is referred to as an ISS-Lyapunov function. Then it holds that one may pick a nonlinear L_∞ gain γ in Equation (A1) of the form, which is given by Sontag (1995)

$$\gamma(s) = \alpha_1^{-1} \circ \alpha_2 \circ \alpha_3^{-1} \circ \alpha_4(s), \quad \forall s > 0 \tag{A4}$$

where the notation $\circ$ stands for the composition operator between two functions.

Proposition A1 (Input to State practically Stable, ISpS) The system $\dot{x} = f(x,u)$ is ISpS if and only if there exists an ISpS-Lyapunov function.

Consider the stability of the closed-loop interconnection of two systems shown in Figure A1.

Theorem A1 Consider a system in composite feedback form (cf. Fig. 1)

$$\sum_{\tilde{z}w}: \begin{cases} \dot{x} = f(x,\omega) \\ \tilde{z} = H(x) \end{cases} \tag{A5}$$

$$\sum_{w\tilde{z}}: \begin{cases} \dot{y} = g(y,\tilde{z}) \\ \omega = K(y,\tilde{z}) \end{cases} \tag{A6}$$

of two ISpS systems. In particular, there exist two constants $d_1 > 0$, $d_2 > 0$, and let β_ω and β_ξ of class KL, and γ_z and γ_ω of class K be such that, for each ω in the L∞ supremum norm, each $\tilde{z}$ in the L_∞ supremum norm, each $x \in R^m$ and each $y \in R^m$, all the solutions $X(x;\omega,t)$ and $Y(y;\tilde{z},t)$ are defined on [0,∞) and satisfy, for almost all $t \geq 0$.

$$\|H(X(x;\omega,t))\| \leq \beta_\omega(\|x\|,t) + \gamma_z(\|\omega_t\|_\infty) + d_1 \tag{A7}$$

$$\|K(Y(y;\tilde{z},t))\| \leq \beta_\xi(\|y\|,t) + \gamma_\omega(\|\tilde{z}_t\|_\infty) + d_2 \tag{A8}$$

Under these conditions, if

$$\gamma_z(\gamma_\omega(s)) < s (resp. \gamma_\omega(\gamma_z(s)) < s), \ \forall s > 0. \tag{A9}$$

then the solution of the composite systems (A5) and (A6) is ISpS.

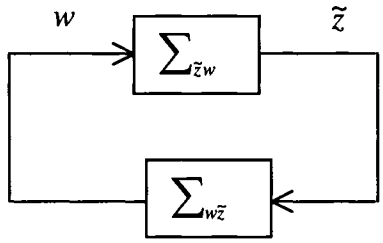

Figure A1 Feedback connection of interconnection systems

VITA

Thongchai Phairoh received his M. Eng and B. Eng degree from King Mongkut's Institute of Technology North Bangkok, Thailand, in 1986 and 1997 respectively, all in mechanical engineering.

From 2000 to 2006, he was a research and teaching assistant in mechanical engineering, at Old Dominion University. From 1993 to 2000, he was lecturer at mechanical engineering at Mahidol University, Thailand. From 1988-1993, he worked as project coordinator at the National Research Council of Thailand. From 1986-1988, he worked as design engineer at Phamaceutical and Medical Supply, Thailand.

In 1996, he received the outstanding award of faculty and staff, Faculty of Engineering, Mahidol University. In 1997, he received the third prize thesis award of Faculty of Engineering, King Mongkut's Institute of Technology North Bangkok. In 2001, he was named outstanding graduate student of mechanical engineering, Old Dominion University.

Journal Publication

Phairoh T., and Huang J.K., Adaptive Ship Roll Mitigation by Using U-tube Tank, accepted Ocean Engineering.

Li Q., Phairoh T., Huang J.K., and Mei C., Adaptive Control of Nonlinear Free Vibrations of Composite Plates Using Piezoelectric Actuators, Accepted AIAA.

Phairoh T., and Huang J.K., Modeling and Analysis of Ship Roll Tank Stimulator Systems, Ocean Engineering, Vol.32, Issues 8-9, June 2005, pp1037-1053.

Conferences

Li Q., Phairoh T., Huang J.K., and Mei C., Adaptive Control of Nonlinear Free Vibrations of Beams and Composite Plates Using Piezoelectric Self-Sensing Actuators, AIAA Structures, Structural Dynamics & Material Conference, 18-21 April 2005, Austin, Texas.

Technical Reports

Phairoh T., and Demuren A., Cellular Automata and State Space Representation Applied to Land Use Modeling, March, 2006.

Phairoh T., and Huang J.K., Identification of a Linear Two-Process Model for Performance Prediction, January, 2006.

Huang J.K., and Phairoh T., Feasibility Analysis of Using the Ship Roll Stimulation System as a Roll Mitigation Device, Prepared for Craft Engineering, November, 2002.

Huang J.K., Mielke R., Fergen P., and Phairoh T., Modeling and Analysis of Ship Roll Stimulation System, November, 2001.